

Hypoxia tolerance and exercise
of an Arctic key stone species the Polar cod
Boreogadus saida
under global change scenarios

Master's thesis

Carolin Julie Neven

M.Sc. Marine Biology

Supervised by Dr. Felix Christopher Mark¹ & Prof. Dr. Guy Claireaux²

¹ Alfred-Wegener-Institut, Helmholtz-Zentrum für Polar- und Meeresforschung (AWI)

² Institute français de recherche pour l'exploitation de la mer (IFREMER Brest, UMR LEMAR 6539)

University of Bremen
June 2021

To my family.

My parents Heike and Heinz,
my brother Christopher
and my grandma
Oma Anni

Table of contents

List of Figures and Tables	iii
Figures.....	iii
Tables	viii
List of Formulas.....	ix
List of Abbreviations	x
Abstract	xii
1 Introduction.....	1
1.1 Polar cod <i>Boreogadus saida</i> – an Arctic keystone species.....	1
1.2 Changing Arctic – a threat to Polar cod?.....	3
1.3 Underlying physiological concepts.....	7
1.3.1 Aerobic metabolic scope	7
1.3.2 Limiting oxygen level curve	8
1.3.3 Oxygen and capacity limited thermal tolerance	10
1.4 State of the Art and resulting key research.....	13
1.4.1 Temperature.....	13
1.4.2 Hypoxia tolerance.....	15
1.4.3 Importance of key research and its objectives.....	15
2 Materials & methods.....	16
2.1 Fish acclimation and keeping	16
2.2 Static respirometry – baseline SMR and SMR measurements.....	17
2.3 Swimming performance and MMR measurements	20
2.4 Data handling	23
2.4.1 Oxygen consumption.....	23
2.4.2 Baseline standard metabolic rate.....	24
2.4.3 Standard metabolic rate.....	24
2.4.4 Maximum metabolic rate	25
2.4.5 Absolute aerobic scope	25
2.4.6 Factorial aerobic scope.....	25
2.4.7 LOL curve and P_{crit}	26
2.4.8 Critical swimming speed.....	26
2.4.9 Gait transition speed	27

2.4.10	Evaluation of burst activity.....	27
2.4.11	Statistical analysis.....	27
3	Results	29
3.1	Mortality.....	29
3.2	Respiration measurements	29
3.2.1	Baseline standard metabolic rate.....	29
3.2.2	Standard metabolic rate.....	30
3.2.3	Maximum metabolic rate	31
3.2.4	Aerobic scope	33
3.2.5	LOL curve and P_{crit}	37
3.3	Swimming performance	39
3.3.1	MR at different water velocities.....	39
3.3.2	Gait transition speed	40
3.3.3	Critical swimming speed.....	43
4	Discussion	45
4.1	Temperature effect on metabolic and swimming capacity.....	45
4.2	Hypoxia tolerance of Polar cod at low and high temperatures	48
4.2.1	Hypoxia tolerance of Polar cod at 10°C.....	48
4.2.2	Hypoxia tolerance of Polar cod at different temperatures	54
4.3	Underlying mechanisms	57
4.4	Ecological implications	61
5	Conclusion	66
6	References.....	lxviii
	Appendix	lxxviii
	Acknowledgements	lxxix

List of Figures and Tables

Figures

Figure 1	Polar cod (<i>Boreogadus saida</i>). Experimental animal with the ID 59. Caught in Billefjorden, Svalbard.....	1
Figure 2	Position of Polar cod in the Arctic food web. This figure exemplifies the central position of Polar cod in the Arctic food web. Note that diet composition is simplified to a high degree as Polar cod feed on amphipods, benthic crustations, chaetognaths, teleosts among others (adapted after Welch 1992).	3
Figure 3	Temperature developments in the Arctic. a: Depicted is the predicted temperature increase until the period 2081 to 2100 compared to 1986 – 2005 depending on the representative concentration path scenario (RCP) for greenhouse gas emissions in different regions in the world. The Arctic region is the region expected to warm the most rapidly in a global comparison (IPCC 2014). b: Temperature change over the Arctic Sea surface relative to the period of 1986 – 2005 for winter (left) and summer (right). Different colours mark predicted temperature development according to the RCP (adapted after IPCC 2013, Annex I).	5
Figure 4	Study area. a: The Arctic comprising the area north of 60°N (Clarke 1983) (https://www.reddit.com/r/MapPorn/comments/5t7ktf/arctic_topographic_map_by_hugo_ahlenius_950x950/ , 29.01.21). b: Svalbard archipelago with position of Billefjorden (78°34'59.99" N 16°27'59.99" E), Isfjorden and Hornsund. Billefjorden is the origin of the experimental animals used in the present study. (https://upload.wikimedia.org/wikipedia/commons/thumb/b/bd/Svalbard_relief_location_map_conic.jpg/496px-Svalbard_relief_location_map_conic.jpg , 27.06.21).	5
Figure 5	Model of the limiting oxygen level curve. At an oxygen saturation of 100% the aerobic metabolic scope is maximised. With decreasing ambient oxygen saturation, the limiting oxygen level curve (LOL curve, red) declines together with the MMR (red) (P_{cmax} ; in case of oxy regulation of MMR P_{cmax} can be found at lower oxygen levels than 100%). RMR and SMR can be regulated and therewith kept independent from decreasing ambient oxygen saturation until a distinct ambient oxygen level. At the intercept of MMR or LOL curve with RMR the limiting oxygen level (LOL) is reached. This results in a restriction of aerobic performances like locomotion and a shift of RMR from oxy regulation to oxy conforming. At P_{crit} the LOL curve or MMR intercepts with the SMR causing the aerobic metabolic scope to be nil. Thus, only energy for maintenance is available. Short-term survival is not compromised. At ambient oxygen saturations below P_{crit} anaerobic metabolism is required to sustain life. Survival is therefore limited (scope of survival) and defined by the duration of the hypoxic situation (modified after Claireaux and Chabot 2016).	10

Figure 6 Conceptual model of oxygen and capacity limited thermal tolerance (OCLTT). The upper graph displays the aerobic scope in relation to temperature whereas the lower graph depicts the rate of aerobic performance like swimming or growth in relation to temperature. Furthermore, key temperatures are displayed. The thermal optimum window is situated between the lower and upper pejus temperature. In this thermal range aerobic scope and aerobic performance are at their maximum. At the pejus temperature aerobic scope starts to decrease due to a mismatch between oxygen supply and oxygen demand resulting in a decrease in the rate of aerobic performance. Increasing temperature leads to a further loss of aerobic scope and aerobic performance ultimately resulting in a loss of aerobic animal function when the critical temperature is reached. Beyond T_{crit} , oxygen supply capacity is not sufficient to fuel maintenance cost aerobically and the animal depends on anaerobic metabolism for energy production. Life beyond T_{crit} is thus temporally limited and finally leads to death (T_d). By restricting oxygen supply, hypoxia (red arrows) will lead to a narrowing of the thermal window by shifting T_{crit} and to a decrease of the aerobic scope within the thermal optimum range. Thus, hypoxia is expected to decrease performance optima (modified after Pörtner 2010). .. 12

Figure 7 Static respirometry setup - reservoir tanks. Two reservoir tanks (black) with a volume of 170l connected via U-pipes were separated into five compartments each, with one compartment containing one respiration chamber. Compartments were closed with transparent covers to prevent evaporation. The upper reservoir tank was additionally covered with a white plastic sheet to ensure similar light conditions in both tanks. Water was gassed with nitrogen and oxygen to derive the desired oxygen saturation of the respective PO_2 level. Gassing was placed in an empty compartment not containing a respiration chamber. Ambient temperature and PO_2 were measured in the upper reservoir tank. Homogeneity of water was derived via a circulation pump circulating water within and between the two tanks. Half of the water volume was exchanged weekly. Furthermore, water was disinfected using a UV-light integrated in the circulation circle. 18

Figure 8 Static respirometry setup – Respiration chamber placed in a compartment of the reservoir tank. Each respiration chamber was connected to a flush- and a recirculation pump that could be controlled by the AutoResp software via a DAQ-M instrument. The flush pump introduced fresh water from the reservoir tank for 2.5 min. Excess water was removed via an outlet. After the flush pump was shut off prohibiting water renewal, water in the respiration chamber was recirculated via the recirculation pump for 17.5 min. Of these 17.5 min the first 30 sec were free from MO_2 measurements to let water homogenise. During the remaining 17 min MO_2 was measured via an optode that was integrated within the recirculation circle and connected to a four-channel meter. Ambient PO_2 and temperature were measured using a four-channel meter likewise. The desired oxygen saturation in the reservoir tanks was derived by gassing with nitrogen and oxygen. Nitrogen input was controlled by the DAQ-M instrument whereas O_2 input was set manually. Inlets of N_2 and O_2

were placed in an empty compartment and are only shown on the figure to explain the setup. Figure adapted after www.loligosystems.com. 19

Figure 9 Swim tunnel setup. The swim tunnel was placed in a reservoir tank and connected to a flush pump that facilitated water renewal. Excess water was released through an outlet leading into the reservoir tank. During the measurement cycle the flush pump was working for 2.5 min to re-establish O₂ saturation in the tunnel. During the wait and measuring phase, the flush pump was shut off and water was circulated via the propeller producing a water current. The propeller was driven by an external motor that was adjusted via a control unit (red), the DAQ-M instrument and the AutoResp software. The velocity could be programmed to increase automatically every 11 min concurrently with the new beginning of the measurement cycle. MO₂ and temperature within the tunnel and ambient O₂ saturation were measured via a four-channel meter using optodes and a temperature sensor. The water of the reservoir tank was gassed with N₂ and O₂ to derive the desired ambient O₂ saturation. The amount of N₂ was set in the AutoResp software and controlled by the DAQ-M instrument. An additional circulation pump in the reservoir tank ensured homogenisation of water within the tank. The fish was placed in the swimming chamber of the swim tunnel in which the water entered through a honeycomb-like structure to create an even water current and left the chamber through a grid. Resting at the grid for three minutes was taken as termination of the experiment. Figure adapted after <https://swimtunnel.com/home/>..... 22

Figure 10 Baseline standard metabolic rate. Dots show metabolic rates (MR) of the individuals tested in mmol O₂/kg/h over the PO₂ range used for the calculation of the baseline SMR (treatments 100 – 60%). Black line depicts baseline SMR (2.12 mmol O₂/kg/h), which was calculated after Chabot et al. 2016 as described in chapter 2.4.2. 30

Figure 11 Standard metabolic rate over decreasing O₂ saturations displayed by a polynomial regression model. Orange line shows the general tendency of SMR over ambient O₂ saturations, orange shaded area indicates standard error (SE) of the regression model. Orange dots show metabolic rates measured at the O₂ levels. Dark orange rhombs depict individual SMR calculated at each oxygen level.....31

Figure 12 Maximum metabolic rate over decreasing O₂ saturations displayed as polynomial regression model. Blue line shows general tendency of MMR over ambient O₂ saturation levels. Blue shaded area indicates SE of the regression model. Blue dots show metabolic rates measured at the O₂ saturation levels. Dark blue rhombs depict individual MMR calculated at each PO₂ level. 32

Figure 13 Maximum-, standard- and baseline standard metabolic rate with aerobic metabolic scope derived from 23 multiple used individuals. All metabolic rates (MR) measured in the swim tunnel (blue) and static respirometry (orange) approach are displayed as dots in relation to the ambient PO₂ levels at which they were assessed. Blue line and dark blue shaded area show MMR as

regression model with respective SE of the model. MMR was derived from the MR measured in the swim tunnel set up. Dark orange line and orange shaded area display the SMR as regression model with SE of the model. SMR was calculated from MR measured in the static respirometry approach. Black line marks calculated baseline SMR. Shaded light blue area between MMR and SMR indicates the AAS defined as difference between MMR and SMR. 33

Figure 14 Absolute aerobic scope at different O₂ saturation levels. Bars and error bars represent the mean AAS with SD per PO₂ level. Numbers depict significant differences between treatments with numbers on top of the error bar state the treatments to which significant difference was observed. The following oxygen saturations could be compared: 80, 50, 40, and 25% O₂ (**Table 2**); 100 – 50% O₂ (**Table 3**); and 40-25% O₂ (p=0.46). 34

Figure 15 Factorial aerobic scope at different O₂ saturation levels. Bars and error bars represent the mean FAS with SD per treatment. Numbers depict significant differences between oxygen saturations with numbers on top of the error bar state the oxygen levels to which significant difference was observed. Following oxygen saturations could be statistically compared: 100-50% + 30% O₂ (**Table 4**); 60 and 40% O₂ (p<0.001); 40 and 25% O₂ (p=0.0063); 30 and 25% O₂ (p=0.04). 36

Figure 16 Limiting oxygen level curve after Claireaux & Chabot 2016. Displayed are the intercept between MMR (blue line) and a regression (dashed line) fit to individual MMR measured at ambient O₂ from 40 – 20% with the baseline SMR. Red circle marks the intercept from which a P_{crit} of 4.51 kPa (S_{crit}: 21.6% O₂) could be inferred. Yellow dashed lines mark the PO₂ range mathematically predicted as scope of survival. 37

Figure 17 Determination of P_{crit} using the R script of Claireaux & Chabot 2016. PO₂ at which mean MMR (blue line) intercepts with baseline SMR (yellow line) was determined using the five lowest mean MMR measured over the PO₂ range tested (red circles) to fit a regression. 38

Figure 18 LOL curve and P_{cmax}. This graph displays the mean MMR (blue line) and mean SMR (orange line) over decreasing oxygen saturation levels. P_{crit} is depicted as intercept between a regression fit to the individual MMR measured at ambient O₂ levels 40 - 20%. Further displayed are the intercept between MMR and SMR at 30% ambient O₂ and the P_{cmax} as the ambient oxygen saturation at which the MMR starts to decrease. P_{cmax} was visually determined to lie between 14.62 – 10.45 kPa ambient oxygen saturation (70% and 50% O₂). 38

Figure 19 Metabolic rates over increasing water velocities. Boxplots show MR measured in the swim tunnel setup. Significant differences of MR between velocities are indicated by letters. For clarity reasons only the significant differences representing the general tendency are shown. For the complete outcome of the Pairwise Wilcoxon Rank Sum Test see **Table 5**. 39

Figure 20	Gait transition speed over decreasing O₂ saturation levels. No significant difference was observed between the PO ₂ levels (n per treatment: 100%= 5, 80%=6, 70%=6, 60%=6, 50%=6, 40%=5, 30%=5, 25%=2, 20%=0).	41
Figure 21	Total number of bursts over decreasing ambient oxygen saturations. Per PO ₂ level the mean was calculated out of the total number of bursts per individual and is depicted with SE. No significant differences between the PO ₂ levels were observed.....	42
Figure 22	Relative number of burst (per min) over decreasing PO₂ levels. Per PO ₂ level the mean was calculated out of the relative number of bursts per individual and is depicted with SE. No significance between the PO ₂ treatments could be observed. n per treatment: 100%= 5, 80%=6, 70%=6, 60%=6, 50%=6, 40%=5, 30%=5, 25%=2).....	42
Figure 23	Critical swimming velocity over oxygen saturation levels. No significant difference was observed between U _{crit} at the different PO ₂ levels investigated (n per O ₂ level: 100% - 30%=6, 25%=3, 20%=2).....	43
Figure 24	Swimming activity over O₂ saturation levels. Experimental duration was divided into two different phases. Inactive time was defined as time when fish did either sit in the swim chamber or were stuck at the grid at the end of the swimming chamber. Swimming time was defined as time spent swimming plus periods when fish used the grid to push themselves forward against the water current. Both phases are displayed as the mean percentage of the complete experimental duration together with the respective SD.....	44
Figure 25	The effect of temperature on inter-species critical oxygen level (P_{crit}; black line) and intra-species P_{crit} (coloured lines). The figure is originating from Rogers et al.2016 and supplemented with data for Polar cod coming from the present study and the master’s thesis of Sarah Kempf.....	56

Tables

Table 1	P-values of Paired Wilcoxon Rank Sum Test testing for significant differences between MMR measured at different ambient oxygen levels. MR measured at all oxygen treatments were pooled and the highest 5% were excluded as outliers. Statistical analysis was performed on the highest 15% of MR values per individual taken together per PO ₂ level. Significant differences of MMR between PO ₂ levels are marked in red.	32
Table 2	P-values of the statistical comparison of AAS between ambient O₂ levels 80, 50, 40 and 25%. As data at these PO ₂ levels were normally distributed but did not show homoscedasticity a Welch-ANOVA was applied followed by a Games Howell post-hoc test. The outcome of the Games Howell post-hoc test is displayed. Significant differences of AAS between PO ₂ levels are marked in red.....	34
Table 3	P-values of the statistical comparison of AAS between ambient O₂ levels 100 – 50%. As data at these PO ₂ levels were not normally distributed but showed homoscedasticity a Kruskal Wallis test was applied followed by a Pairwise Wilcoxon rank sum test. The outcome of the Pairwise Wilcoxon rank sum test is displayed. Significant differences of AAS between PO ₂ levels are marked in red.	35
Table 4	P-values of the statistical comparison of FAS between ambient PO₂ levels 100 – 50 + 30%. As data at these PO ₂ levels were not normally distributed but showed homoscedasticity a Kruskal-Wallis test was applied followed by a Pairwise Wilcoxon rank sum test. The outcome of the Pairwise Wilcoxon rank sum test is displayed. Significant differences of FAS between PO ₂ levels are marked in red.	36
Table 5	P-values of Paired Wilcoxon Rank Sum Test testing for significant differences between MR measured at different velocity intervals. Significant differences in MR between velocity intervals are marked in red.	40
Table 6	Burst counts at different temperatures. This table shows relative burst counts (per minute) and total burst counts assessed in the present study at 10°C and by Sarah Kempf at 1.23 °C.51	
Table 7	Baseline SMR, SMR and RMR of B. saida measured at different temperatures and by different studies. Measuring and calculation method vary between studies.....	58
Table 8	Solubility of oxygen at different temperatures. Displayed is the oxygen content in sea water at 100% oxygen saturation and normal pressure (101.325 kPa). https://www.internetchemie.info/chemie-lexikon/daten/s/sauerstoffgehalt-salzwasser.php	lxxviii

List of Formulas

- (1) **Metabolic rate**..... 24
- (2) **Critical swimming speed**.....26
- (3) **Gait transition speed**.....27
- (4) **Q₁₀ value**.....46

List of Abbreviations

AAS	absolute aerobic scope
ANOVA	analysis of variance
AS	aerobic metabolic scope
ATP	adenosine triphosphate
AWI	Alfred-Wegener-Institute Helmholtz Centre for Polar and Marine Research
BL	body length
<i>B. saida</i>	<i>Boreogadus saida</i> , Polar cod
EPOC	post-exercise oxygen consumption
FAS	factorial aerobic scope
IPCC	Intergovernmental Panel on Climate change
kPa	kilopascal
LOL curve	limiting oxygen level curve
m	meters
mmol	millimole
MMR	maximum metabolic rate
MO ₂	oxygen consumption
MR	metabolic rate
O ₂	molecular oxygen
OCLTT	oxygen and capacity limited thermal tolerance
PCr	phosphocreatine
P _{cmax}	ambient partial oxygen pressure at which MMR starts to decrease
P _{crit}	critical oxygen partial pressure
PO ₂	partial pressure of oxygen
Q ₁₀	Q10 temperature coefficient
RCP	representative concentration path for greenhouse gas emissions
RMR	routine metabolic rate
rpm	rotation per minute
S _{crit}	critical ambient oxygen saturation

SD	standard deviation
SDA	specific dynamic action
SE	standard error
SMR	standard metabolic rate
T_{crit}	critical temperature
T_{opt}	optimum temperature
T_{QB}	break temperature for incremental Q_{10}
TSB	time spent bursting
U_{crit}	critical velocity
U_{gait}	gait changing velocity

Abstract

The Arctic is the region on Earth expected to experience the highest rate of warming caused by climate change. Ocean warming is directly and indirectly decreasing oxygen concentration in the ocean, therewith confronting marine biota with a change of two crucial abiotic factors. Polar cod *Boreogadus saida* is an Arctic key stone species due to its central position in the food web.

In order to contribute to a better understanding of its upper thermal limits and the synergistic effects of warming and decreasing oxygen availability on its metabolic and swimming capacity, Polar cod were acclimated to a temperature hypothesised to belong to its upper thermal limit (10°C) over 10 months. Using static and swim tunnel respirometry 10°C were found to clearly belong to the pejus temperature range of Polar cod although aerobic scope and swimming capacity were maintained at this temperature. No metabolic compensation was observed for standard metabolic rate that increased by a factor of five. A significant PO₂ effect on maximum metabolic rate and aerobic scope was observed when measuring metabolic and swimming capacity at decreasing ambient oxygen levels. Polar cod displayed oxy regulation over the whole PO₂ range tolerated. Critical velocity stayed stable until 40% ambient O₂ saturation whereas gait transition velocity decreased non-significantly at 50% O₂. Temperature had a strong negative effect on hypoxia tolerance by increasing P_{cmax} and P_{crit} to 12.53 and 5.22 kPa O₂, respectively. We observed that water masses of 10°C can be tolerated in short-term by Polar cod but do not allow for population survival. Hypoxia tolerance was found to be strongly decreased at the long-term incubation temperature but still remained high in inter-species comparison and with respect to 10°C as pejus temperature. Future research should address hypoxia tolerance of Polar cod during acute warming to understand the physiological impacts during marine heatwaves.

1 Introduction

The Arctic plays a crucial role within the climate system of our Earth (Larsen et al. 2014). At the same time, it is the region that is expected to experience the most rapid change in abiotic parameters due to climate change (Larsen et al. 2014). Changes in temperature, oxygen concentration and ice cover for example will not only impact the global climate but also the Arctic ecosystem by affecting its inhabitants (Larsen et al. 2014). As species distribution and interaction is defined by the thermal window (Pörtner and Farrell 2008; Deutsch et al. 2020), and thermal tolerance by oxygen availability and supply capacity of the organism (Pörtner 2010; Pörtner et al. 2017), knowledge about physiological limitations of species are crucial to predict possible ecosystem changes in the future Arctic.

1.1 Polar cod *Boreogadus saida* – an Arctic keystone species

The Polar cod *Boreogadus saida* (Lepechin 1774) (**Figure 1**) is the most abundant planktivorous fish species in the Arctic (Aune et al. 2021) and plays a key role in the Arctic food web (Aune et al. 2021; Drost et al. 2014; Brewster et al. 2018).

It belongs to the family Gadidae, reaches an age of about seven years and is with 40 cm maximal length a rather small species (Aune et al. 2021; Bradstreet 1986).



Figure 1 Polar cod (*Boreogadus saida*). Experimental animal with the ID 59. Caught in Billefjorden, Svalbard.

Polar cod display a circumpolar distribution (Aune et al. 2021; Majewski et al. 2016) with their southernmost distribution in the North Atlantic, specifically the Polar front in the Barents Sea, the fjords of Greenland and cold waters off Northern Labrador and Newfoundland (Drost et al. 2014). *B. saida* occupies a diverse suite of habitats throughout its geographic range (Majewski et al. 2016; Crawford et al. 2012). It is found in high abundance in a depth range of 250 - 350 m (Crawford et al. 2012) but also findings as deep as 930 m depth were reported (ADFG 1986). Although generally

described to be a pelagic species (Crawford et al. 2012), bottom trawling surveys reviewed in Majewski et al. 2016 report a numerical dominance of this species in bottom waters throughout the Beaufort Sea (Renaud et al. 2012). Also sea ice is chosen as abode by Polar cod as reported by Gradinger and Bluhm 2004 who observed Polar cod to reside as single individuals or in small groups with not more than 28 individuals within sea ice wedges. They ascribe this habitat choice to an advantage for visual predator avoidance. This diverse habitat use of Polar cod is also reflected in its thermal niche. The animals are able to tolerate temperatures close to the freezing point of seawater due to their anti-freeze glycoproteins (Gradinger and Bluhm 2004; Falk-Petersen et al. 1986; Osuga and Feeney 1978) and were caught by AWI research cruises in a temperature range of -1.8 – 0°C. Crawford et al. 2012 found Polar cod mainly residing either in the upper water layer with temperatures above 1.5°C or in deeper Atlantic water with temperatures above 0°C. A similar finding was reported by Crawford and Jorgenson 1996 who observed that Polar cod in unstratified water were present throughout the water column, experiencing temperatures between -1.3 to -0.3°C. In times of stratification however, they were exclusively found in the upper water layer, which was with temperatures above 2°C significantly warmer than the water masses beneath (-1.5°C). Within these surface waters *B. saida* encounters a thermal range of 2 – 7°C (Crawford and Jorgenson 1996; Olsen 1962) and was even reported in warmer water masses of up to 9°C (Moulton and Tarbox 1987) and 13.5°C (Craig et al. 1982). By contrast, eggs, larvae and early juveniles of Polar cod are known to depend on under-ice habitat (Bradstreet 1986; Aune et al. 2021).

Polar cod appears to have a sluggish moderately active lifestyle. Gradinger and Bluhm 2004 observed no escape response of Polar cod residing in ice crevices when divers approached the animals. Also Lønne and Gulliksen 1989 report Polar cod as moderately active choosing a hiding strategy rather than a fleeing response to avoid predation. Another behaviour hypothesised to be a strategy for the decrease of predation pressure is the formation of immense fish schools (Welch et al. 1993). Schools with a mean densities of 307 to 91 fish/m³, an estimated biomass of 20835 t and a school surface of 4.6 hectares were reported (Crawford and Jorgenson 1996). The reason for the formation of these schools is not known yet (Welch et al. 1993) but beside shelter (Welch et al. 1993) also food abundance is hypothesised as possible trigger (Crawford and Jorgenson 1996). It is clear by contrast, that these schools are prone to mass feeding events. Welch et al. 1993 could observe intense predation of Polar cod schools by primarily black-legged kittiwakes (*Rissa tridactyla*), northern fulmars (*Fulmars glacialis*), harp seals (*Phoca groenlandicus*), beluga (*Delphinapterus leucas*) and narwhals (*Monodon monoceros*). This is giving an impression of the central position of Polar cod in the food web (**Figure 2**). This fish species is an important constituent within the diet of 11 species of marine mammals, 20 species of marine birds and four species of fish (Lowry and Frost 1981), with the latter being suggested to be an underestimation by Crawford et al. 2012. Polar cod itself mainly feed on zooplankton essentially

copepod and amphipod species (Hop and Gjørseter 2013; Renaud et al. 2012) but depending on habitat and season also benthic crustaceans and fish are part of their diet (Hop and Gjørseter 2013; Aune et al. 2021). Thus, by transferring energy from primary to the tertiary trophic level, *B. saida* is playing a pivotal role in the Arctic ecosystem (Bradstreet 1986; Welch 1992; Hop and Gjørseter 2013; Aune et al. 2021). Its key role in the marine food system is furthermore a result of its high biomass, its circumpolar distribution and its nutritional value as the lipid content of the liver of Polar cod can be as high as 60 - 65% (Hop and Gjørseter 2013).

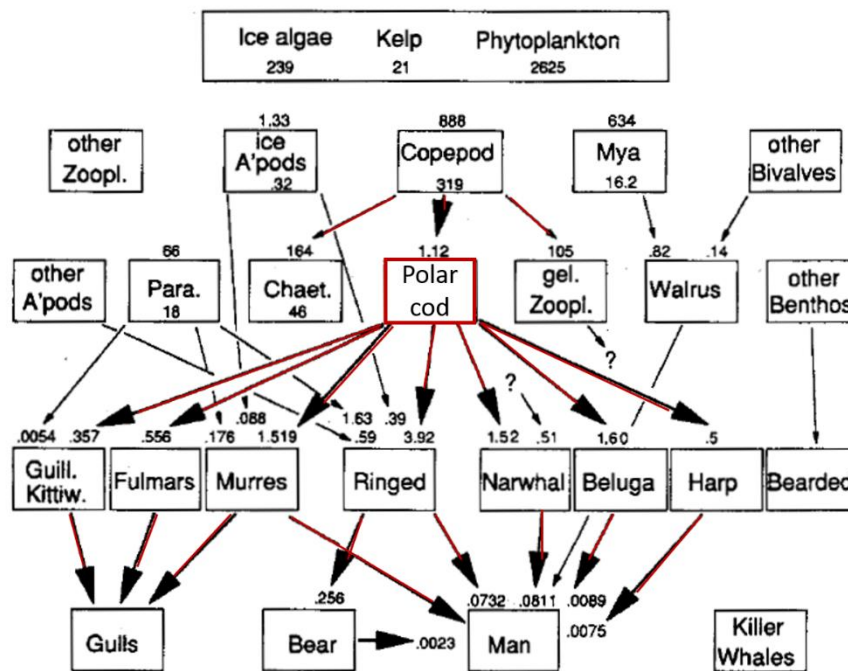


Figure 2 Position of Polar cod in the Arctic food web. This figure exemplifies the central position of Polar cod in the Arctic food web. Note that diet composition is simplified to a high degree as Polar cod feed on amphipods, benthic crustations, chaetognaths, teleosts among others (adapted after Welch 1992).

1.2 Changing Arctic – a threat to Polar cod?

The habitat of Polar cod is, however, prone to pivotal changes due to climate change. Caused by anthropogenic greenhouse gas emission the Earth experiences a global increase of temperature. The surplus of thermal energy is to more than 90% stored in the oceans causing ocean warming (IPCC 2014). Despite thermal year-to-year and decadal fluctuations, globally the temperature of the upper 75 m of the oceans experienced a clear warming trend of 0.11°C per decade between 1971 and 2010. In deeper layers this trend is less pronounced but still present with 0.04°C per decade at 200 m and less than 0.02°C per decade at 500 m depth (Rhein et al. 2013). Considering future developments until the year 2100, the representative concentration path scenarios for greenhouse gas emission RCP2.6

and RCP8.5 predict the ocean surface temperature to increase by 1°C and >3°C, respectively, relative to 1986 – 2005. Water masses in a depth of 1000 m are expected to warm by 0.5°C (RCP2.6) and 1.5°C (RCP8.5) until the end of this century, likewise (Collins et al. 2013).

The Arctic is the region on Earth that is expected to experience the highest rate of warming, a phenomenon called Polar amplification (Larsen et al. 2014, Masson-Delmotte et al. 2013, **Figure 3**). This is due to elevated temperatures of northward directed Atlantic water masses and a decrease in albedo due to sea ice loss (Masson-Delmotte et al. 2013). The increase in temperature above Arctic Sea surface until 2100 is predicted to be ~ 4 - 16°C in winter and ~1 - 5°C in summer compared to the period of 1989 – 2005 and depending on the emission scenario (IPPC 2013, Annex I, **Figure 3**). Zooming in to the study area of this thesis which is Billefjorden (78°34'59.99" N 16°27'59.99" E), a fjord at the west coast of the Svalbard archipelago (**Figure 4**), similar warming trends can be expected. In Isfjorden, which is the fjord connecting Billefjorden with the ocean, an overall warming trend of 1.9°C was observed over the period of 1912 – 2009 (Pavlov et al. 2013). This warming trend is not only caused by energy uptake at the ocean surface but also due to changes in the hydrographic dynamics of the fjords (Promińska et al. 2018). Promińska et al. 2018 report complete absence of winter cooled water in Hornsund at the southern tip of Svalbard in 2012 and a strongly decreased presence of these water mass in 2014. Therewith, Hornsund shows the same warming trend like other Svalbard fjords resulting from a increasing presence of warm Atlantic origin waters over locally formed waters (Promińska et al. 2018).

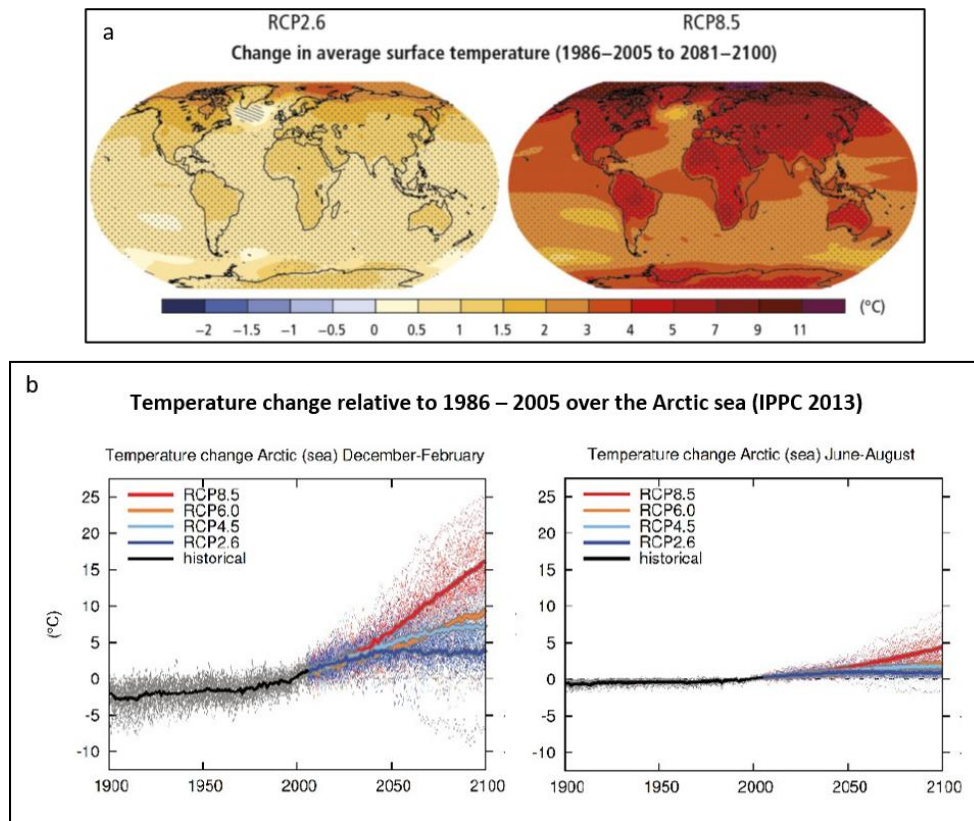


Figure 3 Temperature developments in the Arctic. **a:** Depicted is the predicted temperature increase until the period 2081 to 2100 compared to 1986 – 2005 depending on the representative concentration path scenario (RCP) for greenhouse gas emissions in different regions in the world. The Arctic region is the region expected to warm the most rapidly in a global comparison (IPCC 2014). **b:** Temperature change over the Arctic Sea surface relative to the period of 1986 – 2005 for winter (left) and summer (right). Different colours mark predicted temperature development according to the RCP (adapted after IPCC 2013, Annex I).

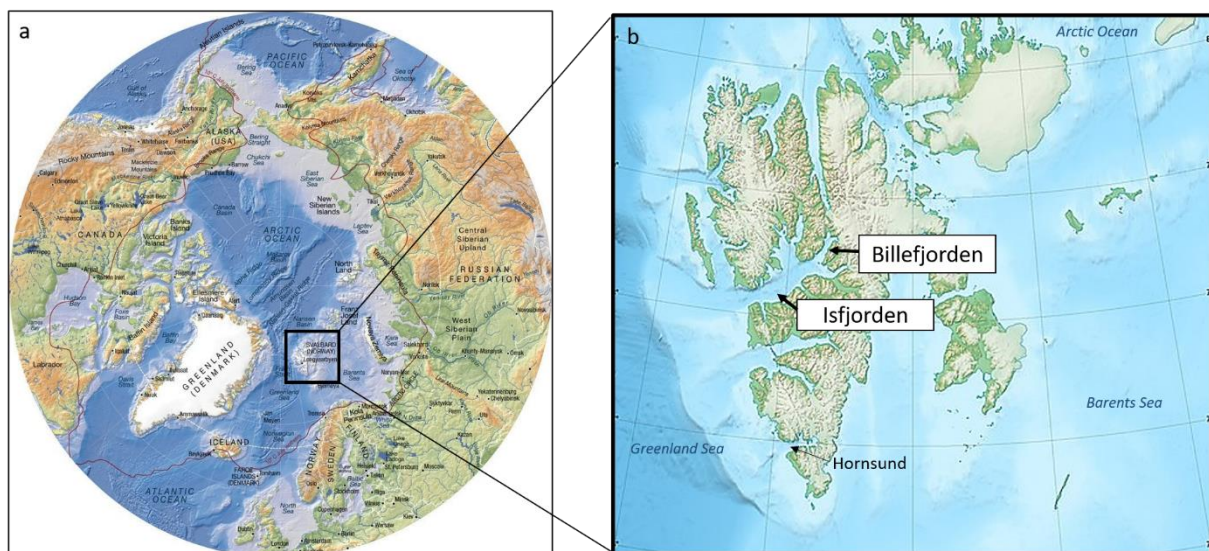


Figure 4 Study area. **a:** The Arctic comprising the area north of 60°N (Clarke 1983) (https://www.reddit.com/r/MapPorn/comments/5t7ktf/arctic_topographic_map_by_hugo_ahlenius_950x950/, 29.01.21). **b:** Svalbard archipelago with position of Billefjorden (78°34'59.99" N 16°27'59.99" E), Isfjorden and Hornsund. Billefjorden is the origin of the experimental animals used in the present study. (https://upload.wikimedia.org/wikipedia/commons/thumb/b/bd/Svalbard_relief_location_map_conic.jpg/496px-Svalbard_relief_location_map_conic.jpg, 27.06.21).

But increasing habitat temperature is not the only change Polar cod will have to face due to climate change. Another phenomenon observed is the decrease in dissolved oxygen (O₂) in the world's oceans (Breitburg et al. 2018; Keeling et al. 2010). This observation is directly linked to warming as an increase of temperature decreases oxygen solubility in the water (Breitburg et al. 2018; Keeling et al. 2010). A sea surface temperature increment of 0.2 – 3.8°C is calculated to result in a decrease of oxygen solubility of cold waters (0°C) like in the Arctic by 0.5 - 9.0% (Storch et al. 2014). But ocean warming also indirectly causes a decrease in ocean oxygen content by increasing the upper ocean stratification leading to a decreased ventilation of the interior ocean with well oxygenated water (Breitburg et al. 2018; Keeling et al. 2010). Until the year 2100 the oxygen content of the oceans is projected to fall by 1-7% depending on modulization and emission scenario (Keeling et al. 2010).

Indirect thermal effects can be expected to influence the oxygen content of the study area, likewise. As reported by Promińska et al. 2018, increasing temperatures do preclude the formation of sea ice which is normally producing dense and salty winter cooled water due to brine release during sea ice production. Due to the high density of winter cooled water, this water mass sinks to become the bottom layer within the fjords (Cottier et al. 2005) and therewith ventilates this water layer. A decrease in sea ice and winter cooled water formation can thus be expected to decrease annual replacement of winter cooled water and the replenishment of the bottom layer with oxygen. Although Polar cod feeds mainly on pelagic animals like zooplankton, in times of low zooplankton availability demersal crustaceans make up a major fraction of its diet (Aune et al. 2021). Thus, but also due to the general residing of this species in bottom waters (Majewski et al. 2016; Renaud et al. 2012) decreased ventilation of Arctic fjords and the oceans could lead to habitat loss and loss of feeding grounds for Polar cod. Also from a more general perspective decreased ambient oxygen should be seen as potential threat to *B. saida*, as fishes are among the taxa being the most sensitive towards hypoxic events suffering from negative effects on biological performances like survival, abundance, development, metabolism, growth and reproduction (Sampaio et al. 2021). The partial pressure of oxygen (PO₂) defining hypoxia is thereby species specific and describes the PO₂ that elicits stress in the organisms. Furthermore, the PO₂ level being hypoxic for a species highly depends on temperature (Keeling et al. 2010; Farrell and Richards 2009). This gives rise to the question how Polar cod will be affected when facing increased temperature and decreased oxygen availability concurrently.

When temperature increases and oxygen declines, marine organisms are directly affected. Ambient temperature decreases oxygen availability by lowering the oxygen solubility of the water (and the blood) and concurrently increases the oxygen demand of organisms due to augmented metabolic rates (Storch et al. 2014; Farrell and Richards 2009). The tight interrelation between temperature and hypoxia is not only expressed in the thermal dependence of hypoxic thresholds but also in the way that hypoxia restricts the thermal tolerance of a species (Pörtner 2010; Claireaux and Chabot 2016).

Thus, temperature and oxygen availability have strong directive, controlling and limiting effects (Fry 1947, 1971) as single parameters but especially in combination due to their synergistic workwise (McBryan et al. 2013). Therefore, these factors heavily impact the distribution and abundance of species (Pörtner 2010, 2001b; Deutsch et al. 2020). In order to be able to gauge the effect of climate change on the Arctic ecosystem it is of pivotal importance to gain knowledge about the sensitivity of key stone species like Polar cod towards warming and deoxygenation by investigating their physiological limits and responses to these parameters.

1.3 Underlying physiological concepts

By affecting their metabolism, environmental factors like temperature and oxygen availability influence an organism's activities such as locomotion, reproduction and growth (Fry 1947, 1971; Claireaux and Chabot 2016). The capacity for these activities defines species distribution and abundance (Pörtner and Farrell 2008; Deutsch et al. 2020; McBryan et al. 2013). Hence, investigating the physiological impact of temperature and oxygen scarcity helps to understand the future fate of Polar cod as key stone species in the Arctic. Therefore, this study investigated the effect of temperature and hypoxia on several metabolic parameters and an aerobic performance trait based on the physiological concepts that will be introduced in the following.

1.3.1 Aerobic metabolic scope

Most animals generate adenosine triphosphate (ATP) by oxidation of food. Thus, the oxygen consumption of an animal is reflecting its energy metabolism (Farrell and Steffensen 2005).

To infer how much energy or oxygen is available for certain performances like swimming or growth the concept of aerobic metabolic scope (AS) can be used. The aerobic metabolic scope is defined as difference between the maximum and the standard metabolic rate (**Figure 5**). The standard metabolic rate (SMR) is the minimal amount of oxygen needed to sustain life. Therefore, it refers to an animal that is neither growing, nor in a reproductive state, nor digesting or displaying locomotive activity, thus only consuming oxygen to fuel essential homeostatic activities for cells and the organism as a whole (Chabot et al. 2016). Digestion, for example, can increase the oxygen consumption over several days (Chabot et al. 2016). The difference between SMR and maximum metabolic rate during digestion is called specific dynamic action (SDA) (Farrell and Steffensen 2005). Maximum metabolic rate (MMR) by contrast is the highest rate of oxygen consumption an animal can attain under a specified set of environmental conditions (Farrell and Richards 2009). Or differently spoken the maximum rate of

oxygen consumption of a fish swimming steadily (Fry 1971). Thus, the aerobic metabolic scope (difference of MMR and SMR) represents the metabolic capacity that allows for aerobic excess activities like growth or reproduction (Fry 1947, 1971; Claireaux and Chabot 2016; Chabot et al. 2016). As an intermediate between SMR and MMR the routine metabolic rate (RMR) is defined as oxygen consumption reflecting SMR plus a certain amount of additional activity such as locomotion or digestion (Fry 1971; Chabot et al. 2016; McBryan et al. 2013).

Environmental influences on fishes' activity and performances are essentially mediated through aerobic metabolism or oxygen consumption (Chabot and Claireaux 2008). Therefore, the framework of AS is the basis for concepts describing the influence of environmental factors like temperature and oxygen availability on the aerobic metabolism of organisms.

1.3.2 Limiting oxygen level curve

The limiting oxygen level (LOL) curve is a model describing the effect of ambient oxygen availability on the AS of an animal (**Figure 5**) (Claireaux and Chabot 2016). At 100% ambient oxygen saturation the AS is maximised. With decreasing ambient oxygen saturation oxygen supply becomes limited. The PO_2 at which oxygen supply fails to cover the maximum demand for oxygen is termed P_{cmax} . Concordantly, at P_{cmax} the MMR starts to decrease (Pörtner 2010; Rogers et al. 2016). A decrease in MMR is resulting in a decline of AS and thus reduces oxygen or energy available for activities surpassing maintenance (Claireaux and Chabot 2016). At the intercept of MMR and SMR, AS is nil. Thus, oxygen supply does not allow to cover more than the maintenance costs. (Claireaux and Chabot 2016). This ambient oxygen level is called critical oxygen partial pressure (P_{crit}) or *level of no excess activity* and is an important parameter to define hypoxia tolerance (Claireaux and Chabot 2016; Rogers et al. 2016). P_{crit} expressed as ambient oxygen saturation is called S_{crit} (Claireaux et al. 2000). Although at P_{crit} short-term survival is not compromised, the ambient oxygen availability does not provide for long-term survival as there is neither capacity for foraging nor digestion. At PO_2 levels below P_{crit} SMR cannot be sustained aerobically and the fall in aerobic ATP synthesis must be compensated by anaerobic ATP production (Claireaux and Chabot 2016). However, anaerobic ATP production is restricted due to its dependence on glycogen stores, the tolerance of the organisms to metabolic end products like lactate and the organism's potential for end product removal. Therefore, the duration of hypoxia determines the survival at ambient oxygen levels below P_{crit} (Claireaux and Chabot 2016; Farrell and Richards 2009). The capacity to sustain life at PO_2 below P_{crit} defines the scope of survival (Claireaux and Chabot 2016). The intercept of MMR and RMR is also considered in this concept and termed limiting oxygen level (LOL). The LOL takes the initial metabolic rate of a fish into account that is not at SMR. As the

energy costs of a fish at RMR are higher than at SMR ambient PO_2 becomes limiting at higher levels than for a fish at SMR (Claireaux and Chabot 2016).

When fish are exposed to decreasing ambient oxygen saturations there are two main strategies to respond to that situation. One of these strategies is oxy conforming meaning that the oxygen consumption of the fish decreases with ambient oxygen saturation. The other is oxy regulation, which enables the fish to maintain stable oxygen uptake independent of ambient PO_2 (Rogers et al. 2016; Farrell and Richards 2009; Pörtner 2010). In most fishes this regulation of oxygen consumption can only be sustained over a distinct range of ambient oxygen saturations. At PO_2 lower than that range, the regulatory mechanisms like increased ventilation, cardiac output and increased gill perfusion are not sufficient anymore to regulate oxygen uptake. Thus, oxygen consumption becomes conforming with ambient oxygen availability (Rogers et al. 2016; Pörtner 2010; McBryan et al. 2013; Claireaux and Chabot 2016). These two strategies are describing the interaction between SMR and RMR with ambient PO_2 , however, and are resulting in a second definition of P_{crit} .

In a review by Rogers et al. 2016 P_{crit} marks the ambient PO_2 at which oxygen uptake at SMR and RMR cannot be maintained and leads to a transition from oxy regulating to oxy conforming. According to Rogers et al. 2016 this translates into several levels of P_{crit} . The first of these levels is P_{cmax} , the second is the level of PO_2 at which RMR cannot be sustained and declines. And the third P_{crit} is defined as PO_2 at which a decline of SMR takes place indicating an insufficient aerobic covering of maintenance costs. Of the studies reviewed by Rogers et al. 2016 84% assessed the P_{crit} of fishes as P_{crit} of RMR, which in the framework of the LOL curve is termed LOL. In this study, the critical oxygen partial pressure (P_{crit}) will be defined after Claireaux and Chabot 2016, thus as the ambient PO_2 at which AS is nil, what is similar to the third definition of P_{crit} reviewed in Rogers et al. 2016.

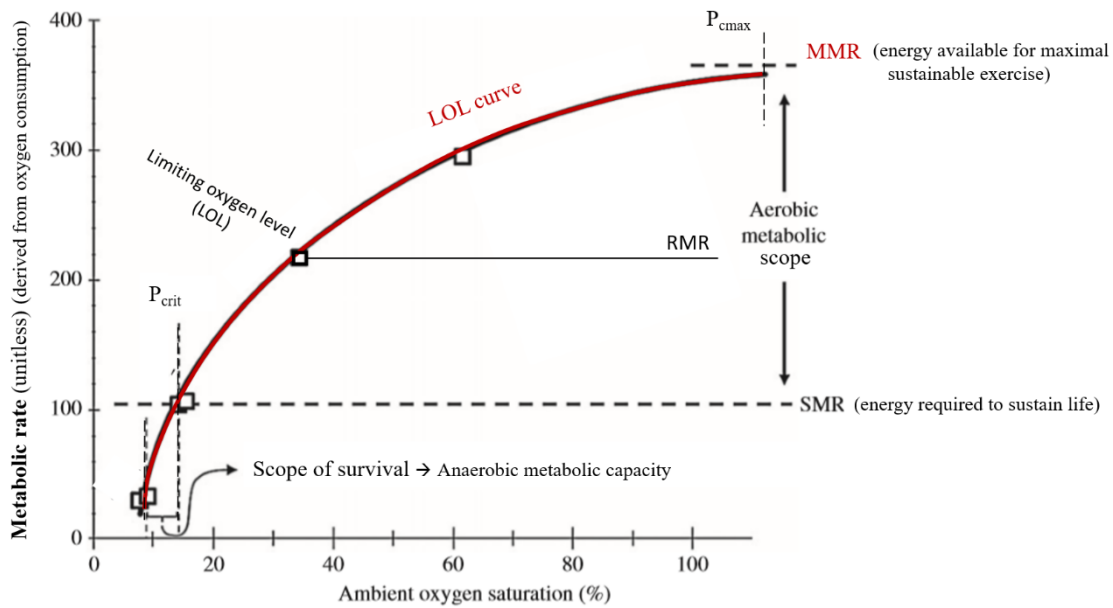


Figure 5 Model of the limiting oxygen level curve. At an oxygen saturation of 100% the aerobic metabolic scope is maximised. With decreasing ambient oxygen saturation, the limiting oxygen level curve (LOL curve, red) declines together with the MMR (red) (P_{cmax} ; in case of oxy regulation of MMR P_{cmax} can be found at lower oxygen levels than 100%). RMR and SMR can be regulated and therewith kept independent from decreasing ambient oxygen saturation until a distinct ambient oxygen level. At the intercept of MMR or LOL curve with RMR the limiting oxygen level (LOL) is reached. This results in a restriction of aerobic performances like locomotion and a shift of RMR from oxy regulation to oxy conforming. At P_{crit} the LOL curve or MMR intercepts with the SMR causing the aerobic metabolic scope to be nil. Thus, only energy for maintenance is available. Short-term survival is not compromised. At ambient oxygen saturations below P_{crit} anaerobic metabolism is required to sustain life. Survival is therefore limited (scope of survival) and defined by the duration of the hypoxic situation (modified after Claireaux and Chabot 2016).

1.3.3 Oxygen and capacity limited thermal tolerance

The concept of oxygen and capacity limited thermal tolerance (OCLTT) relates the framework of aerobic metabolic scope to temperature (**Figure 6**). It investigates the AS over the whole temperature range tolerated and explains thermal tolerance limits by an insufficient oxygen supply at the upper and lower range of the thermal window (Pörtner 2010; Pörtner et al. 2017). By investigating the magnitude of aerobic scope and aerobic performance like swimming or growth over the thermal range tolerated by a species it is possible to define key temperatures like the thermal optimum (T_{opt}) or thermal optimum window, the upper and lower pejus temperatures and the upper and lower critical temperature T_{crit} (Pörtner 2010; Pörtner et al. 2017). At T_{opt} or within the thermal optimum window AS and therewith aerobic performance are maximized (Pörtner 2010). After the thermal optimum AS and aerobic performance start to decrease, which is defining the upper pejus temperature and marking the onset of the upper thermal limit of that species (Pörtner 2010; Farrell and Steffensen 2005; Pörtner et al. 2017). The word pejus is hereby referring to the worsening of animal functioning between pejus

and critical temperature (Pörtner 2010; Farrell and Steffensen 2005; Pörtner et al. 2017). The critical temperature can be defined as temperature at which one or more vital physiological functions collapse resulting in ceasing of animal function (Pörtner 2010). The acute thermal window of a species and its capacity for thermal acclimation together form its thermal niche (Pörtner 2010).

The underlying mechanisms of the described temperature sensitivity of AS can be found in a mismatch of oxygen supply capacity of an organism and its oxygen demand. Increasing temperature accelerates biochemical and physiological processes (Farrell and Steffensen 2005) until a point where cardiorespiratory efficiency is not sufficient to cover oxygen demand (Farrell and Steffensen 2005; Pörtner 2010; Pörtner et al. 2017). This results in a decrease of aerobic scope as more and more oxygen is needed to cover increasing baseline costs (SMR) and less is available for MMR. Decreasing MMR and increasing SMR finally cause a decline in aerobic scope and therewith aerobic performance (Pörtner 2010).

As oxygen limitation can not only result from internal supply limitations but also from external oxygen availability the interaction of temperature and hypoxia can be integrated in the OCLTT-concept (Pörtner 2010). For example, the thermal reduction of oxygen affinity of haemoglobin potentially limiting oxygen uptake at the gills would be expected to increase P_{cmax} and P_{crit} (McBryan et al. 2013). With regard to the curve relating aerobic scope and aerobic performance to temperature, hypoxia would cause a narrowing of the curve, thus reducing T_{crit} (**Figure 6**). Furthermore, hypoxia is expected to lead to a reduction in aerobic scope at the optimum temperature (McBryan et al. 2013; Pörtner 2010).

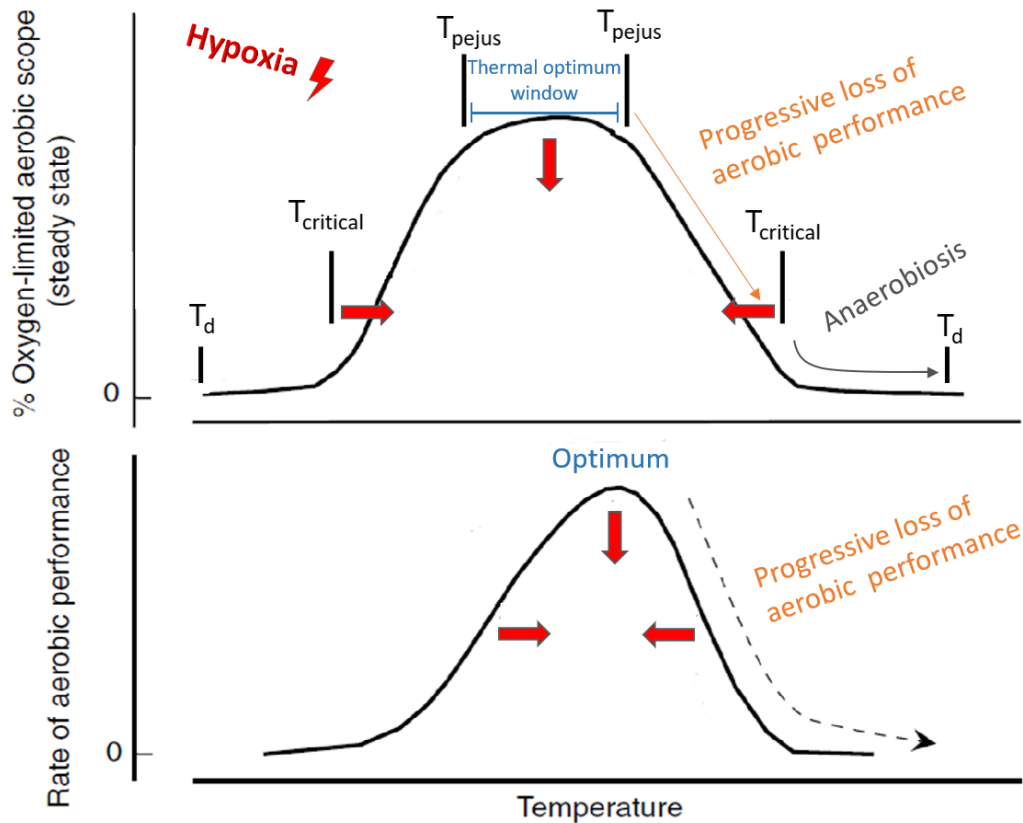


Figure 6 Conceptual model of oxygen and capacity limited thermal tolerance (OCLTT). The upper graph displays the aerobic scope in relation to temperature whereas the lower graph depicts the rate of aerobic performance like swimming or growth in relation to temperature. Furthermore, key temperatures are displayed. The thermal optimum window is situated between the lower and upper pejus temperature. In this thermal range aerobic scope and aerobic performance are at their maximum. At the pejus temperature aerobic scope starts to decrease due to a mismatch between oxygen supply and oxygen demand resulting in a decrease in the rate of aerobic performance. Increasing temperature leads to a further loss of aerobic scope and aerobic performance ultimately resulting in a loss of aerobic animal function when the critical temperature is reached. Beyond T_{crit} , oxygen supply capacity is not sufficient to fuel maintenance cost aerobically and the animal depends on anaerobic metabolism for energy production. Life beyond T_{crit} is thus temporally limited and finally leads to death (T_d). By restricting oxygen supply, hypoxia (red arrows) will lead to a narrowing of the thermal window by shifting T_{crit} and to a decrease of the aerobic scope within the thermal optimum range. Thus, hypoxia is expected to decrease performance optima (modified after Pörtner 2010).

To sum up, the concepts of aerobic metabolic scope, limiting oxygen level curve and oxygen and capacity limited thermal tolerance facilitate the explanation and investigation of interacting effects of ocean warming and deoxygenation on Polar cod. To predict distribution ranges and population sizes knowledge about key temperatures like critical temperatures and the breadth of the thermal window are essential (Pörtner 2010; Pörtner and Farrell 2008). Assessing how hypoxia will affect the thermal window of Polar cod and vice versa how higher temperatures will affect the tolerance of *B. saida* against hypoxic events or generally decreased oxygen availability is therefore crucial to predict the population development of this Arctic key species in the future Arctic Ocean.

1.4 State of the Art and resulting key research

1.4.1 Temperature

Thermal tolerance of *B. saida* has been investigated so far by assessing its thermal window and thermal acclimation potential.

In the implemented studies the acclimation potential and critical temperature regarding acute warming have been explored in a range of 0 - 8°C. They suggest a thermal optimum between 3 and 6°C and a critical temperature between 8 and 16°C. Furthermore, it could be shown that different performances like mitochondrial efficiency, growth or swimming appear to have different temperature tolerances.

The thermal window of Polar cod has been investigated in several regards. The SMR as important parameter for long term survival (Chabot et al. 2016) was investigated over a temperature range of -1.5 – 8°C including early studies and recent acclimation experiments (Holeton 1974; Steffensen et al. 1994; Hop and Graham 1995; Kunz et al. 2016; Kunz et al. 2018). Also the RMR as an approximation of SMR was investigated over a similar temperature range (1 - 6.5°C) (Drost et al. 2014; Drost et al. 2016). Noteworthy, although the definition and calculation of SMR and RMR vary between the studies, a general overview about the temperature response of *B. saida* can still be gained.

The Q_{10} value facilitates to investigate the thermal dependence or independence of a chemical reaction or physiological process (Bennett 1990). In general, it describes the change in velocity of a chemical reaction or physiological process that occurs for every 10°C change in temperature. Considering fishes, a Q_{10} value of about two indicates thermal independence and acclimation potential, whereas $Q_{10} > 2$ indicates an increasing thermal dependence of the process that cannot be regulated by the organism (Holeton 1974; Farrell and Steffensen 2005).

Schurmann and Christiansen 1994 determined the preferred temperature range of Polar cod to be 2.4 – 4.4°C by letting the animals choose out of a temperature range of 0 – 8°C using a shuttle box system. The thermal optimum for heart rate between 3.2 – 3.6°C together with a Q_{10} value of ca. 2 for heart rate until 5.5 - 8.0 °C found by Drost et al. 2014 is in accordance with the preferred temperature range. The finding of a decline in cardiorespiratory performance after a temperature of 5.4°C (Drost et al. 2016) relates to the earlier findings, likewise.

Growth experiments indicate an optimal temperature for growth close to the temperature preference of Polar cod. Kunz et al. 2016 investigated fishes originating from the west coast of Svalbard and suggest an optimal temperature for growth between 3 - 6°C. Laurel et al. 2016 and Laurel et al. 2017 investigated *B. saida* sampled in the Beaufort Sea and found growth to be near maximum at 5°C. However, growth was not significantly decreased at 9°C. When looking at different age classes Laurel

et al. 2017 could show a decrease of growth rate starting at 6.4°C for the 1 year class and at 9°C for the 0 year class. As Kunz et al. 2016 investigated animals around the age of 2 years growth optima seem to vary over the ontogenetic development. All studies investigating growth marked, however, a high growth rate at temperatures below 2°C indicating the adaptation of Polar cod to cold temperatures.

Suggested upper thermal limits for *B. saida* vary between studies. Drost et al. 2014 investigated the maximum heart rate in an acute warming experiment with fishes acclimated to 0°C. They found the maximum heart rate to be at 10.5°C and detected cardiac arrhythmia to occur at 12.5°C with the latter being suggested as the upper critical temperature. Kunz et al. 2016 by contrast suggest a long term upper thermal limit of the study species at 8°C as they found mortality only to occur at this temperature by contrast to the lower incubation temperatures which were 0, 3 and 6°C. This suggestion is supported by the fact that the mitochondrial function in cardiac muscle was observed to be decreased at 8°C due to a decreased ATP production efficiency (Leo et al. 2017) and ability for metabolic compensation disappeared at temperatures higher than 6°C (Kunz et al. 2016; Kunz et al. 2018). By contrast Laurel et al. 2016 who incubated Polar cod to 0, 5, 9 and 16°C did report mortality only for the 16°C incubation. They report that after the second week at 16°C, fishes showed severe signs of stress resulting in mortality that started to occur after 4-5 weeks. Thus, they suggest 16°C as possible long-term upper thermal limit of Polar cod. Overall, the exact definition of the upper thermal maximum of *B. saida* still requires further investigation.

The acclimation capacity of Polar cod was tested over an overall temperature range of 0 to 8°C as mentioned above. Drost et al. 2016 determined the temperature at which cardiac arrhythmia would occur in animals acclimated to 3.5 and 6.5°C. They observed that the critical temperature (T_{crit}) was increased due to the acclimation to higher temperatures reaching 15.1°C for 3.5°C acclimated animals and 18.2°C in animals acclimated to 6.5°C. Furthermore, Drost et al. 2016 showed an acclimation response of the heart rate in a temperature range from 1 – 6.5°C with a Q_{10} value of 1.7. The same study together with Kunz et al. 2018 were the first to investigate the AS of Polar cod supplemented by the investigation of swimming performance as further parameter of thermal tolerance by Kunz et al. 2018. The studies show that AS could be increased until a maximum at 6.5°C (Drost et al. 2016; Kunz et al. 2018) but was decreased at 8°C although maximum metabolic rate still inclined from 6°C to 8°C (Kunz et al. 2018). The decreased AS at 8°C can be traced back to a loss of metabolic compensation resulting in a strong increase of SMR at 8°C as mentioned above (Kunz et al. 2016; Kunz et al. 2018).

Despite the changes in AS, swimming performance measured as maximum water velocity reached until exhaustion (U_{crit}) was not affected throughout the temperature range of 0 to 8°C (Kunz et al. 2018). The maintained aerobic performance at 8°C is therewith questioning 8°C as upper thermal limit of Polar cod.

1.4.2 Hypoxia tolerance

With regard to hypoxia tolerance of *B. saida* very little is known. The only data existing to my knowledge were generated in the frame of the master's thesis of Sarah Kempf who investigated the hypoxia tolerance of *B. saida* at 2.5°C. Her investigations revealed a high hypoxia tolerance of Polar cod with a P_{crit} of 1.01 kPa PO_2 .

To my knowledge the combined effect of temperature and hypoxia on *B. saida* has never been subject of investigation before.

1.4.3 Importance of key research and its objectives

According to the state of research, it is of high importance to fill the previously described gaps of scientific knowledge by examining the hypoxia tolerance and capacity for aerobic performance of Polar cod at a potential upper thermal limit temperature.

To do so, the first objective of this study was to contribute to a better understanding about the upper thermal limit of Polar cod as inconsistencies exist between suggested upper thermal limits also with regard to the observation of this species at 9 - 13.5°C water temperature in the wild. For this purpose, Polar cod were acclimated to a temperature of 10°C over 10 months and metabolic capacities and capacity for exercise at this temperature were assessed. Thus, the first objective aims to resolve the question if 10°C can be assigned to the upper thermal limit of Polar cod. Due to reduced mitochondrial efficiency and a decrease in AS observed at 8°C, the upper thermal limit suggested between 8 and 16°C and the thermal niche of Polar cod observed in the wild I hypothesise that 10°C will be close to its upper pejus temperature (hypothesis 1).

The second objective was to assess how metabolic and swimming capacity of *B. saida* were affected by a combination of temperature and hypoxia in order to predict the influence of changing abiotic parameters on the future ecological development of this Arctic key stone species. Therefore, the metabolic and swimming capacity of the 10°C acclimated fishes were assessed under decreasing ambient oxygen saturations. As I hypothesised 10°C to lie close to the upper pejus temperature of Polar cod I expect the maximum oxygen supply capacity to decrease at high ambient PO_2 levels (P_{cmax}) leading to a restriction of swimming performance beginning at high PO_2 levels, likewise (hypothesis 2). The third objective was to investigate the temperature effect on hypoxia tolerance to evaluate to what degree a temperature of 10°C alters the hypoxia tolerance of Polar cod. Thus, the P_{crit} and anaerobic swimming capacity were assessed with the latter in order to assess the scope of survival. I hypothesised that P_{crit} will be strongly increased compared to 2.5°C but that the scope of survival will stay unaffected by temperature (hypothesis 3).

2 Materials & methods

2.1 Fish acclimation and keeping

The study animals were caught October 2018 on a research cruise with RV Heincke, Alfred Wegener Institute Helmholtz Centre for Polar and Marine Research, AWI (HE519) using a fish-lift connected to a pelagic trawl.

They were originating from Billefjorden, Svalbard (**Figure 4**) and were taken from a depth of 150 m and from a water mass with a temperature of -1.5°C and an oxygen concentration of 5.75 ml/l.

The animals were directly transported to the laboratories of the Alfred Wegener Institute (AWI) in Bremerhaven where they were stepwise ($+1.5^{\circ}\text{C}$ per month) acclimated to the experimental temperature of 10°C over seven months starting in December 2019 at a temperature of $0.0 \pm 1^{\circ}\text{C}$. As the experiments of the present study started in October 2020 the experimental animals were acclimated to a temperature of 10°C for three months before the start of the experiments. Acclimation and experimental temperatures were maintained by using thermostated rooms. Animals were fed with squid (*Loligo vulgaris*) and mussels (*Mytilus edulis*) and exposed to a diurnal cycle of 12 hours light and darkness, respectively.

In total 16 individuals were investigated which had a size of 17.5 - 22 cm with an average of 19.79 ± 1.94 (standard deviation, SD) cm. Individuals weighed 26.6 - 73.9 g with an average of 41.3 ± 10.1 g. Weight of the individuals was measured three times during the experimental period as exact weight was required for the calculation of the oxygen consumption, which was determined as $\text{mmol O}_2/\text{kg}/\text{h}$. Fish were weighed before the start of the experimental period with a mean weight of 47.39 ± 12.93 g. After the termination of the static respirometry experiments at oxygen levels 100 - 60% fish mean weight was reduced by 6.6 ± 4.25 g resulting in a mean weight of 40.8 ± 12.93 g. The last weighing was conducted after the termination of the swim tunnel experiments at 50% ambient oxygen saturation. Mean animal weight increased by 0.69 ± 3.28 g to a mean of 40.91 ± 9.31 g.

In both experimental approaches (static respirometry and swim tunnel respirometry) seven adult cod were tested ($n=7$) per ambient oxygen level. For several oxygen saturation levels, the same individuals were used (chapter 3.1) and distinguishment of individuals was obtained by implanted passive glass transponders (PIT tag, FDX-B, 7 x 1.35 mm, Loligo Systems Denmark).

2.2 Static respirometry – baseline SMR and SMR measurements

The research questions outlined in chapter 1.4.3 were investigated using two experimental approaches from which the first is static respirometry.

Static respirometry does allow for an investigation of energy metabolism under different ambient oxygen saturations by the measurement of oxygen consumption (MO_2). From those oxygen consumption measurements, the baseline standard metabolic rate (baseline SMR) and the standard metabolic rate (SMR) were calculated subsequently contributing to the assessment of the aerobic metabolic scope (AS). For more detail see chapter 2.4.2, 2.4.3 and 2.4.5.

Two reservoir tanks (170 l) (**Figure 7**) were used to maintain ambient oxygen saturation and to facilitate PO_2 reestablishment in the respiration chambers during the experiment. Each reservoir tank was separated in five compartments via impermeable plastic walls. One compartment was used to accommodate one respiration chamber. Water circulation within and between the reservoir tanks was facilitated via outlets at the end of the separating walls and U-pipes connecting the two reservoir tanks. Water circulation was furthermore supported by a circulation pump. The empty compartments were used to place the ambient circulation pump and the temperature and ambient oxygen sensor.

Tubular Perspex respiration chambers with a volume of 1800 ml were used (Loligo Systems ApS, Denmark) (**Figure 8**). Each respiration chamber was connected to a flush and recirculation pump, facilitating the following measurement cycle:

By using the intermittent flow function of the automated respirometry software, AutoResp (version 2.3.0, Loligo Systems ApS, Denmark) a measurement cycle of in total 20 min was applied. This cycle consisted of 2.5 min open mode (flush- and recirculation pump working, water was flushed in from reservoir tank) to re-establish ambient oxygen saturation in the chambers, 30 sec wait phase (only recirculation pump working) to establish a homogeneous oxygen saturation in the respiration chamber after flushing and 17 min measurement phase (only recirculation pump working, one measurement of oxygen saturation per sec). From these oxygen saturation measurements, the oxygen consumption rate of each animal was calculated using the package 'FishResp' (Morozov et al. 2019) of the statistical software R (chapter 2.4.1).

The duration of each period of the measurement cycle was established in a pre-experiment to ensure a complete re-establishment of the desired oxygen saturation in the chamber, a stable oxygen saturation after flushing and a measuring phase allowing reliable oxygen consumption measurements.

The measurement of oxygen saturation was achieved using two fully automated four chamber respirometry systems (Complete medium chamber system, Loligo Systems ApS, Denmark) which were controlled using the AutoResp software mentioned above. As one oxygen meter port was needed to measure ambient oxygen saturation seven respiration chambers could be connected to the remaining oxygen measurement ports to assess oxygen consumption of the animals. The AutoResp software also allowed to acquire the oxygen saturation and temperature data and to control the ambient oxygen saturation and the measurement cycle in the respiration chambers via a DAQ-M instrument (Loligo Systems ApS, Denmark) (**Figure 8**). The desired ambient oxygen saturation according to the respective oxygen treatment was maintained by constant gassing with compressed air and nitrogen.

As probe for oxygen saturation measurements fiber-optic mini sensors (optodes) were used, which were connected to a four-channel meter (Loligo systems ApS, Denmark, Witrox 4 oxygen meter for mini sensors). Optodes were calibrated within the experimental setup by means of a two-point calibration gassing the reservoir tank with nitrogen or oxygen resulting in 0% and 100% oxygen saturation. The calibration was conducted before the start of the experiments and repeated after the termination of the measurements at 60% O₂.

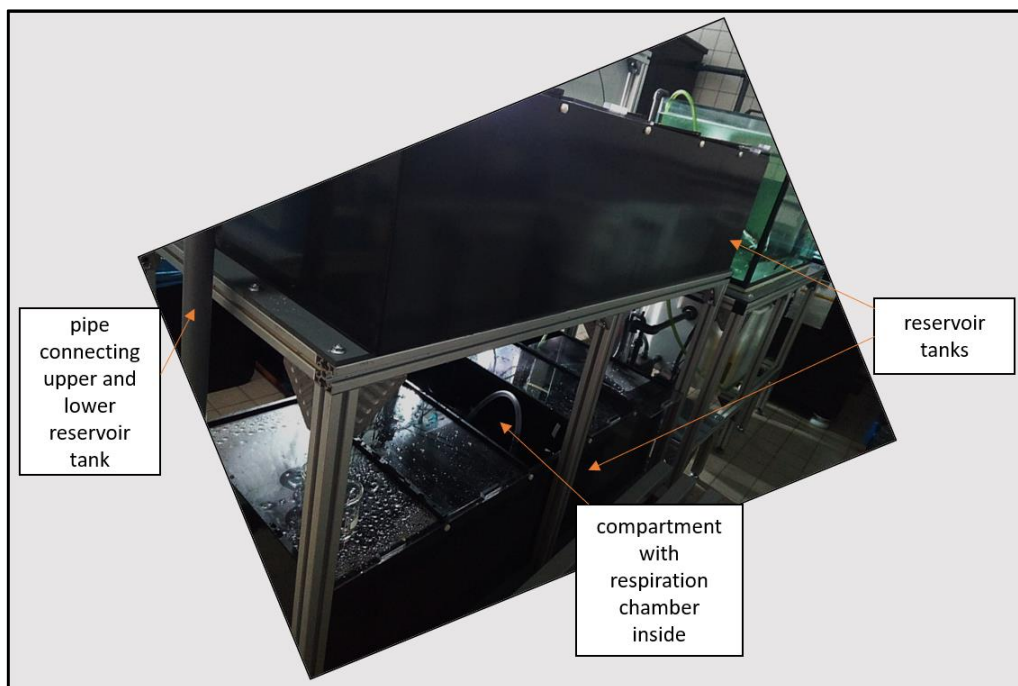


Figure 7 **Static respirometry setup - reservoir tanks.** Two reservoir tanks (black) with a volume of 170l connected via U-pipes were separated into five compartments each, with one compartment containing one respiration chamber. Compartments were closed with transparent covers to prevent evaporation. The upper reservoir tank was additionally covered with a white plastic sheet to ensure similar light conditions in both tanks. Water was gassed with nitrogen and oxygen to derive the desired oxygen saturation of the respective PO₂ level. Gassing was placed in an empty compartment not containing a respiration chamber. Ambient temperature and PO₂ were measured in the upper reservoir tank. Homogeneity of water was derived via a circulation pump circulating water within and between the two tanks. Half of the water volume was exchanged weekly. Furthermore, water was disinfected using a UV-light integrated in the circulation circle.

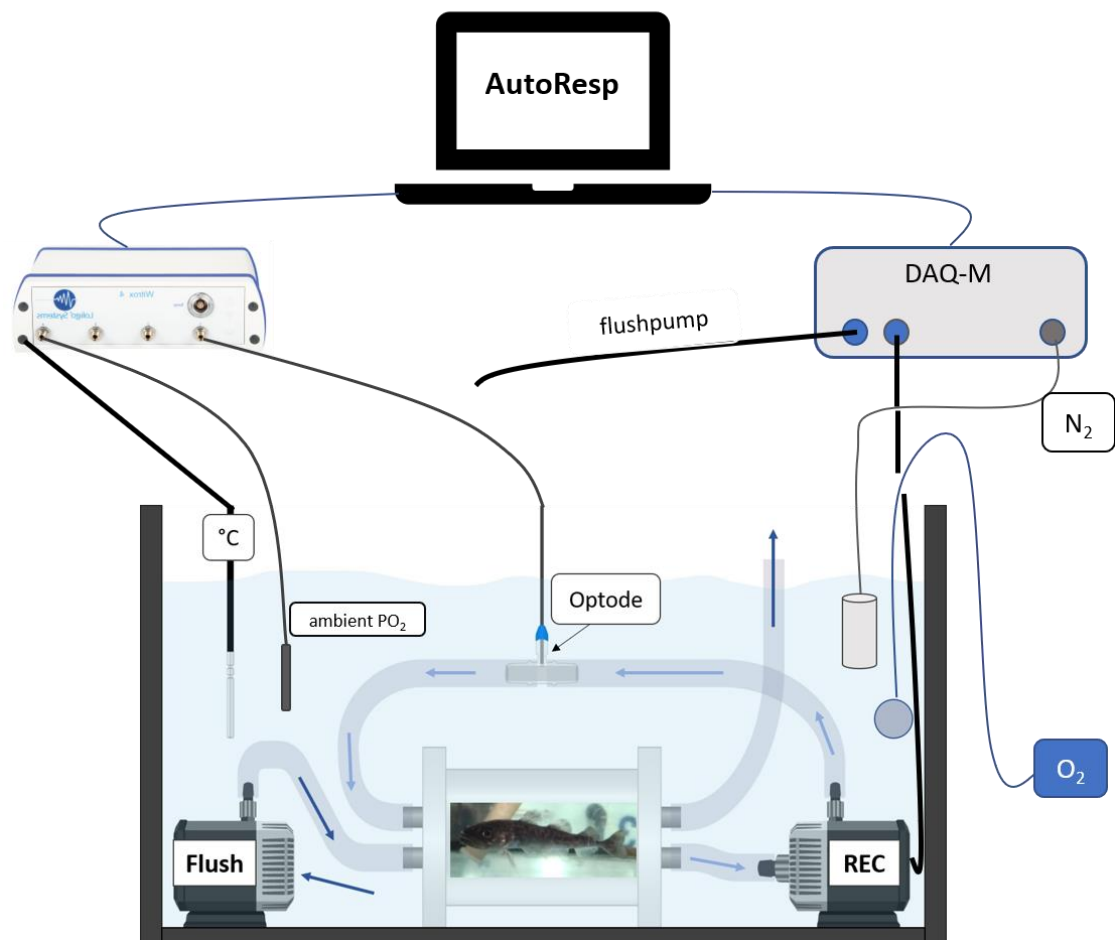


Figure 8 **Static respirometry setup – Respiration chamber placed in a compartment of the reservoir tank.** Each respiration chamber was connected to a flush- and a recirculation pump that could be controlled by the AutoResp software via a DAQ-M instrument. The flush pump introduced fresh water from the reservoir tank for 2.5 min. Excess water was removed via an outlet. After the flush pump was shut off prohibiting water renewal, water in the respiration chamber was recirculated via the recirculation pump for 17.5 min. Of these 17.5 min the first 30 sec were free from MO₂ measurements to let water homogenise. During the remaining 17 min MO₂ was measured via an optode that was integrated within the recirculation circle and connected to a four-channel meter. Ambient PO₂ and temperature were measured using a four-channel meter likewise. The desired oxygen saturation in the reservoir tanks was derived by gassing with nitrogen and oxygen. Nitrogen input was controlled by the DAQ-M instrument whereas O₂ input was set manually. Inlets of N₂ and O₂ were placed in an empty compartment and are only shown in the figure to explain the setup. Figure adapted after www.loligosystems.com.

The range of oxygen saturation levels applied was determined in a pre-experiment.

Animals were placed in the respiration chambers at 100% oxygen saturation. Subsequently flush pumps were shut off resulting in a prevention of water exchange with the reservoir tank. This situation was maintained, and oxygen saturation was measured until an animal first lost equilibrium due to low oxygen saturation in the chamber. As soon as loss of equilibrium was observed oxygen saturation in the respiration chamber was re-established by starting the flush pump and the lowest PO₂ measured was taken as a possible individual P_{crit}. No animals were lost in this experiment.

Following the output of this experiment, O₂ saturation levels were chosen to be 100, 80, 70, 60, 50, 40, 30, 25 and 20% for the static respirometry approach. Each oxygen saturation was applied for 54 h of which 24 hours were two full nights.

For the main experiment as for the pre-experiments fishes were starved for at least two and maximum four days (depending on experimental order of the individuals) to exclude increased metabolic rates due to specific dynamic action. Hop et al. 1997 reported a gut evacuation time from repletion of average 51 hours in a temperature range of -1.5 to -0.5 °C. With regard to the higher experimental temperature of this study a starvation time of 46 h was assumed to be sufficient and was also applied by Drost et al. 2016 who investigated metabolism of Polar cod at 6.5°C.

Animals were caught with a net and transferred in the respiration chambers so that one chamber contained one individual.

Measurements at 100, 80 and 70% oxygen saturation were taken with a break of 4 days in between for which animals were transferred in the collection tank. Measurements at 60, 40 and 25% O₂ saturation were taken directly subsequent to the 70, 50 and 30% O₂ saturation levels, respectively.

The MO₂ measurements at the 50 -25% O₂ saturation levels were taken separately by Dr. Felix Mark 12 weeks after the first row of experiments (levels 100-60% O₂). The temporal break between measurements at 40% and 30% O₂ lasted 2 days.

The respiration chambers were cleaned weekly by taking them out of the experimental setup, rinsing and wiping them out with tap water and setting them up to dry for two days.

All experiments were conducted under dusky light conditions intending to provoke a relaxed condition in the animals with a minimum of locomotory activity.

2.3 Swimming performance and MMR measurements

The second experimental approach used was swim tunnel respirometry, an approach facilitating to evaluate the metabolic rate during exercise and the swimming performance of *B. saida*. Applying a critical swimming speed (U_{crit}) protocol (Brett 1964), oxygen consumption during exercise was provoked to maximise. From these MO₂ measurements maximum metabolic rate (MMR) could be derived (chapter 2.4.4). Via the documentation of the fish's swimming mode the switch from exceptional aerobic to partly anaerobic metabolism was assessed. This is based on the knowledge that an even swimming mode is facilitated by slow muscle contractions, which are aerobically fuelled by red muscles (Johnston 1977; Lurman et al. 2007). Tail kicks so called bursts, displayed for example during escape reactions, do require fast muscle contractions and are powered by white muscles, which

are using anaerobic pathways for energy production (Johnston 1977; Jayne and Lauder 1994; Beamish 1978).

Following the possible P_{crit} of 5.43 – 4.09 kPa O_2 (26 -19.6% O_2) derived in the pre-experiment described in chapter 2.2 the oxygen saturation levels were chosen to be 100, 80, 70, 60, 50, 40, 30, 25, 20% for the swim tunnel experiment.

A Brett-type swim tunnel respirometer of 5l (30 x 7,5 x 7,5 cm, Loligo Systems ApS, Denmark) was used, which was placed in a reservoir tank to ensure constant temperature and oxygen saturation (**Figure 9**). Ambient oxygen saturation and oxygen saturation in the swim tunnel were measured using fibre optic mini sensors (optodes) which were connected to a four-channel oxygen meter (Loligo systems ApS, Denmark, Witrox 4 oxygen meter for mini sensors). This device also allowed to measure the temperature in the swim tunnel. The desired oxygen saturation of the respective O_2 level was controlled by the AutoResp software via a DAQ-M instrument (Loligo Systems ApS, Denmark) and was achieved by constant gassing with air and nitrogen. The installation of an additional circulation pump in the reservoir tank facilitated to homogenise oxygen saturation within the tank.

Water velocity was set in the AutoResp software and steered via the DAQ-M instrument and a control unit regulating the engine that drove a propeller within the swim tunnel (Loligo Systems ApS, Denmark) (**Figure 9**). The engine speed was calibrated against velocity of the water by using a water flow sensor. The measurement cycle also controlled by the AutoResp software via a DAQ-M instrument had a total duration of 11 min and was composed of 1.5 min flushing period, 2.2 min waiting period and 7.3 min measuring period (for further detail see chapter 2.2). The duration of the respective periods was established in a pre-experiment for reasons described in chapter 2.2.

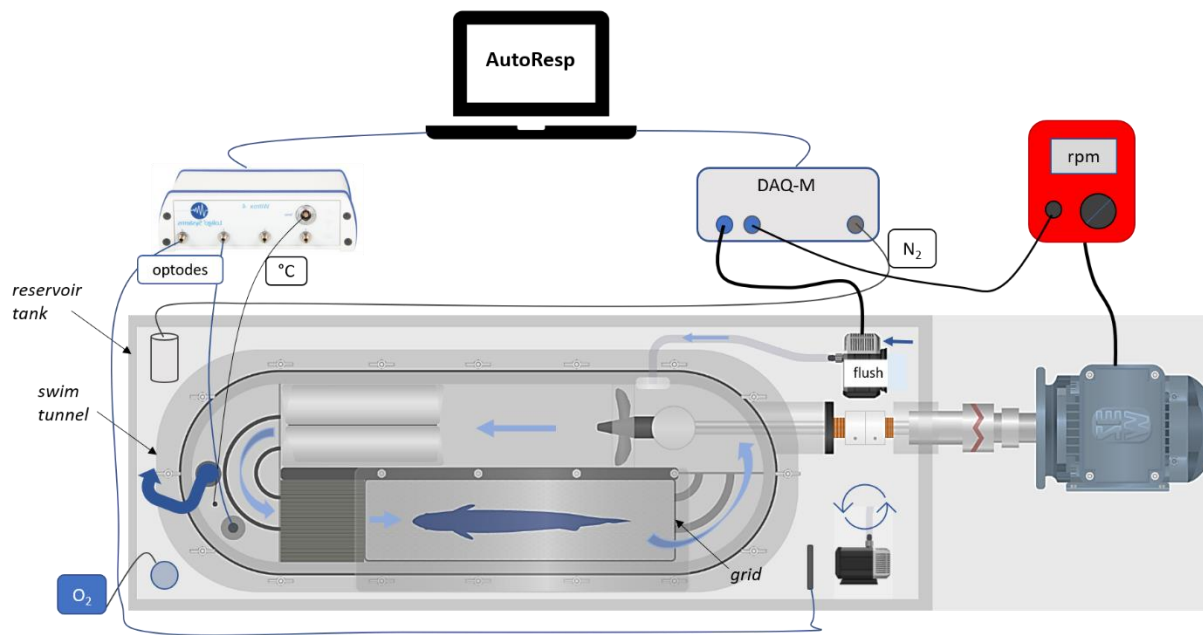


Figure 9 Swim tunnel setup. The swim tunnel was placed in a reservoir tank and connected to a flush pump that facilitated water renewal. Excess water was released through an outlet leading into the reservoir tank. During the measurement cycle the flush pump was working for 2.5 min to re-establish O₂ saturation in the tunnel. During the wait and measuring phase, the flush pump was shut off and water was circulated via the propeller producing a water current. The propeller was driven by an external motor that was adjusted via a control unit (red), the DAQ-M instrument and the AutoResp software. The velocity could be programmed to increase automatically every 11 min concurrently with the new beginning of the measurement cycle. MO₂ and temperature within the tunnel and ambient O₂ saturation were measured via a four-channel meter using optodes and a temperature sensor. The water of the reservoir tank was gassed with N₂ and O₂ to derive the desired ambient O₂ saturation. The amount of N₂ was set in the AutoResp software and controlled by the DAQ-M instrument. An additional circulation pump in the reservoir tank ensured homogenisation of water within the tank. The fish was placed in the swimming chamber of the swim tunnel in which the water entered through a honey-comb-like structure to create an even water current and left the chamber through a grid. Resting at the grid for three minutes was taken as termination of the experiment. Figure adapted after <https://swimtunnel.com/home/>.

Fish were starved for at least two and maximum four days before the experiment (chapter 2.2). They were caught and transferred to the swim tunnel with a plastic bag precluding air exposure with the intention to reduce handling stress. A white plastic cover placed on the reservoir tank was used to minimize effects of disturbance and light condition was dimmed to mimic a light regime corresponding to the habitat.

An acclimation period of in total two hours was applied before the start of the U_{crit} protocol. The acclimation period started with 30 min without water flow, followed by a pre-conditioning to a water velocity of 1.2 BL (body length) per sec for 1 h and 25 min and was terminated with a velocity of 1.4 BL/sec for 5 min. Subsequently to the acclimation period the U_{crit} protocol began at a velocity of 1.4 BL/sec. The velocity was increased by 0.15 BL/sec every 11 min, concurrently with the start of a new measurement cycle. The velocity was increased stepwise, until the fish refused to swim for three minutes. This definition of the termination of the experiment was chosen to ensure that *B. saida* as a

sluggish species achieved a state according to exhaustion. After the fish displayed the defined state of exhaustion the water velocity was immediately decreased to 1.4 BL/sec for another 10 min to give the animal the possibility to recover before it was transferred back to the collection tank.

In order to assess the swimming performance burst behaviour was documented during the entire U_{crit} protocol by counting all burst displayed during the experiment and noting the time of occurrence. U_{crit} as well as the gait-transition speed (U_{gait}) were determined as described in chapter 2.4.8 and 2.4.9.

Per day one to two experiments were conducted allowing to investigate a maximum of 2 animals. The swim tunnel was cleaned at the end of the day by removing all loose parts from the tunnel and by flushing and wiping the tunnel and the loose parts with tap water. Water of the whole system was exchanged, and the loose parts returned to the experimental setup.

2.4 Data handling

2.4.1 Oxygen consumption

The oxygen consumption and therewith the metabolic rates (MO_2) were calculated from oxygen saturation measurements using the R package “FishResp”. The calculation was based on the following equation (Morozov et al. 2019):

$$MO_2 = (\Delta PO_2 \cdot \Delta t^{-1} \cdot (V - d \cdot M)) \cdot M^{-1} \quad (1)$$

were ΔPO_2 is the change in water PO_2 (kPa), V is the volume of the respirometer (l), d is the density of an animal body (1000 kg/m^3), M is the mass of the fish (kg) and Δt is the elapsed time (h).

The bacterial respiration in the respiration chambers was measured over 15 h and accounted for 1.56% of the fish’s respiration. Thus, data were corrected for this background respiration using the “post.test method” of the “FishResp” package in R.

In the swim tunnel bacterial respiration was measured over five measuring circles and accounted for less than 1% of the fish’s respiration. Therefore, data were not corrected for background respiration.

2.4.2 Baseline standard metabolic rate

To ensure that the animals were in a relaxed condition facilitating the measurement of an oxygen consumption representing SMR, the first 36 hours in the respiration chamber were taken as acclimation period. Thus, only the second night (19:00 – 07:00 h) of the experiment was used for SMR calculation. By visual analysis it was assured that MO_2 had stabilized after the defined acclimation period (Drost et al. 2016).

The calculation of the baseline SMR was done after Chabot et al. 2016 in R, using the package “Mclust”. As stable metabolic rates of the fish were found at oxygen levels 100, 80, 70 and 60%, only the MO_2 measured during these experiments was used. The data of the mentioned ambient oxygen saturations were pooled and the lowest 5% were discarded as outliers. The mean value of the remaining lowest 15% was determined and taken as baseline SMR.

2.4.3 Standard metabolic rate

To ensure that the animals were in a relaxed condition the first 36 hours of the experiment were taken as acclimation period. Thus, only MO_2 measurements during the second night of the experiment were used to calculate the SMR. By visual analysis it was assured that MO_2 had stabilized after the defined acclimation period.

The SMR was determined per O_2 level and calculated in R, using the package “Mclust”. From approximately 50 metabolic rates per fish the lowest 5% of metabolic rates of each individual were discarded as outliers. Then, the mean value of the remaining lowest 15% of each fish was calculated and taken as SMR of the respective individual. The SMR per O_2 level was derived building the mean out of the individual SMR of the respective PO_2 level. SD was calculated for each oxygen level, likewise. The general tendency of the SMR over decreasing ambient oxygen levels (**Figure 11**) was visualised using a polynomial regression model. The model was created in R by means of the spline function of the ggplot2 package allowing for a number of three splines.

2.4.4 Maximum metabolic rate

Due to the restricted swimming time of maximum 2.5 hours, the number of measuring points per fish (between 1 and 15 individual metabolic rates) was too small to calculate the mean value of the highest 15% for each fish after the removal of the highest 5% as outliers. Therefore, the data of all oxygen levels were pooled and from these pooled data the highest 5% were discarded. Subsequently, the individual MMR of each fish per oxygen level was determined by calculating the mean of the highest 15% metabolic rates of each individual. If 15% of the metabolic rates was accounting for less than one data point, one metabolic rate was included nevertheless to ensure the representation of each individual tested. The MMR per O₂ level was derived building the mean out of the individual MMR measured at a PO₂ level. SD was calculated for each oxygen level, likewise.

The general tendency of the MMR over decreasing ambient oxygen levels (**Figure 12**) was visualised using a polynomial regression model. The model was created in R by means of the spline function of the ggplot2 package allowing for a number of three splines.

2.4.5 Absolute aerobic scope

The absolute aerobic scope (AAS) is defined as:

$$\text{AAS} = \text{MMR} - \text{SMR}$$

As individuals tested changed over the different O₂ levels (see chapter 2.2 and 3.1) the SMR (chapter 2.4.3) and MMR (chapter 2.4.4) were arranged in all possible combinations per O₂ level. The differences between the newly paired SMR and MMR within one oxygen saturation level were calculated and a SD was determined. Due to interindividual variability calculated differences occurred to be in negative range. Negative differences were excluded resulting in a varying number of individual AAS per treatment from which the mean AAS was derived (100%: 47, 80%: 48, 70%: 37, 60%: 47, 50%: 44, 40%: 34, 30%: 22, 25%: 9 individual AAS).

2.4.6 Factorial aerobic scope

The factorial aerobic scope (FAS) is defined as quotient between MMR and SMR:

$$\text{FAS} = \text{MMR}/\text{SMR}$$

FAS was calculated from all possible combinations of MMR and SMR per O₂ level (see chapter 2.4.5).

2.4.7 LOL curve and P_{crit}

A LOL curve was produced by plotting the mean MMR and baseline SMR over decreasing oxygen levels and determining the intercept of MMR and baseline SMR as P_{crit} (Claireaux and Chabot 2016).

For the exact determination of P_{crit} two different approaches were applied. The first approach allowed to determine the intercept of the baseline SMR with a regression that was fit to the five lowest mean MMR measured over the PO_2 range tested (R script published by Claireaux and Chabot 2016). In the second approach the intercept of MMR with baseline SMR was determined by fitting a regression to the individual MMR calculated for oxygen saturation levels 40 – 20%.

Furthermore, the intercept between MMR and SMR within the LOL curve was assessed.

2.4.8 Critical swimming speed

The critical swimming speed (U_{crit}) was calculated according to Brett (1964):

$$U_{crit} = U_{max} + \frac{vT}{t} \quad (2)$$

where U_{max} is the highest velocity maintained over a complete time interval (t), T is the time spent in the last velocity interval until exhaustion of the fish and v is the velocity increment per velocity interval.

To ensure that a state according to exhaustion was arrived during the swimming exercise three minutes of swimming refusal were chosen as the end of the experiment (chapter 2.3). Since individuals showed a wide range of swimming performance and thus the development of exhaustion differed, the point of termination of the experiment was adjusted in retrospect to prevent overestimation of U_{crit} . For this purpose, the following procedure was applied: Animals that did not show sustained swimming over a minimum of three minutes were excluded from the determination of U_{crit} . For all other individuals each rest at the grid at the end of the swimming chamber lasting minimum one minute was investigated as possible end. If no sustained swimming lasting at least three minutes was following the rest, the rest was taken as the end of the experiment. If the fish showed ongoing swimming for a minimum of three minutes following the rest, the next break of one minute was investigated until a rest was found after which no sustained swimming of at least three minutes could be observed.

2.4.9 Gait transition speed

The gait transition speed (U_{gait}) was adjusted as:

$$U_{\text{gait}} = U_{\text{max}} + \frac{vT}{t} \quad (3)$$

with U_{max} as the highest velocity maintained for a complete time interval (t) without bursting, T as time spent in the velocity interval provoking the first bursting until the first burst event and v as the velocity increment per velocity interval.

Due to the uneven swimming behaviour of Polar cod in the swim tunnel U_{gait} was adjusted in retrospect by refusing all bursts that did not accumulate to at least five bursts per minute.

2.4.10 Evaluation of burst activity

To evaluate the burst capacity of *B. saida* the total and relative number of bursts of each individual were assessed.

For the assessment of the total number of bursts only bursts were considered that occurred during the adjusted experimental time (chapter 2.4.8) and that were also considered for the calculation of U_{gait} (chapter 2.4.9).

The relative number of bursts was determined by setting the total number of bursts in relation to time. Therefore, the time spent bursting (TSB) was calculated as the time between U_{gait} and U_{crit} minus the time spent inactive during the experiment. Subsequently, the number of bursts per minute TSB was calculated.

From the individual total and relative numbers of bursts the mean number of total and relative bursts per O_2 level was calculated.

2.4.11 Statistical analysis

The data were tested for normal distribution and homoscedasticity using the Shapiro-Wilk test and the Levene test, respectively. In case of missing normal distribution or homoscedasticity data were logarithmized and tested again. MMR, SMR, U_{gait} , total and relative burst counts and swimming time were analysed for statistical differences between O_2 levels using a Kruskal-Wallis test followed by a Wilcoxon test. Also differences between metabolic rates at different velocities in the swim tunnel experiments were analysed using the mentioned statistical methods. Possible differences of U_{crit} between O_2 levels was evaluated using a one-way ANOVA with Tukey's test as post-hoc test.

As data of the AAS and FAS did neither show normal distribution nor homoscedasticity not all PO₂ groups were compared in once but groups of normal distributed treatments or treatments with equal variances were built and investigated using either the parametric or non-parametric tests mentioned (for further detail see chapter 3.2.4). The level of statistical significance was set at $p < 0.05$ for all statistical tests. Statistical analysis was performed in R 3.6.1.

3 Results

3.1 Mortality

For the measurements of baseline SMR and SMR (static respirometry) at 80% and 50% O₂ saturation one and six fishes had to be replaced, respectively due to fin rot and medical treatment. One and two further individuals died from suffocation during the measurements at 30% and 25% oxygen saturation, respectively (chapter 3.2.2).

During the swim tunnel approach fin rot and medical treatment caused the replacement of five fish for the measurements at 30% O₂. One further individual died at the end of the two-hour acclimation period in the swim tunnel at an oxygen saturation of $20.37 \pm 0.7\%$ O₂.

In total 7 individuals died from fin rot and medical treatment. Four further fish suffocated during the experiments.

3.2 Respiration measurements

The mean temperature the fish experienced during the swim tunnel experiments was 9.9 ± 0.33 °C. The temperature in the static respirometry set up was higher with an average of 11.7 ± 0.52 °C.

3.2.1 Baseline standard metabolic rate

The baseline SMR was measured by static respirometry and calculated after Chabot et al. 2016. Animals were placed into the respiration chambers for at least 36h and only oxygen readings from the second night after introduction were used for the assessment of metabolic rates (MR). MR measured over an PO₂ range of 100 to 60% were pooled and the mean of the lowest 15% after discarding the lowest 5% as outliers was taken as the baseline SMR of *B. saida*. MR used for the calculation were derived from 8 individuals. The calculated baseline SMR of Polar cod accounted for 2.12 mmol O₂/kg/h (**Figure 10**).

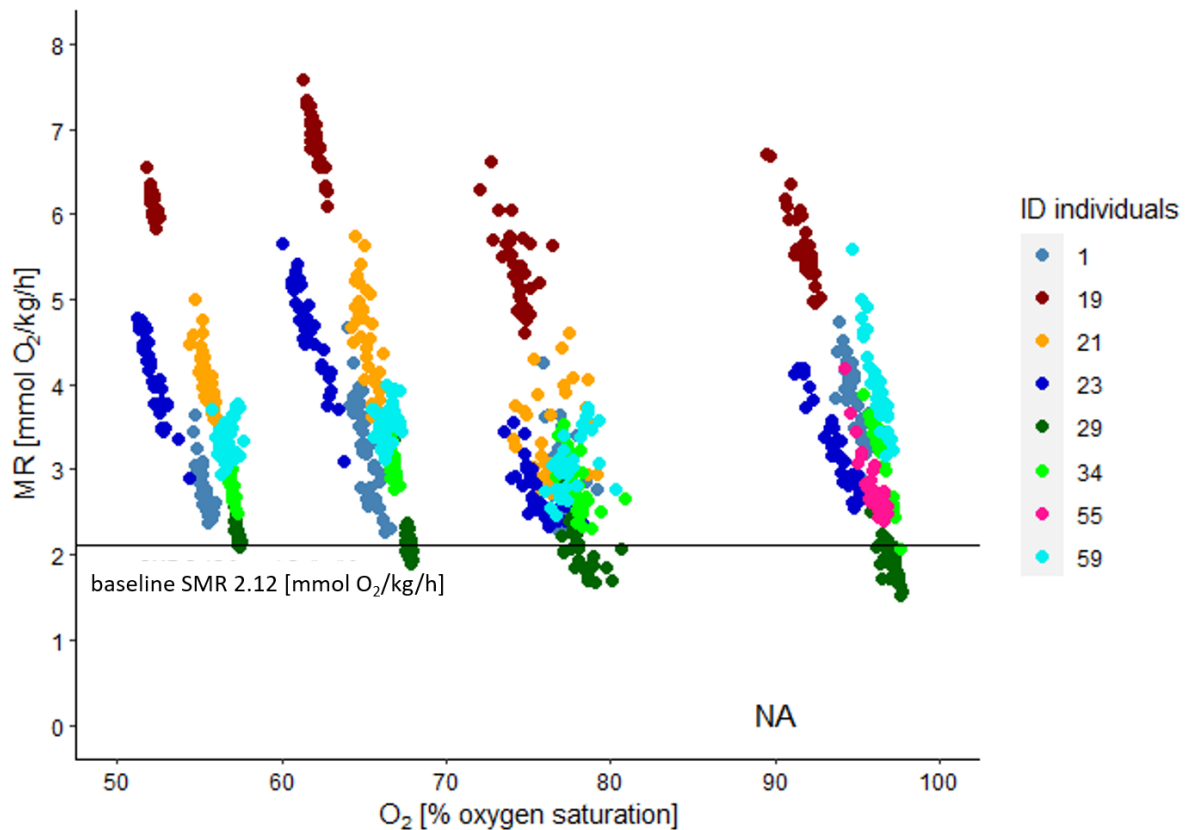


Figure 10 Baseline standard metabolic rate. Dots show metabolic rates (MR) of the individuals tested in mmol O₂/kg/h over the PO₂ range used for the calculation of the baseline SMR (treatments 100 – 60%). Black line depicts baseline SMR (2.12 mmol O₂/kg/h), which was calculated after Chabot et al. 2016 as described in chapter 2.4.2.

3.2.2 Standard metabolic rate

SMR (**Figure 11**) was assessed using the metabolic rates measured during the second night in the static respirometry approach (see chapter 2.4.3). Statistical analysis was performed on the individual SMR pooled per treatment. The Kruskal-Wallis Test, chosen due to missing normal distribution of values and logarithmical values, did not reveal a PO₂ effect on SMR.

Nevertheless, a non-significant increase of the SMR could be observed between the 100% (SMR: 2.7 ± 1.12 mmol O₂/kg/h) and 40% (SMR: 3.88 ± 0.99 mmol O₂/kg/h) oxygen saturation level followed by a non-significant decrease or levelling off of SMR from 40% to 25% (SMR: 2.54 ± 0.89 mmol O₂/kg/h) O₂. The lowest SMR observed occurred at the lowest PO₂ treatment applied (25% O₂: 2.54 ± 0.89 mmol O₂/kg/h).

Due to mortality of two individuals during the MO₂ measurements at 25% after about one hour at an average oxygen saturation of $27.41 \pm 4.18\%$ the experiment was prematurely terminated. Thus, SMR for the 25% oxygen saturation level had to be calculated from five instead of seven individuals and 18 metabolic rates per individual instead of approx. 50 metabolic rates. No MO₂ measurements at an

oxygen saturation of 20% was implemented. As the ambient oxygen saturations during the 25% measurement did scatter and partly covered 20% ambient oxygen saturation, MR measured at 20 + 2.5% O₂ were excluded from the calculation of the SMR at 25% O₂, pooled and used to calculate the SMR at 20% ambient oxygen saturation.

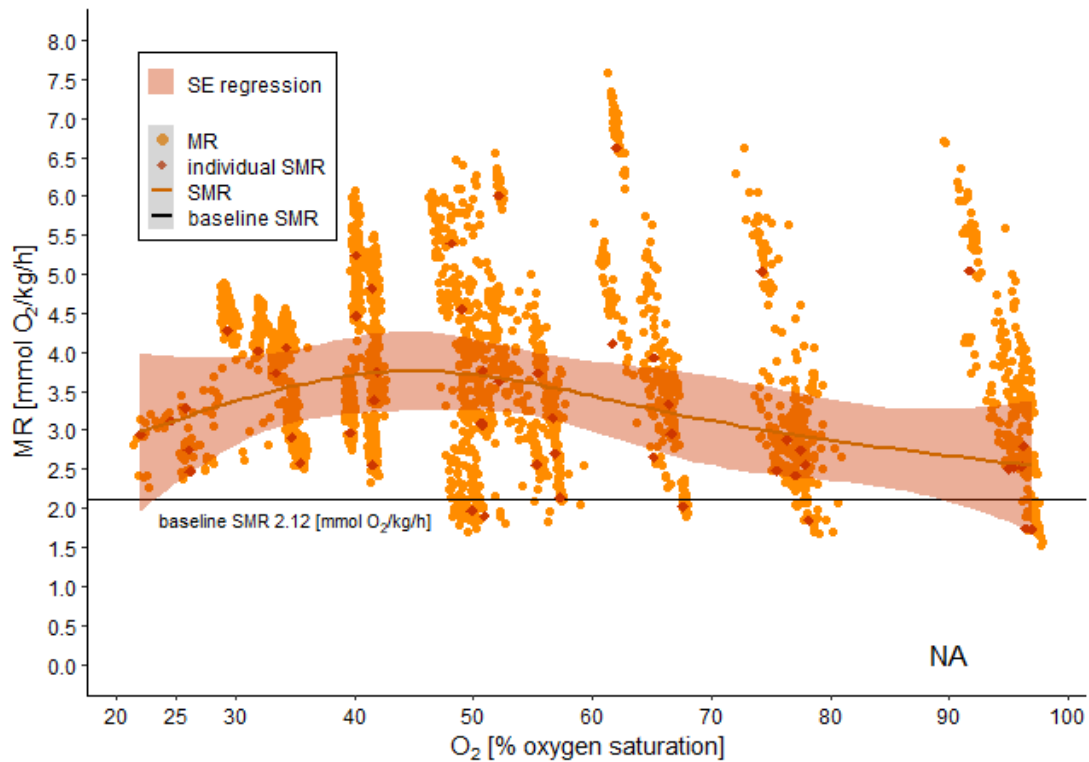


Figure 11 Standard metabolic rate over decreasing O₂ saturations displayed by a polynomial regression model. Orange line shows the general tendency of SMR over ambient O₂ saturations, orange shaded area indicates standard error (SE) of the regression model. Orange dots show metabolic rates measured at the O₂ levels. Dark orange rhombs depict individual SMR calculated at each oxygen level.

3.2.3 Maximum metabolic rate

MMR was calculated from MO₂ measurements during a U_{crit} protocol in the swim tunnel approach (**Figure 12**). Due to loss of equilibrium during the two-hour acclimation time sample size decreased from seven to four for the 25% and 20% O₂ saturation levels, respectively. One fish died at the 20% PO₂ treatment at the end of the acclimation period.

Considering MMR, a significant PO₂ effect was observed ($p < 0.0001$). For p -values between oxygen saturation levels see **Table 1**. MMR stayed relatively stable in an O₂ range between 100 and 70% (max: 6.71 ± 1.76 mmol O₂/kg/h, min: 6.47 ± 1.87 mmol O₂/kg/h) but decreased non-significantly by about 1 mmol O₂/kg/h between 70 and 50% O₂ (max: 6.71 ± 1.76 mmol O₂/kg/h, min: 5.73 ± 1.38 mmol O₂/kg/h). Thus, the P_{cmax} is defined to lie between the 70 and 50% oxygen saturation level and accounts

for 14.62 – 10.45 kPa O₂. MMR measured at 30, 25 and 20% O₂ was significantly lower than at treatments 50% to 100% O₂. Beginning at 40% ambient oxygen MMR displayed a linear decline. MMR equalled SMR at 21.6% ambient O₂ saturation.

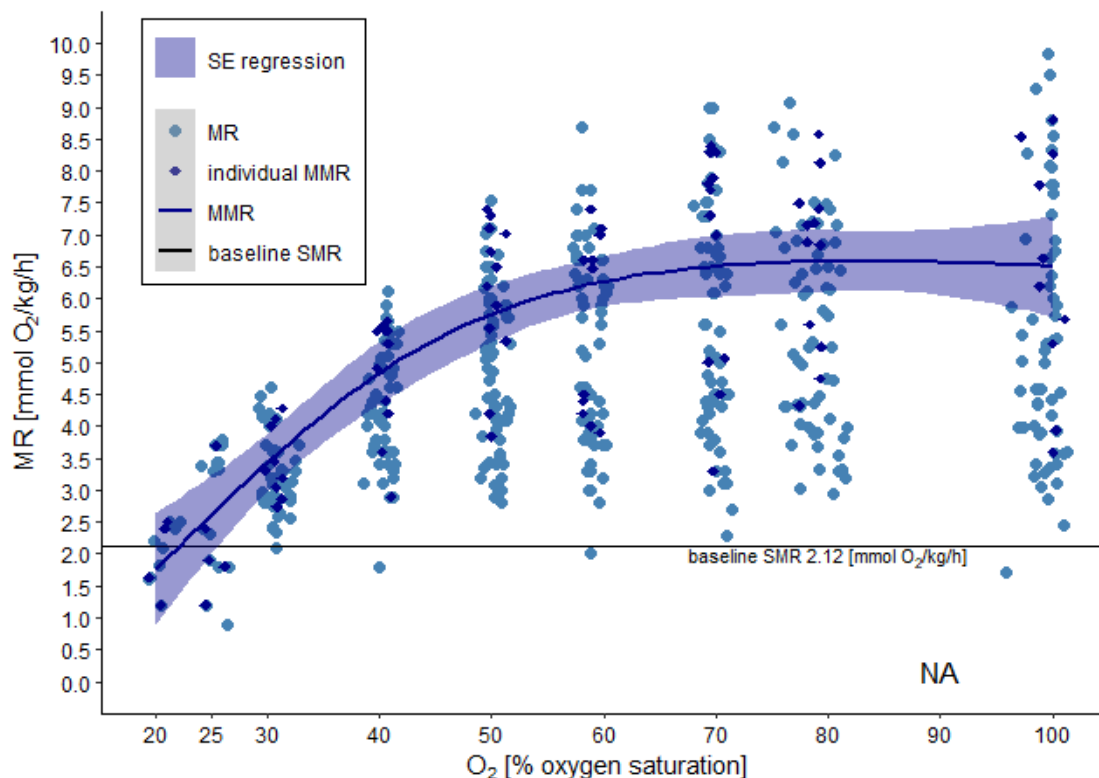


Figure 12 Maximum metabolic rate over decreasing O₂ saturations displayed as polynomial regression model. Blue line shows general tendency of MMR over ambient O₂ saturation levels. Blue shaded area indicates SE of the regression model. Blue dots show metabolic rates measured at the O₂ saturation levels. Dark blue rhombs depict individual MMR calculated at each PO₂ level.

Table 1 P-values of Paired Wilcoxon Rank Sum Test testing for significant differences between MMR measured at different ambient oxygen levels. MR measured at all oxygen treatments were pooled and the highest 5% were excluded as outliers. Statistical analysis was performed on the highest 15% of MR values per individual taken together per PO₂ level. Significant differences of MMR between PO₂ levels are marked in red.

O ₂ level saturation [%]	20	25	30	40	50	60	70	80
25	1.0000							
30	0.1007	1.0000						
40	0.1524	0.2018	0.1774					
50	0.0303	0.0027	0.0017	0.1533				
60	0.1534	0.0311	0.0296	1.0000	1.0000			
70	0.1565	0.0610	0.0203	0.5916	1.0000	1.0000		
80	0.0396	0.0039	0.0002	0.1520	1.0000	1.0000	1.0000	
100	0.0719	0.0360	0.0234	0.8900	1.0000	1.0000	1.0000	1.0000

3.2.4 Aerobic scope

Aerobic scope defined as difference between MMR and SMR is displayed in **Figure 13**.

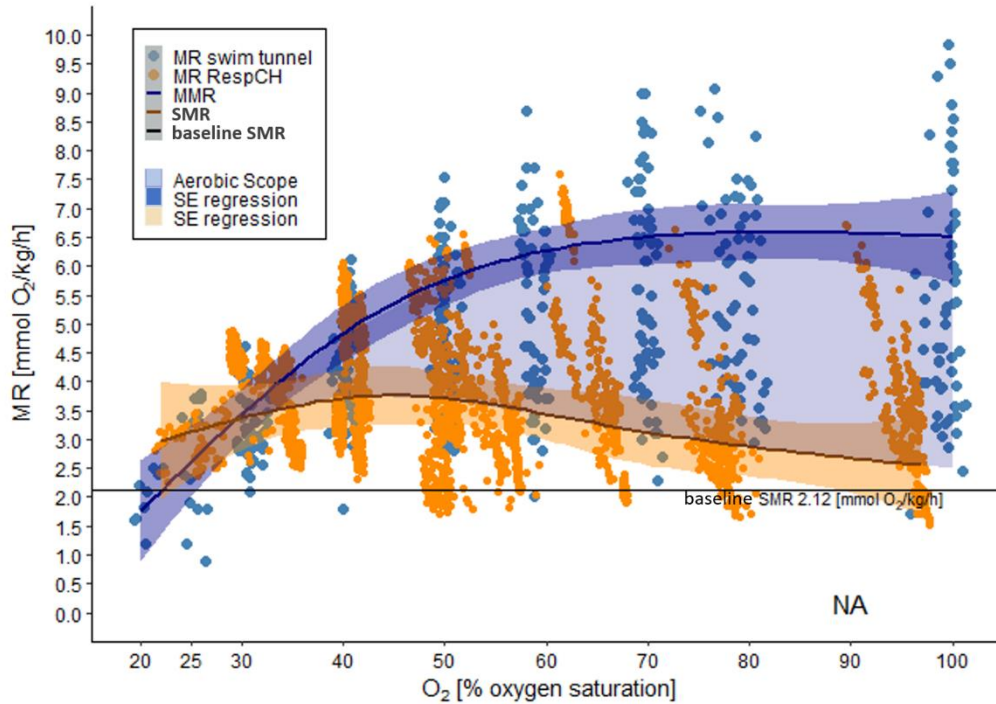


Figure 13 Maximum-, standard- and baseline standard metabolic rate with aerobic metabolic scope derived from 23 multiple used individuals. All metabolic rates (MR) measured in the swim tunnel (blue) and static respirometry (orange) approach are displayed as dots in relation to the ambient PO_2 levels at which they were assessed. Blue line and dark blue shaded area show MMR as regression model with respective SE of the model. MMR was derived from the MR measured in the swim tunnel set up. Dark orange line and orange shaded area display the SMR as regression model with SE of the model. SMR was calculated from MR measured in the static respirometry approach. Black line marks calculated baseline SMR. Shaded light blue area between MMR and SMR indicates the AAS defined as difference between MMR and SMR.

3.2.4.1 Absolute aerobic scope

As data of AAS over the PO_2 range tested were neither normally distributed nor showed homoscedasticity analysis for significant differences of AAS was not possible between all PO_2 levels. Statistical analysis was conducted between the following O_2 saturation levels: 80, 50, 40, and 25% (Welch-ANOVA, **Table 2**), 100 – 50% (Kruskal-Wallis test, **Table 3**) and 40-25% (Kruskal-Wallis test, $p=0.46$).

A significant PO_2 effect on AAS could be observed (**Figure 14**). AAS remained stable between 100-70% O_2 saturation with a mean of 3.58 ± 1.75 mmol O_2 /kg/h ($p=0.49$). AAS at 60 and 50% O_2 was significantly decreased compared to 80% O_2 ($p=0.001$, $p=0.019$) with an AAS of 2.53 ± 1.47 mmol O_2 /kg/h and 2.76 ± 1.53 mmol O_2 /kg/h at 60 and 50% O_2 , respectively. A further significant decrease of AAS was found

between 50 and 40% O₂ (p<0.0001) and 50 and 25% O₂ (p=0.013). AAS did not differ significantly between the three lowest PO₂ levels tested (p=0.46) with a mean AAS of 1.34 ± 0.94 mmol O₂/kg/h.

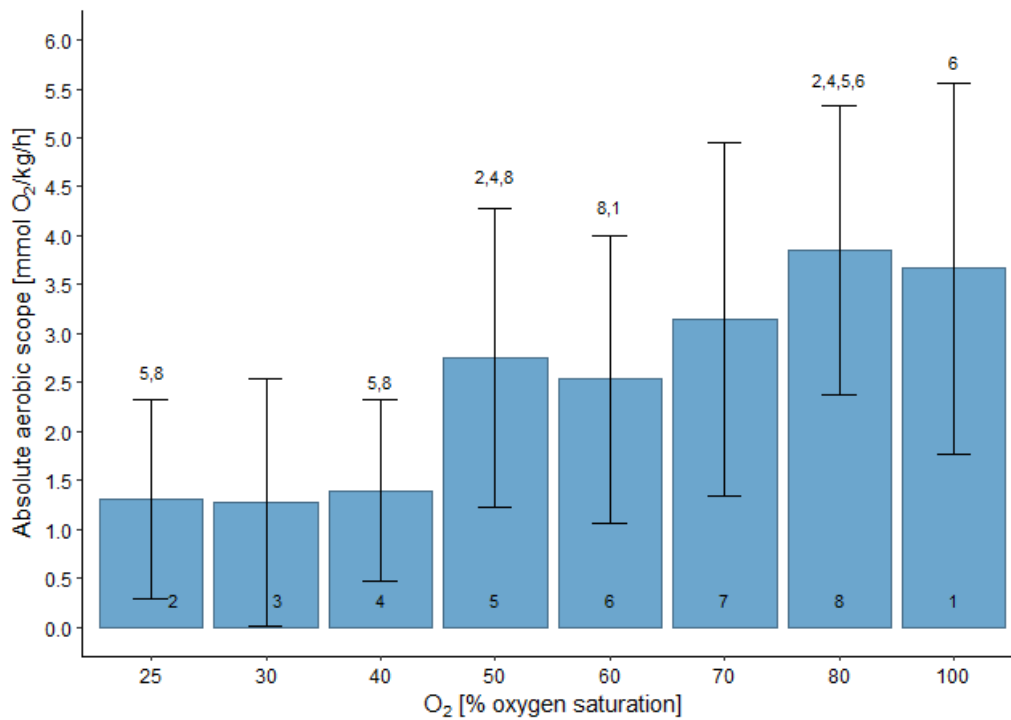


Figure 14 Absolute aerobic scope at different O₂ saturation levels. Bars and error bars represent the mean AAS with SD per PO₂ level. Numbers depict significant differences between treatments with numbers on top of the error bar state the treatments to which significant difference was observed. The following oxygen saturations could be compared: 80, 50, 40, and 25% O₂ (Table 2); 100 – 50% O₂ (Table 3); and 40-25% O₂ (p=0.46).

Table 2 P-values of the statistical comparison of AAS between ambient O₂ levels 80, 50, 40 and 25%. As data at these PO₂ levels were normally distributed but did not show homoscedasticity a Welch-ANOVA was applied followed by a Games Howell post-hoc test. The outcome of the Games Howell post-hoc test is displayed. Significant differences of AAS between PO₂ levels are marked in red.

O ₂ level saturation [%]	25	40	50
40	0.9950		
50	0.0130	3.9200E-05	
80	6.5800E-06	5.3000E-06	0.0040

Table 3 P-values of the statistical comparison of AAS between ambient O₂ levels 100 – 50%. As data at these PO₂ levels were not normally distributed but showed homoscedasticity a Kruskal Wallis test was applied followed by a Pairwise Wilcoxon rank sum test. The outcome of the Pairwise Wilcoxon rank sum test is displayed. Significant differences of AAS between PO₂ levels are marked in red.

O ₂ level saturation [%]	50	60	70	80
60	1.0000			
70	1.0000	0.8481		
80	0.0186	0.0013	0.4932	
100	0.2698	0.0431	1	1

3.2.4.2 Factorial aerobic scope

As was observed for AAS also the data of FAS were neither normally distributed nor showed homoscedasticity over the PO₂ range tested. Thus, analysis for significant differences of FAS was not possible between all PO₂ levels.

The FAS (**Figure 15**) was statistically compared between ambient O₂ levels 100-50% + 30% (**Table 4**), 30 and 25% (p=0.04) and 40 and 25% PO₂ (p= 0.0063) using a Kruskal-Wallis test. A Welch-ANOVA (p < 0.0001) was used for the evaluation of FAS between O₂ levels 60 and 40%.

A significant PO₂ effect on FAS could be observed. In comparison to AAS, FAS stayed stable over a smaller ambient oxygen saturation range (100-80%: p= 1.0, mean FAS: 2.6 ± 0.91) with the first significant decrease of FAS observed at 70% O₂ compared to 80 and 100% ambient oxygen saturation (p=0.001, p=0.014). At oxygen levels 70 - 50% FAS stayed stable as no significant differences of FAS between these oxygen levels could be observed (70 - 50% O₂ with max: 1.94 ± 0.87 and min: 1.84 ± 0.64). Furthermore, a significant decline of FAS between 60% (1.84 ± 0.64) and 40% (1.24 ± 0.41) O₂ was detected (p<0.0001). At the three lowest PO₂ levels FAS was statistically investigated between 40 and 25% O₂ (40%: 1.24 ± 0.41, 25%: 1.02 ± 0.7) and 30 and 25% O₂ (30%: 1.64 ± 1.77). A significant decrease could be found within both comparisons (p=0.0063, p= 0.04).

At 100% O₂ saturation the highest mean FAS of 2.6 ± 1.04 was observed.

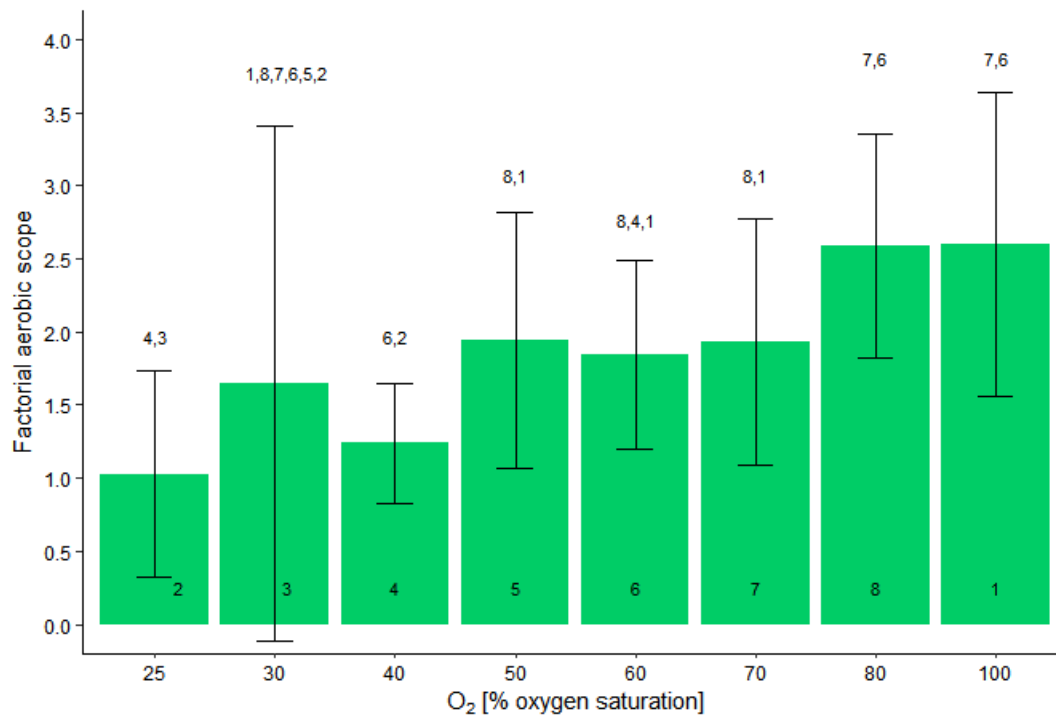


Figure 15 Factorial aerobic scope at different O₂ saturation levels. Bars and error bars represent the mean FAS with SD per treatment. Numbers depict significant differences between oxygen saturations with numbers on top of the error bar state the oxygen levels to which significant difference was observed. Following oxygen saturations could be statistically compared: 100-50% + 30% O₂ (Table 4); 60 and 40% O₂ (p<0.001); 40 and 25% O₂ (p=0.0063); 30 and 25% O₂ (p=0.04).

Table 4 P-values of the statistical comparison of FAS between ambient PO₂ levels 100 – 50 + 30%. As data at these PO₂ levels were not normally distributed but showed homoscedasticity a Kruskal-Wallis test was applied followed by a Pairwise Wilcoxon rank sum test. The outcome of the Pairwise Wilcoxon rank sum test is displayed. Significant differences of FAS between PO₂ levels are marked in red.

O ₂ level saturation [%]	30	50	60	70	80
50	0.0001				
60	1.40E-05	1.0000			
70	8.4000E-05	1.0000	1.0000		
80	6.0000E-08	0.0027	0.0017	0.0010	
100	6.3000E-08	0.01259	0.0020	0.0139	1.0000

3.2.5 LOL curve and P_{crit}

The LOL curve derived from the measurements assessed in this study is depicted in **Figure 16**.

One method to derive the critical oxygen saturation of a species is to assess the intercept of SMR and MMR as P_{crit} is defined as the partial pressure of ambient oxygen at which aerobic scope is nil (Claireaux and Chabot 2016).

In this study two approaches were used to determine the intercept between MMR and baseline SMR and therewith P_{crit} (see chapter 2.4.7). Both, the regression fit to the individual MMR measured at 40 – 20% O_2 (**Figure 16**) and the intercept of the regression fit to the lowest 5 mean MMR measured (**Figure 17**), intercept with the baseline SMR at an ambient oxygen saturation of 21.6% resulting in a P_{crit} of 4.51 kPa O_2 .

P_{cmax} was found to lie between 70 and 50% ambient oxygen saturation (see chapter 3.2.3), thus between 14.62 and 10.45 kPa O_2 . The intercept between MMR and SMR was observed at 30% ambient oxygen saturation (**Figure 18**).

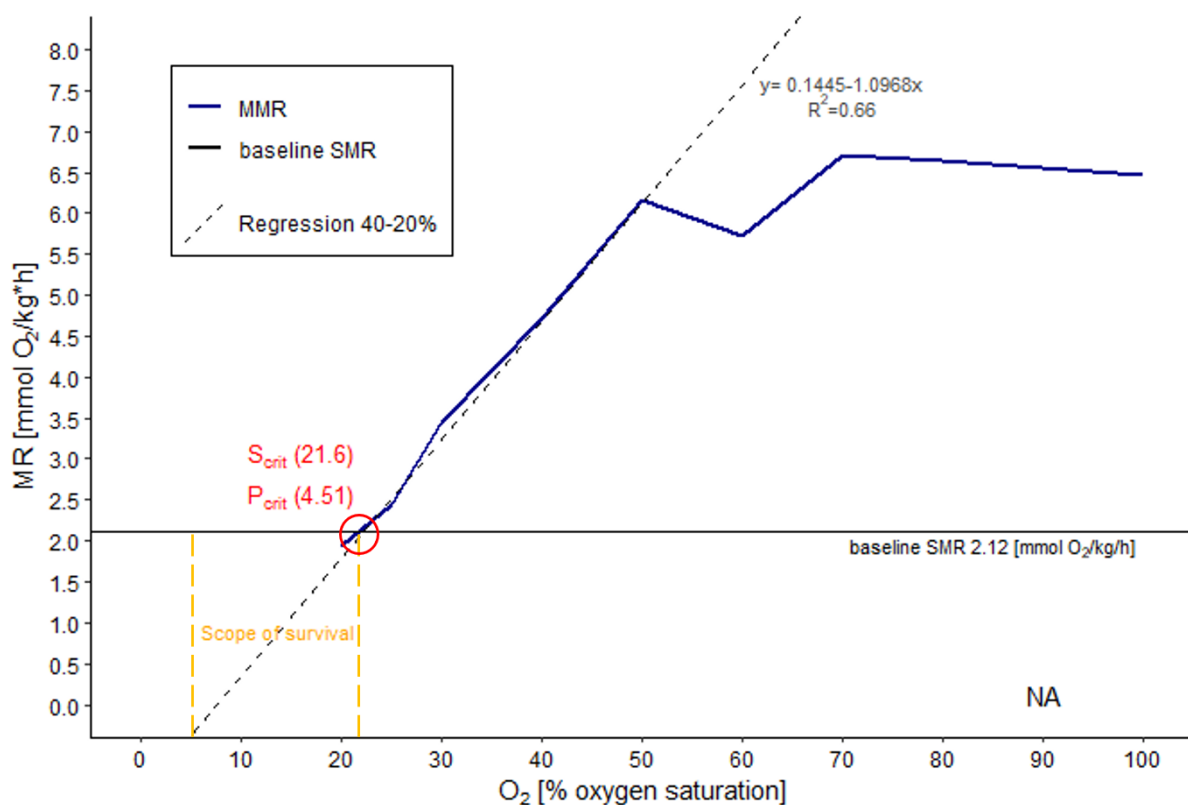


Figure 16 Limiting oxygen level curve after Claireaux & Chabot 2016. Displayed are the intercept between MMR (blue line) and a regression (dashed line) fit to individual MMR measured at ambient O_2 from 40 – 20% with the baseline SMR. Red circle marks the intercept from which a P_{crit} of 4.51 kPa (S_{crit} : 21.6% O_2) could be inferred. Yellow dashed lines mark the PO_2 range mathematically predicted as scope of survival.

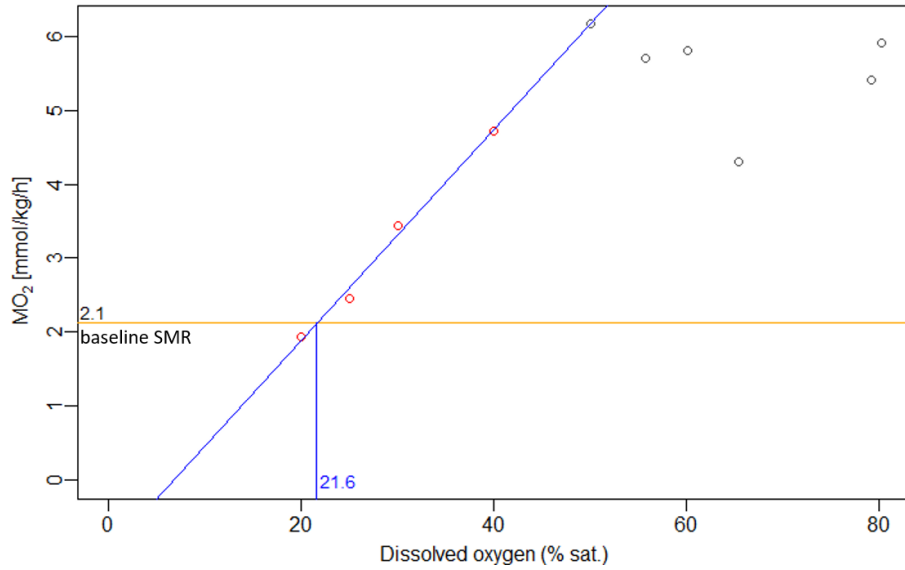


Figure 17 Determination of P_{crit} using the R script of Claireaux & Chabot 2016. PO_2 at which mean MMR (blue line) intercepts with baseline SMR (yellow line) was determined using the five lowest mean MMR measured over the PO_2 range tested (red circles) to fit a regression.

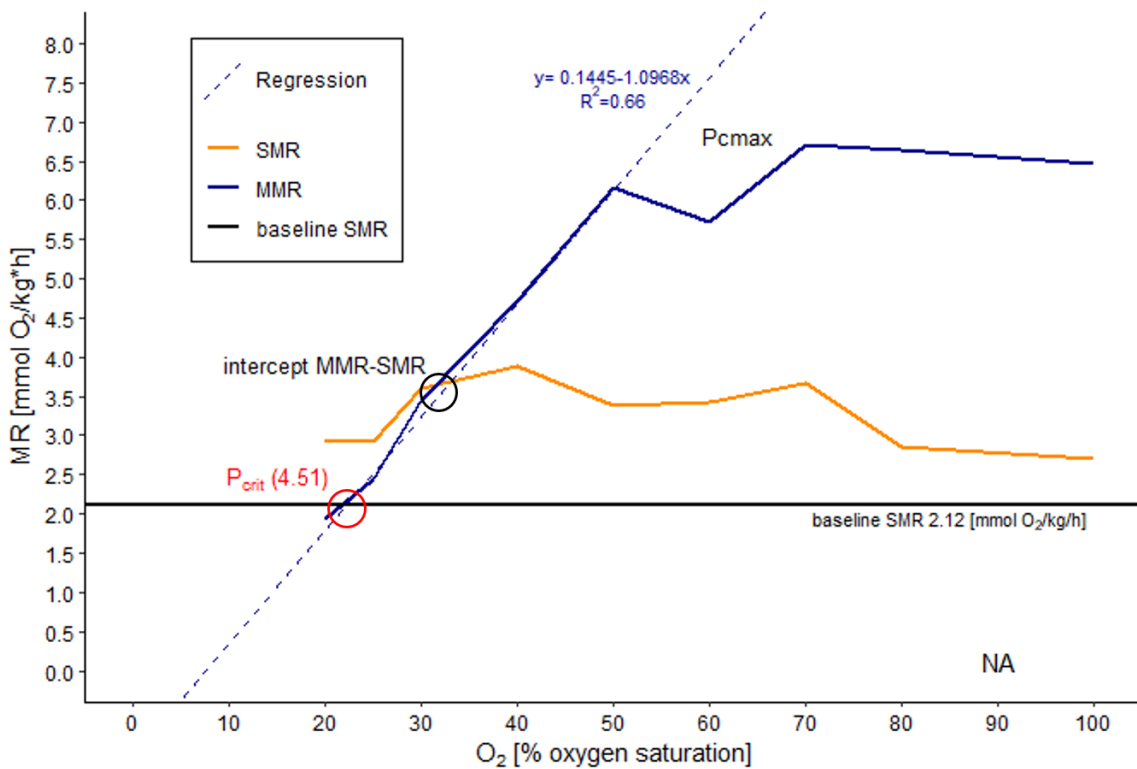


Figure 18 LOL curve and P_{cmax} . This graph displays the mean MMR (blue line) and mean SMR (orange line) over decreasing oxygen saturation levels. P_{crit} is depicted as intercept between a regression fit to the individual MMR measured at ambient O_2 levels 40 - 20%. Further displayed are the intercept between MMR and SMR at 30% ambient O_2 and the P_{cmax} as the ambient oxygen saturation at which the MMR starts to decrease. P_{cmax} was visually determined to lie between 14.62 - 10.45 kPa ambient oxygen saturation (70% and 50% O_2).

3.3 Swimming performance

3.3.1 MR at different water velocities

During the swim tunnel experiments the metabolic rates increased significantly with water velocity ($p < 0.0001$) until 2.9 BL/sec was reached (**Figure 19, Table 5**). Mean MR at 2.9 BL/sec was 6.47 ± 1.49 mmol O₂/kg/h. At velocity intervals following 2.9 BL/sec MR did not further increase significantly but levelled off (mean MR 2.9 – 3.5 BL/sec: max: 6.94 ± 1.21 mmol O₂/kg/h, min: 6.2 ± 0.95 mmol O₂/kg/h). The sample size decreased with increasing water velocity due to exhaustion (n per velocity interval: 1.4= 54, 1.55= 54, 1.7= 50, 1.85= 46, 2.0= 43, 2.15= 39, 2.3= 33, 2.45= 29, 2.6= 24, 2.75= 20, 2.9= 14, 3.05= 9, 3.2= 7, 3.35= 5, 3.5= 3).

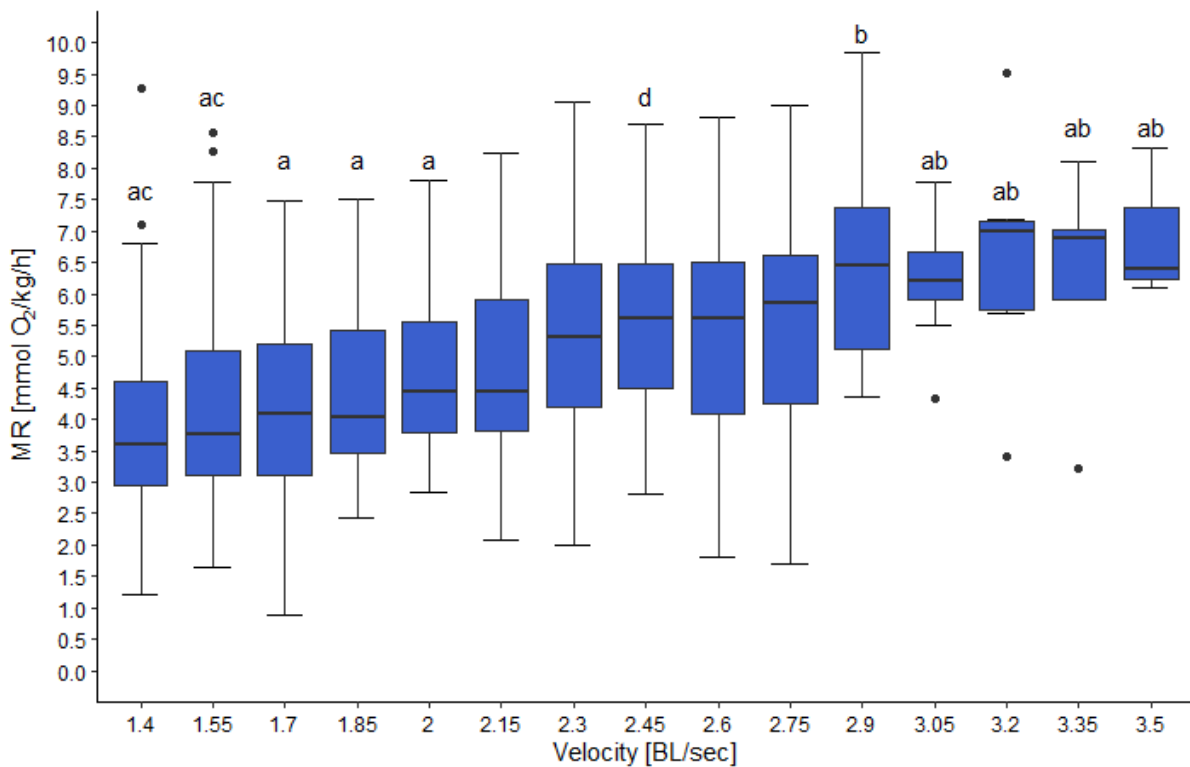


Figure 19 Metabolic rates over increasing water velocities. Boxplots show MR measured in the swim tunnel setup. Significant differences of MR between velocities are indicated by letters. For clarity reasons only the significant differences representing the general tendency are shown. For the complete outcome of the Pairwise Wilcoxon Rank Sum Test see **Table 5**.

Table 5 P-values of Paired Wilcoxon Rank Sum Test testing for significant differences between MR measured at different velocity intervals. Significant differences in MR between velocity intervals are marked in red.

Velocity [BL/sec]	1.4	1.55	1.7	1.85	2	2.15	2.3	2.45	2.6	2.75	2.9	3.05	3.2	3.35
1.55	1.0000													
1.7	1.0000	1.0000												
1.85	1.0000	1.0000	1.0000											
2	0.3766	1.0000	1.0000	1.0000										
2.15	0.2892	1.0000	1.0000	1.0000	1.0000									
2.3	0.0026	0.0820	0.1414	0.6184	1.0000	1.0000								
2.45	0.0022	0.0250	0.0501	0.2173	1.0000	1.0000	1.0000							
2.6	0.0295	0.3392	0.6394	1.0000	1.0000	1.0000	1.0000	1.0000						
2.75	0.0231	0.2005	0.3390	0.5062	1.0000	1.0000	1.0000	1.0000	1.0000					
2.9	0.0008	0.0056	0.0061	0.0122	0.0236	0.3728	1.0000	1.0000	1.0000	1.0000				
3.05	0.0341	0.1089	0.1419	0.1578	0.2321	1.0000	1.0000	1.0000	1.0000	1.0000	1.0000			
3.2	0.1432	0.5647	0.4843	0.9756	0.7949	1.0000	1.0000	1.0000	1.0000	1.0000	1.0000	1.0000		
3.35	1.0000	1.0000	1.0000	1.0000	1.0000	1.0000	1.0000	1.0000	1.0000	1.0000	1.0000	1.0000	1.0000	
3.5	1.0000	1.0000	1.0000	1.0000	1.0000	1.0000	1.0000	1.0000	1.0000	1.0000	1.0000	1.0000	1.0000	1.0000

3.3.2 Gait transition speed

The gait transition speed as the velocity (BL/sec) at which the even swimming mode of an individual was first interrupted by bursting was measured during the U_{crit} protocol realised in the swim tunnel set up. Although statistical analysis globally did reveal significant difference between U_{gait} at the different PO_2 levels (Kruskal-Wallis, $p=0.02$) this finding was not confirmed by the post-hoc test (Wilcoxon-Test). Generally, U_{gait} was relatively stable over an PO_2 range of 100 to 60% air saturation (median: max: 2.1 BL/sec, min: 1.92 BL/sec) with a slight increase towards 60% (median: 100%: 1.93 BL/sec, 60%: 2.1 BL/sec) (**Figure 20**). Compared to higher PO_2 levels U_{gait} at 50 to 25% O_2 saturation was slightly lower (median: max: 1.9 BL/sec, min: 1.53 BL/sec).

The number of animals which allowed to determine U_{gait} varied between the experiments with a distinct decrease for the 25% ($n=3$) and the 20% O_2 saturation levels ($n=0$). At each treatment initially seven fish were tested. At each oxygen level between 100 - 30% O_2 one individual refused to swim (individual varied) so that U_{gait} could only be determined from six individuals. At oxygen levels 100 and 30% one fish and at 40% O_2 two fish finished the experiment without displaying burst-behaviour. At 25% O_2 two fish lost equilibrium during the acclimation period, two individuals refused to swim, and another did not show burst behaviour so that U_{gait} had to be inferred from two specimen. At 20% O_2 saturation, one fish died at the end of the acclimation-period and three further experiments were terminated during the acclimation period due to loss of equilibrium. From the three fish tested in the U_{crit} protocol at 20% O_2 one refused to swim and for none of the remaining individuals burst events were observed. Thus, no U_{gait} could be determined at 20% O_2 .

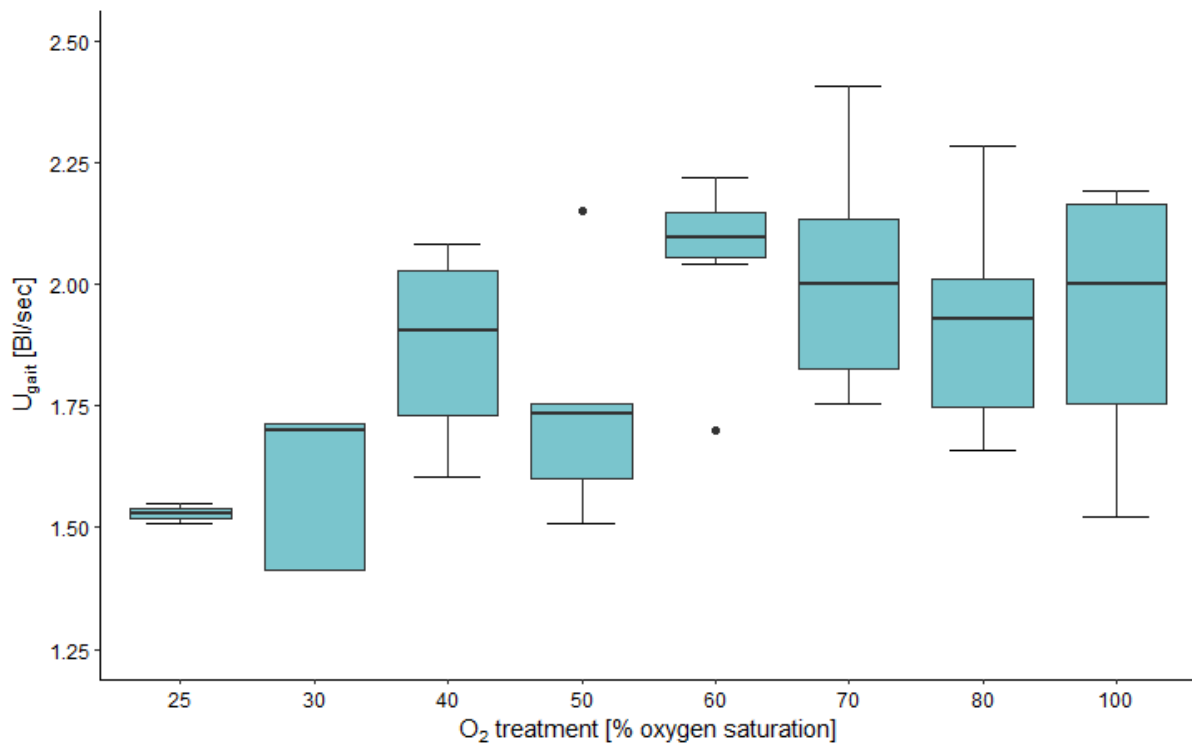


Figure 20 Gait transition speed over decreasing O₂ saturation levels. No significant difference was observed between the PO₂ levels (n per treatment: 100%= 5, 80%=6, 70%=6, 60%=6, 50%=6, 40%=5, 30%=5, 25%=2, 20%=0).

Like U_{gait} also the investigation of the total number of bursts did not reveal a significant PO₂ effect (p=0.23). The total number of bursts stayed relatively stable over an oxygen range between 80 and 40% O₂ saturation (max: 226.33 ± 316.60 bursts (40%), min: 154.00 ± 197.44 bursts (60%)) followed by a non-significant decrease of total burst activity at 30% and 25% O₂ (30%: 62.67 ± 46.97 bursts, 25%: 42.67 ± 68.77 bursts) (**Figure 21**).

Also, the relative burst activity (burst per minute TSB) did not show significant differences between the PO₂ levels tested (p= 0.42) (**Figure 22**). Bursts per minute stayed relatively stable over the entire PO₂ range investigated with the highest relative burst count at 40% ambient O₂ with 5.86 ± 5.18 bursts per minute. The relative burst count was lowest at 25% with 2.87 ± 2.19 bursts per minute.

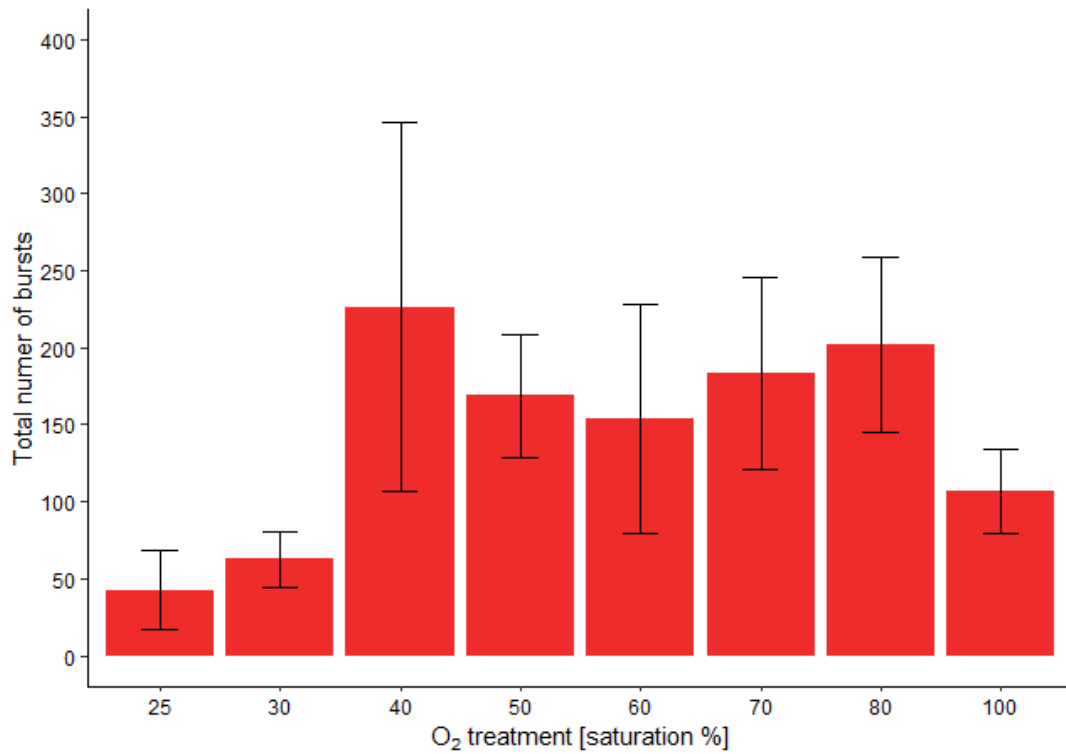


Figure 21 Total number of bursts over decreasing ambient oxygen saturations. Per PO₂ level the mean was calculated out of the total number of bursts per individual and is depicted with SE. No significant differences between the PO₂ levels were observed.

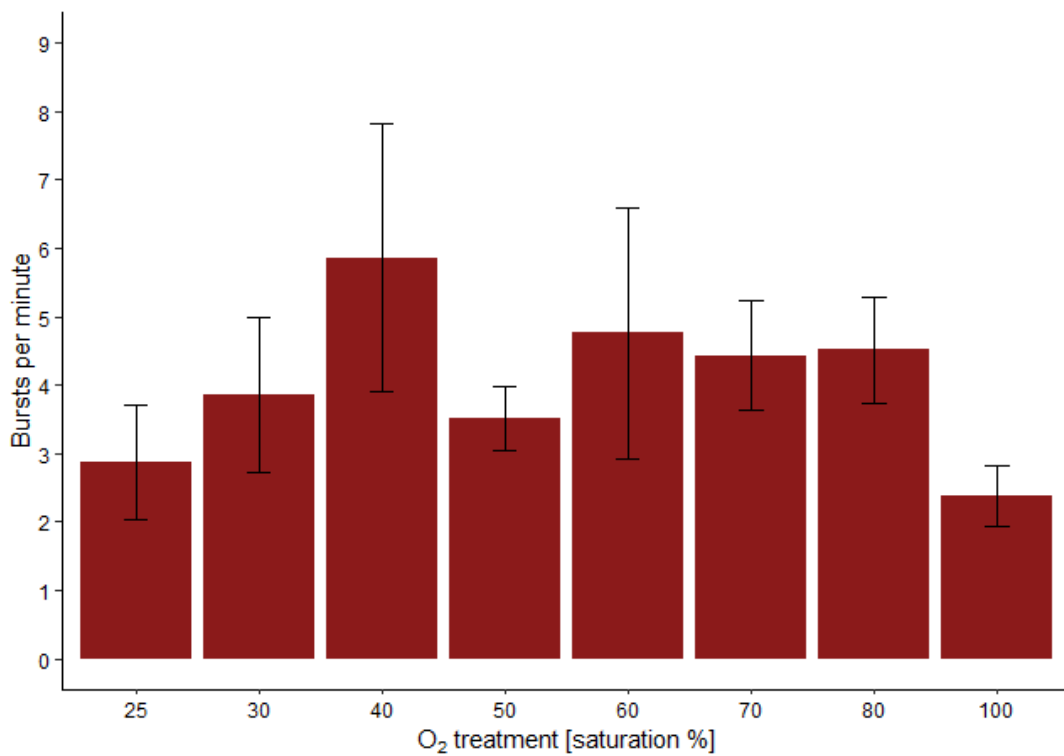


Figure 22 Relative number of burst (per min) over decreasing PO₂ levels. Per PO₂ level the mean was calculated out of the relative number of bursts per individual and is depicted with SE. No significance between the PO₂ treatments could be observed. n per treatment: 100%= 5, 80%=6, 70%=6, 60%=6, 50%=6, 40%=5, 30%=5, 25%=2).

3.3.3 Critical swimming speed

Albeit a global statistical difference between U_{crit} was found between the PO_2 levels tested (ANOVA, $p=0.008$), this finding could not be confirmed by the post-hoc test (Tukey-test). U_{crit} remained relatively stable over a O_2 range from 100 to 40% (median: max: 2.61 BL/sec, min: 2.50 BL/sec) (**Figure 23**). Comparing the mentioned range with the U_{crit} at 30 to 20% (median: max: 1.83 BL/sec, min: 1.59 BL/sec) a decrease in U_{crit} was observed, even though not significant.

At each PO_2 level the swimming performance of seven individuals was investigated of which one (individual varied) refused to swim at O_2 levels 100 – 30%, respectively. Refuse of swimming increased at the 25% oxygenation level to two out of seven individuals. Two further fish could not be tested due to loss of equilibrium during the acclimation period at 25% O_2 . At 20% O_2 two fish lost equilibrium during the acclimation period in the swim tunnel set and one further individual died during the acclimation time. Of the four individuals tested at 20% O_2 one refused to swim resulting in a U_{crit} value derived from $n=3$.

Although the sample size decreased at low PO_2 levels, the time spent swimming during the experiments did not differ over the whole PO_2 range tested ($p=0.72$, **Figure 24**).

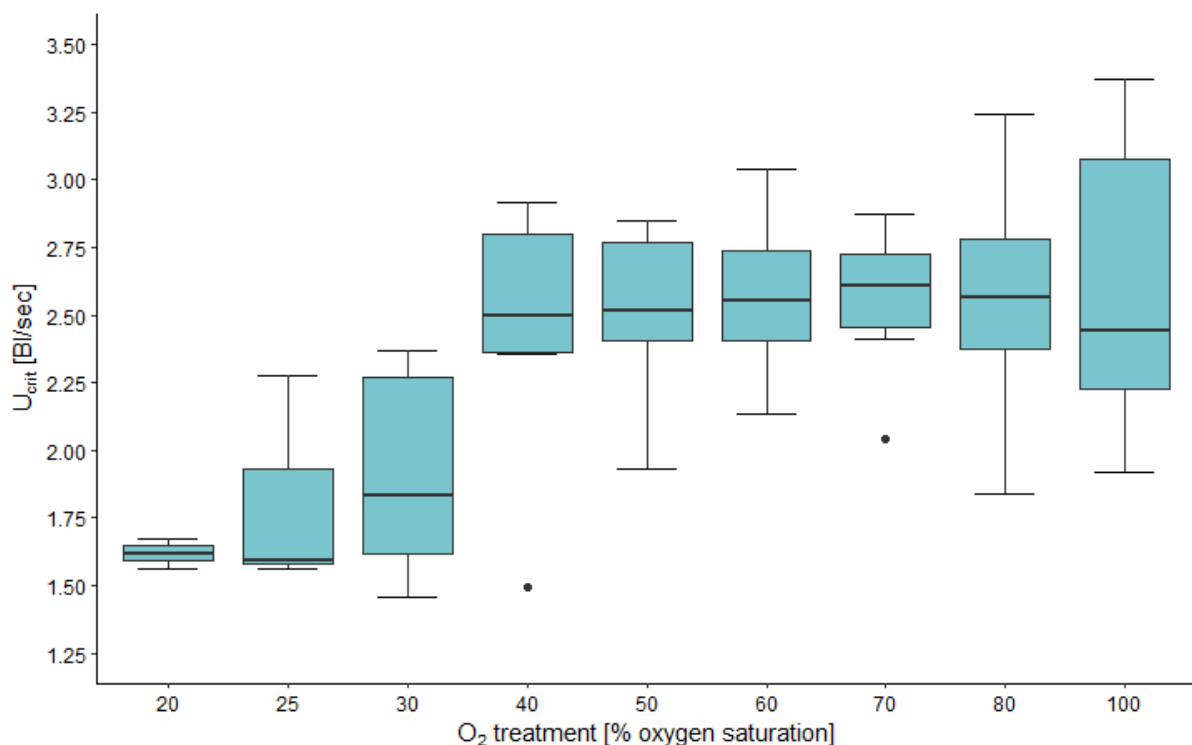


Figure 23 Critical swimming velocity over oxygen saturation levels. No significant difference was observed between U_{crit} at the different PO_2 levels investigated (n per O_2 level: 100% - 30%=6, 25%=3, 20%=2).

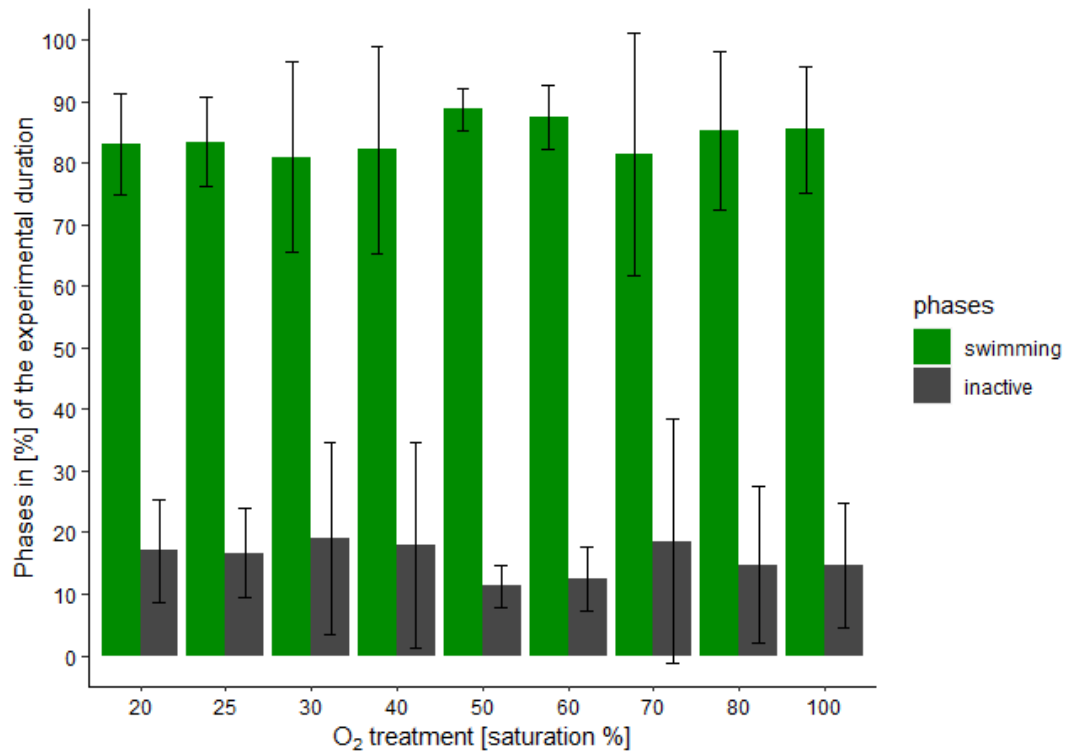


Figure 24 **Swimming activity over O₂ saturation levels.** Experimental duration was divided into two different phases. Inactive time was defined as time when fish did either sit in the swim chamber or were stuck at the grid at the end of the swimming chamber. Swimming time was defined as time spent swimming plus periods when fish used the grid to push themselves forward against the water current. Both phases are displayed as the mean percentage of the complete experimental duration together with the respective SD.

4 Discussion

4.1 Temperature effect on metabolic and swimming capacity

Polar cod investigated in the present study had been acclimated to a temperature of 10°C over a period of 10 months. To investigate the temperature effect on the metabolism of this Arctic species several metabolic parameters and the swimming performance of the animals were assessed. The first chapter of the discussion will be used to relate the temperature of 10°C to the thermal window of Polar cod in order to infer possible ecological implications coming from increasing water temperatures observed in Arctic waters (**Figure 6**).

The first hypothesis of this study states that 10°C is close to the upper pejus temperature of Polar cod. This is inferred from the preferred temperature range of *B. saida* which is reported to be 2.4 - 4.4 °C (Schurmann and Christiansen 1994), the physiological optimum temperature of 3 - 6.5°C (Drost et al. 2014; Drost et al. 2016; Kunz et al. 2016) and the upper thermal limit that is suggested to be between 8 – 16°C (Drost et al. 2014; Drost et al. 2016; Kunz et al. 2018; Laurel et al. 2016) (see chapter 1.4.1). In order to investigate the first hypothesis, the outcome of the present study will be examined in comparison to measurements of the metabolic and swimming capacity of Polar cod at 2.5°C implemented by Sarah Kempf.

In accordance with the definition of pejus temperature the acclimation temperature of 10°C does not appear to be the pejus temperature of Polar cod yet. The pejus temperature is defined as the onset of the upper thermal limit of a species and the temperature at which the aerobic scope of an animal starts to decrease (Farrell and Steffensen 2005; Pörtner et al. 2017) (see chapter 1.3.3). Although the long-term acclimation of Polar cod to a temperature of 10°C did not result in metabolic compensation within the animals, neither the absolute aerobic scope nor the swimming capacity was reduced as will be discussed in the following.

Metabolic compensation describes the restoration of immediate thermal effects on metabolism (Bullock 1955; Precht 1958). Thus, metabolic compensation facilitates animals to acclimate to increased temperature regimes by maintaining their metabolic rate independent from temperature (Precht 1958). A measure to investigate thermal dependence of metabolic processes and therewith acclimation capacity is the Q_{10} value:

$$Q_{10} = \left(\frac{R_2}{R_1} \right)^{\frac{10}{(T_2 - T_1)}} \quad (4)$$

with R_1 being the metabolic rate at the first temperature (T_1) and R_2 being the metabolic rate at the second temperature (T_2). A Q_{10} value higher than two indicates increasing thermal dependence and

therewith absent metabolic compensation (Precht 1958; Bennett 1990; Høleton 1974; Farrell and Steffensen 2005; McBryan et al. 2013). The Q_{10} values presented in the following were calculated by using measurements taken at 2.5°C (Sarah Kempf). Data of both studies were not normalized for weight, but results were comparable since the range of animal weight was similar (2.5°C: 39 ± 9.5 g, 10°C: 41.3 ± 10.1 g).

The Q_{10} values for baseline SMR and SMR found in the present study were with 8.14 and 4.0 respectively far out of the range that would indicate metabolic compensation. This is in line with findings by Kunz et al. 2016 and Kunz et al. 2018 who found the capacity for metabolic compensation being restricted to a temperature range of 0 - 6°C. Thus, it can be concluded that 10°C is beyond the thermal preferendum of the study species (Claireaux and Lagardère 1999).

The increase of the MMR in comparison to 2.5°C is in accordance with a rise of MMR observed in a long-term incubation experiment that applied a temperature range from 0 - 8°C (Kunz et al. 2016; Kunz et al. 2018). The Q_{10} value of 1.56 of the MMR, however, suggests a restricted potential to increase maximum oxygen supply capacity. Whereas MMR was only 1.5 times increased at 10°C compared to 2.5°C the baseline SMR and SMR rose by 5 and 2.5 times, respectively. This difference in plasticity of maintenance and maximum metabolism is a known phenomenon in fish and led to the “*plastic floors and concrete ceiling*” hypothesis (Sandblom et al. 2016; Rodgers and Franklin 2021). This hypothesis summarizes the observation of exponential increase of SMR and RMR with rising temperature but a decreasing or reaching of a plateau of MMR. The word ceiling is hereby referring to the apparent lack of acclimation potential of MMR that does not allow for an increase of MMR with temperature after the ceiling is reached resulting in a progressively declining aerobic scope. The disparity in thermal sensitivity of both metabolic traits observed in Polar cod is reflected in a decrease of the FAS, which declined from 10.2 at 2.5°C to 2.6 ± 1.04 at 10°C. AAS by contrast did not decrease but stayed in a range comparable with 2.5°C (approx. 3.2 mmol O₂/kg/h at 2.5°C, 3.67 ± 1.89 mmol O₂/kg/h at 10°C). This is in contrast to Kunz et al. 2018 who found a decrease in the AAS at 8°C compared to 6°C long-term acclimation temperature.

A temperature effect on the swimming performance was, however, neither observed in the present study nor in the study of Kunz et al. 2018. Indeed, the present research found U_{gait} to be lower (10°C: 1.93 ± 0.28 BL/sec, 2.5°C: 2.49 ± 0.56 BL/sec) and U_{crit} slightly reduced (10°C: 2.60 ± 0.59 BL/sec, 2.5°C: 2.89 ± 0.58 BL/sec) in comparison to the swimming performance at 2.5°C. The decrease of the two parameters does not have to be a direct effect of temperature, however, but is suggested to result from increased swimming activity observed at 10°C compared to 2.5°C. At the higher temperature, the animals increased the time spent swimming by 30% (**Figure 24**) meaning they reduced their inactive time during the U_{crit} protocol. Thus, in the same experimental duration fishes swam 30% more

compared to 2.5°C. This higher swimming activity is hypothesised to have provoked an earlier need for anaerobic swimming and a final exhaustion at slightly lower swimming speeds.

All in all, neither a decrease in aerobic performance nor in AAS are indicating 10°C to be a pejus temperature for Polar cod.

Pörtner et al. 2017 suggest, however, that for the determination of the pejus temperature not only the AS should be considered but the performances of several animal functions to pay attention to the subtle development of the pejus limit. Of the animal functions suggested the break point temperature of heart rate, mitochondrial functioning and aerobic performance measured as exercise and growth have been assessed for Polar cod.

With regard to heart rate two breakpoint temperatures are reported. Fish acclimated to 0°C showed an Arrhenius break temperature of 3.2 – 3.6°C and a break temperature for incremental Q_{10} (T_{QB}) with the Q_{10} value decreasing below 2 at 5.5 – 8.0°C (Drost et al. 2014). Furthermore, it should be mentioned that heart rate showed an acclimation response with a significant increasing of T_{QB} to 7.3°C in fish acclimated to 6.5°C (Drost et al. 2016). Mitochondrial functioning stayed unaffected at 6°C but at 8°C ATP production efficiency was decreased due to increased proton leak together with a lowered Cytochrome c oxidase capacity (Leo et al. 2017). Studies reporting growth rates of Polar cod suggest a growth optimum in a range of 3 – 6°C with the temperature causing decrease of growth rate depending on life stages (Kunz et al. 2016; Laurel et al. 2016; Laurel et al. 2017). For two years old Polar cod a decrease of condition factor and feed conversion efficiency at 8°C compared to 6°C was observed (Kunz et al. 2016). For one year old fishes a decline of growth rate was observed at 6.4°C and for the 0-year class at 9°C (Laurel et al. 2016; Laurel et al. 2017). Polar cod long-term acclimated to 10°C displayed a reduced growth rate, likewise. Furthermore, reproductive activity was suspended at this temperature in comparison to fish that were kept at 0°C (unpublished data Dr. Felix Mark). According to exercise, by contrast, a temperature effect could neither be observed at 8°C (Kunz et al. 2018) nor at 10°C.

Taking the thermal thresholds of the described functions together it can be inferred that there is not one distinct pejus temperature for Polar cod but a pejus temperature range (Pörtner et al. 2013) within which animal performances decrease in a hierarchical order (Pörtner et al. 2008). This can be explained by the fact that temperatures that cause the maintenance costs to rise are causing a conflict in energy budgeting considering excess activities like growth or reproduction (Lefrançois and Claireaux 2003). With regard to the present study this is in accordance with the decrease in FAS observed at 10°C compared to 2.5°C, which is indicating the increased fraction of energy used for maintenance cost apparently restricting growth and reproduction at the study temperature. A hierarchical energy allocation similar to that observed in Polar cod was also reported for Atlantic cod (*Gadus morhua*) and eelpout (*Zoarces viviparus*) caused by an increase in SMR due to cold acclimation (Pörtner et al. 2008). Pörtner et al. 2008 suggest that the covering of increased maintenance costs is to the expense of

energy allocation to growth and fecundity. They suggest likewise that energy allocation to motility might be favoured before growth and reproduction to secure foraging capacity. This could explain the maintenance of swimming performance throughout the pejus temperature range observed in Polar cod. Remaining foraging capacities at these high temperatures are also indicated by observation of *B. saida* at temperatures around 10°C in the wild (Craig et al. 1982; Moulton and Tarbox 1987). Moulton and Tarbox 1987 suggest that Polar cod would visit these high temperature water masses due to prey availability.

In conclusion, the temperature of 10°C is suggested to lie within the pejus temperature range of Polar cod but does still allow for foraging activity in contrast to growth and reproduction. The onset of the pejus temperature range can be expected to lie between 6 and 8°C. For a discussion about further ecological implications please see chapter 4.4.

4.2 Hypoxia tolerance of Polar cod at low and high temperatures

The second and the third research objective aim at the investigation of the combined effect of temperature and decreased oxygen availability on metabolic and swimming capacity of Polar cod as well as at the investigation of the potential temperature effect on its hypoxia tolerance. Chapter 4.2.1 discusses the results of the measurements of metabolic and swimming capacity at decreasing PO₂ levels as well as the P_{crit} found for Polar cod at 10°C. In chapter 4.2.2 the hypoxia tolerance found in the present study will be compared to the hypoxia tolerance found at 2.5°C in order to investigate the effect of the pejus temperature on hypoxia tolerance.

4.2.1 Hypoxia tolerance of Polar cod at 10°C

As introduced in chapter 1.3.2 there are two physiological strategies that fish apply when confronted with decreasing ambient oxygen saturations: oxy conforming and oxy regulation.

The results of the present study show that *B. saida* clearly uses an oxy regulating strategy when being confronted with decreasing oxygen availability. The fishes were able to regulate their SMR to remain at normoxic level over the whole ambient oxygen saturation range tolerated (**Figure 11**). In general maintenance of SMR was found to be facilitated by increased gill ventilation, gill perfusion, cardiac output, the increase of blood carrying capacity by elevation of haemoglobin concentration and increased tissue O₂ extraction (Richards and Farrell 2009). In the case of Polar cod, we can only hypothesise what mechanisms were used to compensate low O₂ availability. The nonsignificant

increase of SMR from 100 to 40% O₂ saturation (**Figure 11**) indicates an increase of metabolic costs resulting from increased ventilation and cardiac output. Claireaux and Chabot 2016 mention that increasing SMR may also be a result from increased activity due to agitation of the animals when oxygen availability becomes restricted. An increased locomotive activity can be excluded, however, as the variability of metabolic rates did not increase at lower ambient oxygen saturations (**Figure 11**).

At oxygen levels lower than 45%, SMR started to level off (**Figure 11**). On the one hand this slight reduction in SMR could indicate a behavioural adjustment expressed as a suppression of the remaining activity in order to reduce oxygen demand (McBryan et al. 2016). On the other hand, the reduced oxygen consumption could also indicate a physiological limitation due to non-sufficient oxygen supply to maintain increased ventilation and cardiac output. As a physiological limitation would probably result in a behavioural adjustment, both explanations combined are possible to explain the effect on SMR, likewise. In case of a physiological limitation survival over several days at oxygen levels below 45% would be critical.

Not only the SMR but also the MMR could be observed to be regulated, however, not over the entire PO₂ range tolerated (**Figure 12, Figure 18**). MMR started to decline between 70 and 50% O₂ so that P_{cmax} as the PO₂ level restricting maximum metabolism lies within this range (14.62 – 10.45 kPa O₂). At oxygen saturation levels lower than 50% the MMR decreased more steeply indicating the restrictions of the exploitation of the cardiorespiratory system that were facilitating the satisfaction of oxygen demand of normoxic maximum metabolism at higher oxygen levels.

The decline of MMR and increase of SMR resulted in a significant decrease of absolute and factorial aerobic scope between higher and lower oxygen levels (**Figure 13, Figure 14, Figure 15**). Surprisingly, this did not provoke the swimming performance to decline as no significant PO₂ effect could be observed for U_{crit}, U_{gait} and swimming time (**Figure 20, Figure 23, Figure 24**).

When allowing for the investigation of non-significant differences, however, trends can be seen. The maximum velocity reached decreased beginning at 30% O₂ (**Figure 23**). This can be seen as rather late since AAS and FAS decreased significantly at higher ambient O₂ levels (**Figure 14, Figure 15**). U_{gait} by contrast was observed to decrease at higher ambient O₂ saturations which were lying within the range of P_{cmax} (**Figure 20, Figure 18**). This indicates a restricted oxygen supply for exercise although no significant difference in AAS could be observed at 50% compared to 60% ambient O₂ yet (**Table 3**).

A reason for missing significance despite non-significant trends could result from high inter-individual variability reflected in the high standard deviations of the measurements.

This interindividual variability is also influencing the determination of the critical oxygen partial pressure P_{crit}. P_{crit} of Polar cod acclimated to 10°C was determined to be 4.51 kPa O₂ (S_{crit} 21.6% O₂) (**Figure 16**). These P_{crit} values seem, however, rather to represent the lower range of interindividual variability. Although three and two individuals at the 25 and 20% O₂ saturation level, respectively, still

swam two other individuals lost equilibrium during the acclimation period in the swim tunnel at both O₂ saturations and one individual died at the end of the acclimation period at 20% O₂. Thus, whereas some individuals clearly reached P_{crit} beginning at 30% ambient O₂ saturation (6.28 kPa) others remained an AS at 20% O₂ that still allowed for excess activity. These high interindividual differences in hypoxia tolerance had not been observed at 2.5°C and may be a result of the exposure of the animals to their upper thermal limit. One could also argue the high inter-individual variability might be a methodological artefact as the loss of equilibrium and death in the swim tunnel setup could have been prevented by reducing the ambient O₂ saturation stepwise instead of introducing the animals directly from normoxic to hypoxic oxygen conditions. Although this is regarded as clear enhancement of the experimental procedure and suggested for future studies the stepwise reduction of PO₂ cannot be expected to change the overall outcome regarding P_{crit}. Despite a stepwise reduction of PO₂ over 21h for the SMR measurement at 30% in the static respirometry setup one fish died after being exposed to 30% O₂ for one hour. After the termination of the measurements at 30%, PO₂ was further decreased for the measurement of SMR at 25% O₂. Although animals had the possibility to acclimate to a O₂ saturation of 30% for 46 h two further specimen died after one hour at an oxygen saturation of 27.41%. The possibility that death was caused due to an oxygen debt taken during the long exposure to 30% O₂ can be excluded as no reduction in MR indicating a switch to anaerobic metabolism could be observed.

In conclusion, I suggest that the survival at oxygen saturations lower than 30% O₂ (6.28 kPa) is critical for Polar cod at 10°C. This is due to mortality beginning at 30% but is also suggested by the intercept of MMR with SMR at this PO₂ level (**Figure 18**) which indicates a vanishing AS and possible requirement of anaerobic metabolism at oxygen saturations below 30%. Thus, the P_{crit} representative for the study species can be expected to lie between 4.51 kPa (S_{crit} 21.6% O₂) and 6.28 kPa (S_{crit} 30% O₂) O₂. It has to be kept in mind, however, that PO₂ levels above P_{crit} in an environment of 10°C do still not facilitate long-term population survival due to prohibited growth and reproduction at this temperature (chapter 4.1).

As pointed out by Pörtner 2010 and Rogers et al. 2016 among others hypoxia tolerance cannot be determined solely by the consideration of the critical partial oxygen pressure. When investigating hypoxia tolerance anaerobic capacity is an important parameter as it is defining the width of the scope of survival and the temporal tolerance against PO₂ below P_{crit}.

In the present study anaerobic swimming capacity has been investigated as proxy for anaerobic metabolic capacity of Polar cod. Anaerobic swimming capacity was measured as absolute and relative bursts counts, Ugait marking the onset of the use of anaerobic metabolism and U_{crit} as maximum velocity reached (Roze et al. 2013; Lurman et al. 2007).

A comparison between burst counts assessed in this study and at 2.5°C is displayed in **Table 6**. The observation that Polar cod was not able to increase burst occurrence despite a higher need for anaerobic swimming indicated by lower U_{gait} at 10°C gives the first indication for a restricted anaerobic swimming capacity of this species. Only looking at the normoxic conditions the total number of bursts was in the same range at both temperatures, but relative burst counts were lower at 10°C than at 2.5°C (10°C: 2.34 ± 1.20 burst/min, 2.5°C: 12.61 ± 9.39 burst/min). This can be explained by an increased TSB resulting from an U_{gait} at lower velocities and an increased swimming activity at 10°C (chapter 4.1). At ambient oxygen levels 70 to 40% the total burst count was about 80% higher at 10°C than at 2.5°C. This higher total burst count could be provoked by the 30% higher swimming activity at 10°C and the 20% lower oxygen concentration in the water (**Table 8**) due to reduced oxygen solubility at the higher temperature. Looking at the general burst capacity throughout the PO_2 range tested the low relative burst counts observed at both temperatures indicate a low burst capacity of Polar cod. This is moreover supported by the observation that decreasing ambient oxygen availability - although provoking a decrease in AS - did not result in an increase of burst occurrence. This is against the expectation that with less oxygen available for aerobic swimming the share of anaerobic bursting would increase.

Table 6 **Burst counts at different temperatures.** This table shows relative burst counts (per minute) and total burst counts assessed in the present study at 10°C and by Sarah Kempf at 1.23 °C.

ambient oxygen level [% saturation]	10°C		1.23°C (Kempf)		10°C		1.23°C (Kempf)	
	mean relative number of bursts (per min)	SD	mean relative number of bursts (per min)	SD	mean total number of bursts	SD	mean total number of bursts	SD
100	2.38	1.21	12.61	9.39	106.67	73.28	146.17	211.93
80	4.51	2.05			201.83	151.61		
70	4.43	2.09	6.23	3.39	183.50	165.97	22.33	21.68
60	4.76	4.84	7.48	7.11	154.00	197.44	18.83	32.87
50	3.51	1.21	13.55	17.42	168.67	104.67	36.33	54.97
40	5.86	5.18	10.42	9.67	226.33	316.57	43.33	35.86
30	3.86	2.99	14.56	9.33	62.67	46.97	47.50	38.04
25	2.87	2.19	10.11	8.96	42.67	68.77	14.83	12.85
20			3.24	4.34			27.50	42.99
15			2.34	3.50			5.50	8.04
10			1.14	2.54			0.83	1.86

The low burst capacity of Polar cod can be also seen when comparing relative burst counts to other species such as European seabass *Dicentrarchus labrax* for example, which is reported to display relative burst counts of 84 bursts per 30 sec (Marras et al. 2010) compared to Polar cod with 6.33 ± 4.16 bursts per minute. The overall burst capacity found during hypoxia challenges at 10 and 2.5°C is in accordance with measurements of Kunz et al. 2018. They assessed the same parameters of swimming performance as were assessed in the present study in animals incubated at 0, 3, 6 and 8°C at normoxic conditions. They determined the anaerobic swimming capacity to be 0 – 5.7%. Another common observation of the present study with Kunz et al. 2018 and the master’s thesis of Sarah Kempf

is that some animals did not display burst behaviour at all further indicating low anaerobic swimming capacities of Polar cod.

In this study the burst capacity was measured to infer the capacity for anaerobic metabolism of Polar cod. This was done in order to gain information about its scope of survival and therewith its hypoxia tolerance. When taking the anaerobic capacity of muscles as proxy for general anaerobic capacity it has to be considered that the anaerobic fuelling of burst swimming is not only realised using glycolytic pathways but also by the use of phosphocreatine (PCr) hydrolysis (Lurman et al. 2007). The lysis of PCr to phosphate and creatin catalysed by creatin kinase results in the reversible transfer of a phosphoryl group to ADP (Nyack 2006; Hochachka and Mossey 1998). This reaction serves for a fast delivery of ATP used for quick muscle contractions during burst swimming but also for a replenishment of ATP stores during times of oxygen scarcity when aerobic ATP production is restricted (Nyack 2006; van Waarde et al. 1983).

Due to the low burst counts per minute of Polar cod, found at 10°C and 2.5°C one could speculate that in *B. saida* the PCr could be replenished during burst swimming between single bursts. This could facilitate the species to fuel the major fraction of bursts by PCr and therewith avoid accumulation of lactate. This speculation makes clear that a deduction of the general anaerobic capacity of Polar cod from burst swimming could lead to an overestimation of capacity for anaerobic glycolysis and therewith survival capacity below P_{crit} . As the replenishment of PCr stores is reported to require more than 30 min to 1 hour (Curtin et al. 1997; Nyack 2006), however, a restoration of PCr stores between bursts appears unlikely. Furthermore, Whiteley et al. 2006 reported a moderate lactacidosis measured in Polar cod after stress exposure indicating a general capacity for anaerobic glycolysis. Thus, it appears likely that both pathways are incorporated in burst swimming. To investigate the contribution of the different pathways to burst capacity one could evaluate PCr concentration during a U_{crit} protocol. Lurman et al. 2007 report that PCr concentration in *G. morhua* remained stable until 80% U_{crit} but was decreased by half at 100% U_{crit} . As no information about the U_{gait} of *G. morhua* exists to my knowledge it is not possible to speculate about the contribution of PCr to the overall burst capacity in this species and infer possible implications for Polar cod.

To conclude, the measurement of burst capacity as proxy for anaerobic metabolism does not appear adequate for several reasons. As discussed above the assessment of burst capacity does not allow to infer differentiated information about anaerobic pathways used and their contribution to burst swimming. Therefore, the predictive power of burst swimming for anaerobic glycolysis is restricted. Furthermore, the high standard deviation of burst counts displays the sensitivity of the measurement of this parameter to subjective bias through the experimenter and the counting method. Together with the finding that anaerobic metabolism during swimming is also used before the onset of burst swimming (Rome et al. 1984; Jayne and Lauder 1994) this further adds to the restricted predictive

power mentioned. Thus, other methods should be used to investigate the anaerobic metabolic capacity of Polar cod in future studies. The measurement of the post exercise oxygen consumption (EPOC) reveals the oxygen debt taken during anaerobic metabolism (Wood 1991). After exercise the glycogen and PCr stores are replenished aerobically and also the accumulated lactate is decomposed aerobically (Curtin et al. 1997; Wood 1991). Thus, measuring EPOC would allow for a more reliable measurement of anaerobic capacity by avoiding subjective bias coming from the experimenter. However, the assessment of EPOC does still not facilitate to distinguish the different anaerobic pathways used. Hence, I suggest that the most appropriate approach to assess the anaerobic metabolic capacity of Polar cod would be the measurement of substrates and end products like PCr and lactate in the context of exercise.

Coming back to the investigation of the scope of survival of Polar cod to complete the assessment of its hypoxia tolerance the restricted burst capacity found in this study and in others (Kempf, (Kunz et al. 2018) still indicates an overall low anaerobic capacity of *B. saida*. This suggestion is confirmed by the temporal tolerance of the animals to ambient oxygen levels that led to mortality. Fish were observed to die after one to two hours at the respective PO_2 level. All in all, this suggests a narrow and temporarily strongly restricted scope of survival for *B. saida* and does contradict the scope of survival mathematically predicted (**Figure 16**).

In polar fish low anaerobic capacities are a common phenomenon and suggested to result from a space constrain in muscle cells due to high mitochondrial densities. High mitochondrial densities compensate for the thermal decrease of metabolic rates and therefore energy production but restrict the space for myofibrillar densities, glycogen stores and glycolytic complexes required for extensive lactate formation (Farrell and Steffensen 2005). Such a muscle design maximizing aerobic energy production is furthermore favoured by a moderately active lifestyle (Farrell and Steffensen 2005) what is suggested to be the case in *B. saida* (Gradinger and Bluhm 2004; Lønne and Gulliksen 1989).

Some reliance on anaerobic metabolism can, however, nevertheless be seen in Polar cod and is also suggested by Whiteley et al. 2006 as mentioned above. For instance, the maintenance of U_{crit} at 40% O_2 saturation (**Figure 20**) despite a significant lower AAS than at 50 and 80% O_2 (**Figure 14**) could be explained by the non-significantly increase of total and relative bursts occurrence at 40% O_2 (**Figure 21, Figure 22**).

In summary, a regulation of SMR and MMR over decreasing PO_2 levels were found in Polar cod at 10°C. As SMR increased until 45% O_2 and P_{cmax} was found to be between 14.62 kPa (70% O_2) and 10.45 kPa (50% O_2) O_2 AAS decreased significantly with the first significant difference observed between 80 and 60% O_2 . No significant PO_2 effect was found by contrast on the swimming performance although non-significant trends could be observed. P_{crit} was found to be in the range between 4.51 kPa and 6.28 kPa O_2 (S_{crit} 21.6 and 30% O_2) and a high interindividual variability was observed especially expressed

towards the lowest oxygen levels tolerated. Burst capacity of Polar cod can be estimated to be low and together with the mortality observed during the experiments suggests a narrow scope of survival.

4.2.2 Hypoxia tolerance of Polar cod at different temperatures

As discussed in chapter 1.2, temperature is expected to affect hypoxia tolerance mainly by increasing the metabolic demand for oxygen and to a lesser degree by concurrently decreasing oxygen solubility of water and blood. Therefore, we stated within the third hypothesis that a temperature of 10°C will decrease hypoxia tolerance of Polar cod. To assess the temperature effect on hypoxia tolerance in the study species the results of the present study will be compared to the hypoxia tolerance measured at 2.5°C by Sarah Kempf in the following.

A clear decrease in hypoxia tolerance of Polar cod could be observed at 10°C. Most strikingly the oxygen saturation range tolerated decreased at the higher temperature resulting in an increased P_{crit} and P_{cmax} as will be discussed more in detail later on.

Despite this strong thermal effect on the tolerated oxygen range the overall regulatory ability of Polar cod did not decrease as can be seen in the ability to regulate its SMR over the whole oxygen saturation range tolerated (**Figure 11**) at both temperatures. The increase of SMR with decreasing PO_2 levels was also observed at 2.5°C, interestingly over a similar oxygen saturation range (2.5°C: until about 35% O_2 , 10°C: until about 40% O_2). This is further emphasizing the strength of the regulatory capacity of Polar cod as the actual oxygen concentration in the water is 20% lower at 10°C compared to 2.5°C (**Table 8**) and the animals had a higher oxygen demand due to a 5-fold higher SMR.

Despite an initial regulation of MMR at 10°C (**Figure 18**) the P_{cmax} was strongly increased to 14.62 kPa – 10.45 kPa (70 – 50%) O_2 at 10°C compared to 9.86 – 5.27 kPa (45 – 25%) O_2 at 2.5°C. This resulted in a non-significant decrease of AS beginning at 70% O_2 at 10°C (**Figure 13**, **Figure 14**) compared to 30% O_2 at 2.5°C. Beyond P_{cmax} MMR decreased at a higher rate (**Figure 18**), which was similar at both temperatures (1 – 1.4 mmol O_2 /h/kg per PO_2 level at 10°C, 1 mmol O_2 /kg/h per PO_2 level at 2.5°C).

The most severe effect of temperature on hypoxia tolerance could be seen when examining the P_{crit} . Whereas Polar cod exhibit a remarkable low P_{crit} of 1.01 kPa (S_{crit} 4.81%) O_2 at 2.5°C a temperature increase of 7.5°C caused the P_{crit} to increase to about 5.22 kPa (S_{crit} 25%) O_2 (see chapter 4.2.1). Although the thermally induced decrease of oxygen solubility in the water accounts for a 20% decline in oxygen concentration at a respective oxygen saturation this cannot solely explain the shift of P_{crit} and P_{cmax} because both parameters increased by 50% compared to 2.5°C. Thus, temperature effects on the organism have to play a role, likewise.

The temperature effect on P_{crit} is a known phenomenon that was also observed in other species and is mainly caused by increasing metabolic demand (Pörtner 2010; McBryan et al. 2013). Pörtner 2010

suggests that P_{crit} rises in parallel with SMR. This relationship could clearly be observed in this study with SMR increasing by 5 times from 2.5°C to 10°C and the increase in P_{crit} lies in the same magnitude (1.01 kPa O_2 at 2.5°C to approx. 5.22 kPa (25%) at 10°C). This is emphasising a strong interrelation between hypoxia tolerance and maintenance costs (Mandic et al. 2009; McBryan et al. 2016; Chabot and Claireaux 2008; Remen et al. 2013). Interestingly with regard to the discussion of 10°C as pejus temperature for Polar cod (chapter 4.1) Pörtner 2010 suggests that beyond pejus temperature hypoxaemia sets in due to thermal limitation and that will finally cause P_{crit} to rise. Thus, the increase of P_{crit} gives a further indication that 10°C lies within the pejus temperature range of Polar cod. Moreover, Pörtner 2010 states that within the thermal optimum and close to pejus temperature P_{cmax} is minimal supporting the finding that 10°C is situated at the upper range of the pejus temperature range as P_{cmax} rose to approx. 12.53 kPa O_2 (60% O_2) at 10°C in comparison to approx. 7.38 kPa O_2 (35% O_2) at 2.5°C. As the thermal optimum for Polar cod is suggested to be between 3 and 6°C (Drost et al. 2014; Kunz et al. 2016; Laurel et al. 2016; Laurel et al. 2017) and the temperature preference between 2.4 and 4.4 °C (Schurmann and Christiansen 1994) a P_{cmax} of 7.38 kPa O_2 can be considered to be close to the P_{cmax} minimum.

Furthermore, with regard to P_{crit} it is interesting that the intercept of MMR with baseline SMR could not be shown experimentally but had to be defined mathematically at 2.5°C as animals ceased swimming at the lowest oxygen levels and also the resulting RMR measured in the non-swimming animals did not decrease below SMR. As discussed in chapter 4.2.1 this is in strong contrast to the observation of high interindividual variability when approaching limiting oxygen levels observed at 10°C. The fact that some animals reached P_{crit} while others still had swimming capacity facilitated the determination of the intercept of MMR and baseline SMR at 10°C experimentally. The higher interindividual variability at 10°C compared to 2.5°C together with a higher P_{cmax} at the higher temperature is also leading to an overlapping SD of SMR with MMR starting at 70% O_2 whereas at 2.5°C SD was not observed to overlap before the intercept of MMR and SMR.

As already suggested (chapter 4.2.1), the observed differences in interindividual variability between the temperatures could be a result of the vicinity of 10°C to the upper critical temperature of Polar cod. That the interindividual variability is due to different weight and sizes of the animals in the different studies is unlikely because both weight and size were lying in the same range in both studies (2.5°C: 19.75 ± 1.35 cm, 39 ± 9.5 g, 10°C: 19.79 ± 1.94 cm, 41.3 ± 10.1 g). General effects of size and weight on metabolic rate could not be assessed statistically as data were neither normally distributed nor exhibited homoscedasticity.

In comparison to other species, the hypoxia tolerance of Polar cod can be defined as high (when considering P_{crit} solely). This can be seen when setting the P_{crit} of Polar cod into relation to the P_{crit} values of a variety of other teleosts reviewed by Rogers et al. 2016 (**Figure 25**). At 2.5°C Polar cod is

one of the species with the lowest P_{crit} . The high hypoxia tolerance is further emphasized by the direct comparison with another subarctic species the Greenland cod *Gadus ogac*. *G. ogac* exhibits a P_{crit} of 8.66 kPa O_2 (S_{crit} 40.4% O_2) at 1°C compared to 1.01 kPa O_2 at 2.5°C for Polar cod (Corkum and Gamperl 2009). Also after a five-fold increase of P_{crit} due to the temperature effect observed, the P_{crit} of *B. saida* remains low in comparison to other species. For example, *G. ogac* displays a P_{crit} of 11.54 kPa O_2 (S_{crit} 54.8% O_2) when acclimated to 8°C for 6 weeks in comparison to 4.51 – 6.28 kPa O_2 (S_{crit} 21.6 - 30% O_2) in Polar cod at 10°C (Corkum and Gamperl 2009). Compared to a temperate gadid species and potential predator (Renaud et al. 2012), the Atlantic cod *Gadus morhua*, the P_{crit} can be found in a similar range for both species at a temperature of 10°C (*G. morhua*: P_{crit} 4.84 kPa O_2 , S_{crit} : 23.2% O_2 at 10°C (Chabot and Claireaux 2008; Schurmann and Steffensen 1997)). Although from an ecological point of view this does not automatically translate in an advantage for Polar cod, it still emphasizes the remarkable hypoxia tolerance of this species when considering that 10°C belong to the thermal optimum window of Atlantic cod (Chabot and Claireaux 2008; Righton et al. 2010) by contrast to Polar cod, which at 10°C is exposed to a temperature of its pejus temperature range.

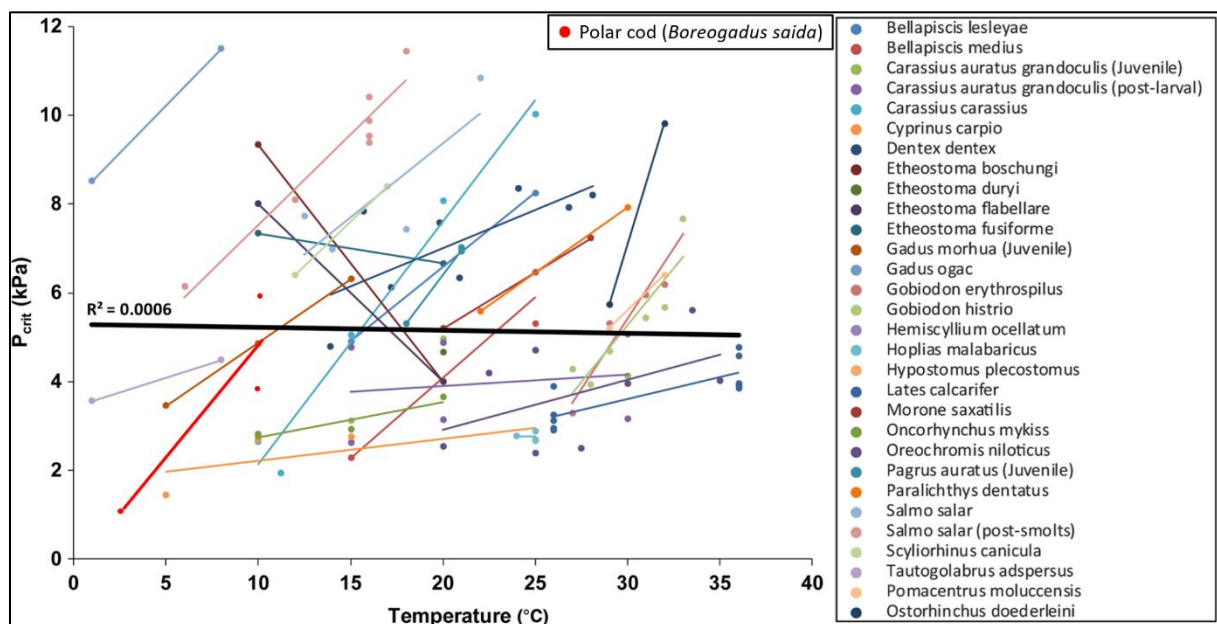


Figure 25 The effect of temperature on inter-species critical oxygen level (P_{crit} ; black line) and intra-species P_{crit} (coloured lines). The figure is originating from Rogers et al.2016 and supplemented with data for Polar cod coming from the present study and the master's thesis of Sarah Kempf.

Another feature of the hypoxia tolerance of Polar cod compared to other teleosts is its ability for oxy regulation. This is enabling this species to maintain its AS over a temperature dependent range of ambient oxygen saturations. As reviewed by Chabot and Claireaux 2008 oxy regulation was not found in Atlantic cod, turbot (*Psetta maxima*), seabass (*Dicentrarchus labrax*) and sole (*Solea solea*). Also Greenland cod did not display an oxy regulative strategy (Corkum and Gamperl 2009). Since the aerobic

scope describes the oxygen available for (excess) activity, capacity for oxy regulation can be regarded as an advantage. A maintained AS does allow to escape hypoxic water, enter moderately hypoxic water to seek shelter or to search for prey as will be discussed more in detail in chapter 4.4 (Domenici et al. 2013; Claireaux et al. 2000; Herbert and Steffensen 2005). But what are the underlying mechanisms that allow Polar cod to display this oxy regulative strategy at low and at high temperatures as well as the extraordinary low P_{crit} ?

4.3 Underlying mechanisms

As could be seen in the chapter 4.2.1 and 4.2.2, Polar cod displays a high hypoxia tolerance with regard to its regulatory capacity and its low P_{crit} . Hereafter, different physiological properties will be discussed to investigate the question which mechanisms facilitate this remarkable hypoxia tolerance.

So far direct responses to declining ambient oxygen levels like increase of ventilation and cardiac output have been discussed. They suit as mechanism supporting the maintenance of SMR independent from ambient oxygen. At ambient oxygen saturations lower than 45 - 35% O_2 SMR levels off but can nevertheless be sustained over quite a range of oxygen levels especially at 2.5°C. This indicates that the hypoxia tolerance of Polar cod does not only rely on direct physiological responses but is also facilitated by general physiological features of this species. The hypothesis of involvement of other physiological mechanisms finds further support when considering the fact that the capacity for oxygen delivery has to be sufficient to cover the additional costs arising from increased ventilatory and cardiac activity. And that at PO_2 levels at which other fish species already face their critical oxygen saturation (Rogers et al. 2016; Corkum and Gamperl 2009).

Factors that could explain the oxy regulation and low P_{crit} of Polar cod aside from direct responses to hypoxia are a high ability for oxygen extraction, delivery and a low oxygen demand as will be discussed more in detail in the following (McBryan et al. 2013; Chabot and Claireaux 2008).

The baseline costs of Polar cod measured by Sarah Kempf at 2.5°C are with 0.44 mmol O_2 /kg/h strikingly low and could be a major reason for the low P_{crit} found for Polar cod at this temperature. An interrelation between hypoxia tolerance and low metabolic demand was also found by Mandic et al. 2009 who investigated several species of sculpins of the family Cottidae and by McBryan et al. 2016 who found this correlation investigating hypoxia tolerance of several subspecies of killifish *Fundulus heteroclitus*. Also Remen et al. 2013 suggests that the metabolic requirement at rest can be used to gauge P_{crit} in post-smolts of Atlantic salmon (*Salmo salar*).

Other studies measuring the SMR of Polar cod found higher SMR at comparable temperatures, however (**Table 7**). Kunz et al. 2016 who measured the SMR of Polar cod and Atlantic cod in the same experimental setup even found the SMR for *G. morhua* to be lower (3°C: 2.1 mmol O_2 /kg/h, 8°C: 2.7

mmolO₂/kg/h) than for *B. saida* (3°C: 3 mmolO₂/kg/h, 8°C: 3 mmolO₂/kg/h). When comparing the P_{crit} of both species around their respective thermal optimum the P_{crit} of *G. morhua* is with about 4.18 kPa (20%) O₂ nevertheless distinctly higher than the P_{crit} found for Polar cod (Chabot and Claireaux 2008; Righton et al. 2010). This suggests that a low metabolic demand cannot be considered as the pivotal mechanism facilitating hypoxia tolerance in the study species.

Table 7 Baseline SMR, SMR and RMR of *B. saida* measured at different temperatures and by different studies. Measuring and calculation method vary between studies.

measurement	temperature °C	mmol O ₂ /kg/h	
SMR	-1.5	1.25	<i>Holeton 1974</i>
SMR	0	3.22	<i>Kunz et al. 2018</i>
SMR	0	3.18	<i>Kunz et al. 2016</i>
RMR	1	1.69	<i>Drost et al. 2016</i>
SMR	1	1.88	<i>Steffensen et al. 1994</i>
baseline SMR	2.5	0.44	<i>Kempf</i>
SMR	2.5	1.1	<i>Kempf</i>
SMR	3	3.03	<i>Kunz et al. 2018</i>
SMR	3	3.18	<i>Kunz et al. 2016</i>

Another physiological feature advantageous for hypoxia tolerance is an increased ability for oxygen extraction. Oxygen extraction is accomplished by several drivers one being the oxygen extraction capacities at the gills. Large gill surface area has been shown in species inhabiting periodically hypoxic environments (reviewed in (Mandic et al. 2009) and an increase of gill surface area as response to acclimation to hypoxia is reported in several teleost species (Nilsson 2007; Love and Rees 2002; Richards and Farrell 2009). In scaleless carp *Gymnocypris przewalskii* a modulation of the gills also with regard to diffusion distance can be seen already after 12 – 24h in severe hypoxia (~3% O₂) (Matey et al. 2008). However, Polar cod neither lives in a habitat with frequent hypoxia events nor were the animals acclimated to hypoxia apart from exposure to hypoxia during the experiments. Furthermore, the cold habitat temperatures of Polar cod do not favour increased gill surface area because of the high oxygen saturations in polar waters and low metabolic demands at these temperatures (Farrell and Richards 2009). Thus, although increased gill surface as response to hypoxia exposure cannot be excluded, an inherent large gill surface of Polar cod resulting in high hypoxia tolerance does not appear likely. It has been shown, however, that warm acclimation leads to an increase in gill respiratory surface area (McBryan et al. 2016) and one could hypothesise that increased gill surface area induced by long-term acclimation to 10°C could have helped Polar cod to maintain some of its hypoxia tolerance at this temperature. As 10°C lies in the pejus temperature range, however, it appears questionable to which extent increased oxygen extraction capacity at the gills would allow to serve for hypoxia

tolerance when normal performances like growth or reproduction are ceased at this temperature already at normoxic conditions.

But the gills are not the only organ at which oxygen extraction takes place.

In Antarctic icequab (*Rhigophila dearborni*) (SMR: 0.52 mmol O₂/kg/h) cutaneous respiration can account for up to 35% of total oxygen uptake (Wells 1986). Also in the Antarctic Icefish *Chaenocephalus aceratus* a portion of 40% of cutaneous respiration of the total respiration was measured (Hemmingsen and Douglas 1970), although claimed to be a potential overestimation by Farrell and Steffensen 2005 since being extrapolated from tail skin. The fraction of cutaneous respiration measured in the nototheniids *Trematomus bernachii* (SMR: 1.55 mmol O₂/kg/h) and *Pagothenia borchgrevinki* (SMR: 1.56 mmol O₂/kg/h) accounted for 9 - 17%, respectively (Wells 1987). Wells 1987 suggests an interrelation between cutaneous respiration, scalelessness and low metabolic rate with species fulfilling the mentioned features having a higher proportion of cutaneous respiration. Likewise, Farrell and Steffensen 2005 marked that an increased contribution of cutaneous respiration in polar fish might be possible due to an overall reduced metabolic rate and increased oxygen solubility in the plasma. Polar cod fulfils the preconditions ascribed to cutaneous respiration partly. The study species possesses reduced scales (Evseenko and Bolshakova 2020) and the SMR measured by some studies lies in the range of the SMR found in the Antarctic species mentioned (**Table 7**). The role of cutaneous oxygen uptake in fish has been discussed critically, however. As reviewed by Farrell and Steffensen 2005, Holeyton 1975 questioned the high share of cutaneous respiration reported. He argued that the fraction of blood transported to the skin and the absorption capacity of this well-oxygenated blood would not be sufficient to facilitate the cutaneous oxygen uptake measured. Furthermore, he addressed the high functional adaptation of the gills. Convection is created using a counter current equipped with a branchial pump whereas cutaneous respiration has to extract from a passive flow along the skin surface. In addition, the blood water diffusion barrier at the skin of *Chaenocephalus aceratus*, the Blackfin ice fish, is an order of magnitude greater compared with gill lamellae. A compensation for the higher diffusion barrier by surface area cannot be expected as depending on the activity level of the fish species the gill area per cm² body surface is up to 8-fold higher (Common mackerel, *Scomber scombrus*: 8.38 cm² gill area per cm² body surface, flounder, *Pseudopleuronectes americanus*: 1.25 cm² gill surface per cm² body surface) (Gray 1954). It is furthermore not clear if oxygen absorbed by cutaneous respiration does supply to the general metabolic demand of the animal or is used exclusively to support metabolism of the skin (Farrell and Steffensen 2005).

Thus, also cutaneous respiration does not appear to have the potential to be the pivotal underlying mechanism of Polar cod's hypoxia tolerance. This is on the one hand due to the physiological constraints discussed above and on the other because it remains questionable to which degree Polar cod fulfil the attributes of fish assumed to be in favour of cutaneous respiration. To my knowledge no

measurements of cutaneous oxygen uptake exists for Polar cod. Investigations in this regard would help to confirm or refuse the suggestion made.

Not only the oxygen uptake is important regarding oxygen supply but also the oxygen transport within and between cells has to be considered.

It has been suggested that the intra- and intercellular diffusion of oxygen is enhanced through high lipid contents in the cell and the membrane (Sidell 1991, 1998). On the basis of increased solubility and diffusivity characteristics of oxygen in lipids it is hypothesised that in the presence of lipid droplets the rate of oxygen diffusion between capillaries and mitochondria is accelerated independent of the PO_2 gradient (Sidell 1991). In terms of hypoxia tolerance this could be an advantage as it could help to sustain the oxygen supply to tissues despite a low oxygen saturation of the blood during low ambient oxygen availability. Also exercise could benefit from this feature due to an enhanced oxygen diffusion to muscle cells even at low ambient PO_2 levels. To further investigate the applicability of this hypothesis the time component would have to be considered by assessing oxygen diffusion rates in lipid rich and lipid poor muscle tissue in relation to oxygen demand of the tissues during exercise.

Furthermore interesting is the fact that the thermally induced reduction of oxygen solubility is minor in nonpolar solvents by contrast to polar solvents like water or cytoplasm (Battino et al. 1968; Sidell 1991). Thus, high lipid contents in cells and membranes could be advantageous for oxy regulation when facing hypoxia and high temperature concurrently.

Polar cod occupies a central position in the Arctic food web due to its high lipid content (Hop and Gjørseter 2013). As reviewed by Hop and Gjørseter 2013 the major lipid fraction is stored in the liver accounting for 60-65% wet weight whereas the muscle lipids are rather low with 3% wet weight. Compared to Antarctic species which Sidell 1991, 1998 is considering with his hypothesis the muscle lipid content of Polar cod is strikingly low not supporting a major contribution of lipids to oxygen diffusion and absorption. However, it has to be noted that the estimate of muscle lipids for Polar cod were derived from whole carcasses (without liver, intestine and gonads) and high muscle lipid content of 37% of the Antarctic species *Trematomus borchgrevinki* and *Dissostichus mawsoni* was derived only from red muscle and is depicting dry weight (Lin et al. 1974). Lipid content in the carcass reported as dry weight is 14% in Polar cod leaving space for a role of lipids in oxygen diffusion. Looking at the reason for high lipid content in polar fish a contribution of lipids to oxygen diffusion and uptake in *B. saida* finds further support.

The low anaerobic capacities in muscles of Polar cod discussed in chapter 4.2.1 could indicate elevated mitochondrial densities (Farrell and Steffensen 2005). High mitochondrial densities in Antarctic and Arctic fish cause a space scarcity not only for glycogen stores but also for energy storage within the cell (Farrell and Steffensen 2005). As lipids have a higher energetical value than protein fishes with high

mitochondrial densities tend to accumulate lipids in their intra and intercellular space in high densities (Farrell and Steffensen 2005). The trend to increased capacity of the beta-oxidation pathway is further supporting the possible interrelation between these observations (Gilles et al. 1989). Therefore, a higher lipid content in Polar cod muscle compared to temperate fish appears possible but clearly requires further investigation. To investigate the role of nonpolar solvents in hypoxia tolerance it would be also interesting to investigate the lipid content of another subarctic species *Gadus ogac* who displays by far a higher P_{crit} than Polar cod (Corkum and Gamperl 2009). To my knowledge no information is available considering lipid content of muscle tissues in this species.

In conclusion, of the physiological mechanisms discussed only an enhanced oxygen affinity and an increased oxygen diffusion rate due to high cellular and membrane lipid content appears to bear a potential as physiological feature underlying the hypoxia tolerance of Polar cod. Also, an interplay of high lipid content and a relatively low oxygen demand could be taken into account. To sincerely consider high lipid contents as underlying feature, however, more knowledge about the actual tissue lipid concentration in Polar cod is required plus temporal and quantitative information about oxygen uptake and diffusion rate in lipid rich tissues in relation to oxygen demand. Future investigations of the physiological features underlying the low P_{crit} and regulative capacity of Polar cod should also consider other physiological mechanism of the respiratory cascade such as blood oxygen affinity for instance.

4.4 Ecological implications

Increasing water temperature and reduced oxygen availability have to be expected for the Arctic Ocean in the future. This study is the first to investigate the physiological responses of Polar cod to decreasing ambient oxygen availability under high temperature. In the following the potential ecological implications resulting from the physiological responses observed in this study will be discussed.

The results of this research show that water masses of 10°C are tolerated by Polar cod and can serve as short term feeding grounds for this species. As described in chapter 4.1 the AS and swimming capacity of Polar cod found at 10°C are in accordance with observation of this species in water masses with a temperature as high as 9 - 13.5°C in the wild (Craig et al. 1982; Moulton and Tarbox 1987). Although a temperature of 10°C is not supportive of a thriving population of Polar cod as growth and reproduction are strongly reduced if not diminished at this temperature (unpublished data Dr. Felix Mark), prey residing in water masses of about 10°C appears to be still available for Polar cod. This is in agreement with the suggestion of Moulton and Tarbox 1987 that an accumulation of zooplankton is the reason for the presence of *B. saida* in high temperature waters.

Although *B.saida* are typically found in a depth range of 350 to 500 m (Crawford et al. 2012; Majewski et al. 2016) the warm water masses they sought were with 6 – 7 m of shallow depth (Moulton and Tarbox 1987). As these shallow waters are extensively prone to ocean warming (IPPC 2014) a future rise in temperature could restrict Polar cod from profiting from prey availability in these water masses. The combination of a temperatures around 10°C and deoxygenation could restrict foraging habitat of this species, likewise. Zooplankton accumulation in the mentioned warm water layer was related to the pycnocline (Moulton and Tarbox 1987). As water masses around pycnoclines are known for potential hypoxia due to intense respiration by animal and bacteria abundance (Domenici et al. 2013; Diaz and Rosenberg 2008) they could be an occasion for Polar cod to encounter hypoxia at high temperatures. At 10°C water temperature, Polar cod displays still a relatively low P_{crit} . Thus, frequent warm water masses with low oxygen availability can be expected to be possible for this species. Due to a decrease of AS starting at 70% O_2 , however, the capacity for concurrent foraging and digestion might be impacted. Jourdan-Pineau et al. 2010 found that the higher MMR in fed seabass (*Dicentrarchus labrax*) during exercise compared to starved animals under normoxic conditions did vanish when exposed to 50% ambient oxygen saturation. This indicates a limitation of meeting the costs of swimming and SDA concurrently at these oxygen levels. Thus, the suitability of water masses around the pycnocline as foraging grounds for Polar cod could be decreased due to high temperature as the oxygen levels at which AS was decreased were 30% higher at 10°C compared to 2.5°C. The observation of a maintained U_{crit} over decreasing oxygen saturation observed in seabass (Jourdan-Pineau et al. 2010) and in the present study cannot be interpreted as indication for sufficient oxygen to cover concurrent exercise and SDA. This has to be inferred from the observation that MMR between fed and starved seabass at decreased PO_2 did not differ thus indicating a prioritisation of aerobic exercise over digestion (Jourdan-Pineau et al. 2010). To predict the suitability of water masses of high temperature and decreased oxygen availability as foraging grounds for Polar cod experiments evaluating MMR of fed animals under exercise would deliver further insight.

Potential future decrease in oxygen availability in bottom water masses in Arctic fjord systems can be hypothesised not to restrict habitat and foraging grounds of Polar cod by contrast. As explained in chapter 1.2 bottom waters in Arctic fjords like Billefjorden, the point of origin of the experimental animals, can be expected to decrease in oxygen availability due to hydrodynamic changes. As these water masses are not expected to heat to a temperature of 10°C (Promińska et al. 2018) it would be useful to gauge the hypoxia tolerance of *B. saida* at temperatures between 2.5°C and 10°C. The strong interrelation of SMR and P_{crit} mentioned in chapter 4.2.2 does allow to infer the thermal sensitivity of hypoxia tolerance (Remen et al. 2013). Although temperature can have a severe influence on hypoxia tolerance in ranges in which AS is not decreased yet as it was shown in the present study and for killifish *Fundulus heteroclitus* (McBryan et al. 2013) hypoxia tolerance of Atlantic cod displayed temperature

insensitivity across its thermal optimum range (Chabot and Claireaux 2008). Therefore, and due to the fact that Polar cod were capable of metabolic compensation within their thermal optimum window (Kunz et al. 2018) it can be suggested that the low P_{crit} and the oxy regulatory capacity observed at 2.5°C may stay in a similar range until a temperature of 6°C (Kunz et al. 2018). Following these conclusions foraging grounds in oxygen reduced fjord bottom waters appear not to be restricted in the future due to Polar cod's remarkable hypoxia tolerance at 2.5°C. A crucial precondition for this conclusion is, however, that benthic communities are tolerant against the extents of oxygen scarcity so that food abundance will not decrease or even vanish (Diaz and Rosenberg 2008).

A known phenomenon about *B. saida* is the formation of big schools (Crawford and Jorgenson 1996; Aune et al. 2021; Welch et al. 1993; Hop et al. 1997) to swarm sizes up to 900 million individuals (Crawford and Jorgenson 1996). As will be discussed hereafter increased temperatures and decreased oxygen availability can be expected to impact school formation and to increase predation risk of Polar cod schools.

An accumulation of an immense number of individuals like mentioned above can be expected to decrease ambient oxygen saturation within the school (Domenici et al. 2013). As was seen in schools of striped mullet *Mugil cephalus* the difference between dissolved oxygen within and outside fish schools with a length of 150 m was differing by up to 28% (McFarland and Moss 1967). Decrease of dissolved oxygen is also observed in aquaculture where a decrease of oxygen saturation in the centre of sea cages is reported to levels as low as 30% O₂ (Oppedal et al. 2011). Thus, the high hypoxia tolerance of Polar cod observed at 2.5°C together with the high oxygen solubility in water at low temperature might be clearly advantageous for the formation of fish schools of the size reported. One could even hypothesize that the extent of the schools is the evolutionary reason for Polar cod to develop high hypoxia tolerance. In turn this also implicates that at higher temperatures when oxygen consumption is increased while oxygen solubility of the water is decreased the formation of schools of the reported size might be problematic (Domenici et al. 2013). For example, with regard to feeding since one suggestion for gathering of Polar cod is prey availability (Moulton and Tarbox 1987; Aune et al. 2021). As discussed above the decreasing AS at oxygen saturations lower than 70% at 10°C could impact foraging and digestion capacity, thus impacting feeding during schooling.

A general decreased ambient oxygen availability was observed to result in a horizontal expansion of school volume to enhance water mixing and oxygen availability for individuals (Domenici et al. 2013). Horizontal volume extension was found to be favoured before vertical expansion potentially due to higher hydrodynamically and thus energetically advantage for the individuals (Abrahams and Colgan 1985; Domenici et al. 2013). A horizontal formation is expected, however, to decrease the chance for visual predator detection (Abrahams and Colgan 1985; Domenici et al. 2013). As the hypoxia tolerance of Polar cod is clearly decreased at a temperature of 10°C compared to lower temperatures the

threshold inducing an increase in school volume can be hypothesized to be at higher oxygen saturations. Thus, it might be possible that a combination of increased temperature and decreased ambient oxygen availability leads to an increased predation risk for Polar cod schools. Whereas the predation of ectothermic species underlies the constraints of decreased oxygen availability likewise (Domenici et al. 2013) mammalian and avian predators that constitute a major fraction of the higher trophic level that is feeding on Polar cod (Welch 1992; Crawford et al. 2012) can be expected to be in advantage when aquatic oxygen gets restricted and temperature does increase (Domenici et al. 2013).

Also for the individual an increased predation risk is suggested due to decreased escape potential. As explained in chapter 4.2.1, at 10°C a change of the general burst pattern was observed. Although total burst capacity did not decrease in comparison to 2.5°C, the number of bursts per minute remarkably declined due to higher swimming time but also due to bursting at lower velocities. In the wild that could translate in reduced escape capacity as phosphocreatine stores and anaerobic capacity might already be partly exploited at the beginning of the escape reaction and thus preventing high burst frequency at the end of chasing or during a surprising predation event. As the general escape capacity of Polar cod is estimated to be low due to minor burst capacity (Kunz et al. 2018) a further decrease of burst potential during predator prey interaction can be estimated as strongly disadvantageous for Polar cod.

The general inspection of hypoxia tolerance of Polar cod at 10°C emphasizes a weakness of the hypoxia tolerance but also a potential for a behavioural escape reaction of this species.

Despite the steep increase of P_{crit} at 10°C, it remains still very low when compared to other species (see chapter 4.2.2). This increase of P_{crit} might be, however, nevertheless threatening for Polar cod due to its narrow scope of survival. Therefore, the remaining swimming capacity until an O_2 saturation of 40% and the general increase of swimming activity at 10°C compared to 2.5°C observed during the experiments could facilitate this species to escape hypoxic water masses and therefore prevent an exposure to P_{crit} . Different strategies can be observed with some species reducing their activity under hypoxic situations and other mostly highly active species increasing activity what is interpreted as avoidance reaction to escape hypoxic zones (Domenici et al. 2013). Atlantic cod was observed to display a mixture of both reactions depending on severity of oxygen scarcity (Claireaux et al. 2000; Herbert and Steffensen 2005). Whereas the outcome of the present study can only indicate that the potential for an avoidance reaction does exist as can be seen in maintained U_{crit} until an oxygen saturation of 40% O_2 , further experiments could reveal which response Polar cod is displaying when given the possibility for escaping hypoxia.

As last point of this chapter the extrapolation of the assessed data to the field will be addressed. With regard to an extrapolation it has to be considered that an increase of water temperature to 10°C is only predicted for surface waters (IPPC 2014), while the depth mainly chosen by Polar cod (Crawford et al. 2012; Majewski et al. 2016) probably will inherit lower water temperatures. Thus, *B. saida* in the wild will not have the chance to acclimate to a constant temperature of 10°C before encountering hypoxic situations. Moreover, an acclimation is not reasonable for this species since 10°C as pejus temperature is not supporting population survival. Cross acclimation meaning the investigation of the impact of one environmental stressor after the acclimation to another stressor showed that long-term acclimation to high temperatures clearly improves hypoxia tolerance (McBryan et al. 2013). Future research should thus consider the effect of temperature on hypoxia tolerance during acute warming to pay attention to an ecologically more relevant scenario like marine heatwaves (Hu et al. 2020; Fazel-Rastgar 2020).

5 Conclusion

The present study is the first to investigate the combined effect of ocean warming and deoxygenation on an Arctic key stone species the Polar cod.

The first objective was to contribute to a better understanding about the upper thermal limit of the study species. Concordantly, the temperature of 10°C was hypothesised to be close to the upper pejus temperature of *B. saida*. The outcome of the present study confirms this first hypothesis. Although Polar cod maintained their swimming capacity and AS compared to measurements at 2.5°C, the finding that P_{cmax} strongly increased together with physiological limitation of other processes at or before the study temperature clearly assign 10°C to the pejus temperature range. Based on the literature discussed I further suggest the beginning of the pejus temperature range to lie between 6 and 8°C. With regard to ecological implications this suggests that Polar cod are able to tolerate 10°C short-term, for foraging activities for instance. A permanent thermal environment of 10°C by contrast threatens population survival of the study species.

The second objective aimed at investigating the combined effect of a temperature of 10°C and hypoxia on the metabolic and swimming capacity of *B. saida*. Based on the first hypothesis I expected the maximum oxygen supply capacity to decrease at high ambient PO_2 levels (high P_{cmax}) leading to a restriction of swimming performance beginning at high PO_2 levels, likewise. P_{cmax} and the swimming performance observed confirm the second hypothesis, as a decrease in both parameters was observed at ambient O_2 levels of 30% higher oxygen saturation than at 2.5°C. Despite the clear impact of a combination of high temperature and hypoxia on metabolic and swimming capacity, the overall swimming performance stayed comparable to swimming observed at 2.5°C until 40% ambient O_2 . Ecologically this could be advantageous for Polar cod to escape moderate hypoxic water masses or to frequent moderate hypoxia for shelter.

To investigate to what degree the temperature of 10°C alters the hypoxia tolerance of Polar cod was the third research objective. The hypothesis that P_{crit} would be strongly increased at 10°C compared to 2.5°C was confirmed. P_{crit} at 10°C was observed to be with 5.22 kPa (S_{crit} 25% O_2) five times higher compared to 2.5°C. Within the inter-species comparison - and considering 10°C belonging to the pejus temperature range - hypoxia tolerance of *B. saida* at 10°C remains very high. Further it was hypothesised that the scope of survival will stay unaffected by temperature increase. Due to high SD of burst counts at both temperatures the investigation of the second hypothesis was restricted. Also, with regard to burst capacity as proxy for whole organism's anaerobic capacity, it is highly recommended to use the measurement of lactate or PCr in future investigations aiming at the assessment of the scope of survival of Polar cod. Due to the time course of mortality observed and the

fact that relative burst counts were low at both temperatures, a narrow scope of survival is indicated. This suggests a hypoxia tolerance strategy building on low P_{crit} rather than survival capacity at PO_2 levels below P_{crit} .

Additionally, potential underlying mechanisms of the hypoxia tolerance of Polar cod have been discussed in the present study. Of the mechanisms considered, which were low metabolic demand, cutaneous and gill respiration and increased oxygen diffusion rates in tissues facilitated by high lipid content, only the latter is suggested to bear a potential to facilitate the low P_{crit} and the high regulative capacity observed. The identification of the mechanisms or features underlying the hypoxia tolerance of Polar cod are a clear avenue for future research.

The outcome of this master's thesis underlines the high hypoxia tolerance of Polar cod even at an upper thermal limit temperature. Therefore, a combination out of increased temperature, as it is expected for the Arctic Ocean, and decreasing oxygen availability does not appear to be the major threat for adult specimen of the study species. Only considering the abiotic factors investigated, *B. saida* can be expected to keep its central role as key species in the Arctic food web.

6 References

- Abrahams, M. V.; Colgan, P. W. (1985): Risk of predation, hydrodynamic efficiency and their influence on school structure. In *Environmental Biology of Fishes* 13 (3), pp. 195–202.
- ADFG (1986): Alaska habitat management guide: life histories and habitat requirements of fish and wildlife. Juneau.
- Aune, M.; Raskhozheva, E.; Andrade, H.; Augustine, S.; Bambulyak, A.; Camus, L. et al. (2021): Distribution and ecology of polar cod (*Boreogadus saida*) in the eastern Barents Sea: A review of historical literature. In *Marine environmental research* 166, pp. 105–262.
- Battino, R.; Evans, F. D.; Danforth, W. F. (1968): The solubilities of seven gases in olive oil with reference to theories of transport through the cell membrane. In *Journal of the American Oil Chemists' Society* 45 (12), pp. 830–833.
- Beamish, F. W. (1978): Swimming capacity. In *Fish Physiology* 7, pp. 101–187.
- Bennett, A. F. (1990): Thermal dependence of locomotor capacity. In *The American journal of physiology* 259 (2), 253 - 258.
- Bradstreet, M. SW. (1986): Aspects of the biology of Arctic cod (*Boreogadus saida*) and its importance in Arctic marine food chains. Central and Arctic Region.
- Breitburg, D.; Levin, L. A.; Oschlies, A.; Grégoire, M.; Chavez, F. P.; Conley, D. J.; Zhang, J. (2018): Declining oxygen in the global ocean and coastal waters. In *Science* 356 (6371).
- Brewster, J. D.; Giraldo, C.; Choy, E. S.; MacPhee, S. A.; Hoover, C.; Lynn, B. et al. (2018): A comparison of the trophic ecology of Beaufort Sea Gadidae using fatty acids and stable isotopes. In *Polar Biology* 41 (1), pp. 149–162.
- Bullock, T. H. (1955): Compensation for temperature in the metabolism of poikilotherms. In *Biological Reviews* 30 (3), pp. 311–342.
- Chabot, D.; Claireaux, G. (2008): Environmental hypoxia as a metabolic constraint on fish: the case of Atlantic cod, *Gadus morhua*. In *Marine pollution bulletin* 57 (6-12), pp. 287–294.
- Chabot, D.; Steffensen, J. F.; Farrell, A. P. (2016): The determination of standard metabolic rate in fishes. In *Journal of fish biology* 88 (1), pp. 81–121.
- Claireaux, G.; Chabot, D. (2016): Responses by fishes to environmental hypoxia: integration through Fry's concept of aerobic metabolic scope. In *Journal of fish biology* 88 (1), pp. 232–251.
- Claireaux, G.; Lagardère, J.-P. (1999): Influence of temperature, oxygen and salinity on the metabolism of the European sea bass. In *Journal of Sea Research* 42, pp. 157–168.

- Claireaux, G.; Webber, D. M.; Lagardère, J.-P.; Kerr, S. R. (2000): Influence of water temperature and oxygenation on the aerobic metabolic scope of Atlantic cod (*Gadus morhua*). In *Journal of Sea Research* 44 (3-4), pp. 257–265.
- Clarke, A. (1983): Life in cold water: the physiological ecology of polar marine ectotherms. In *Oceanography and marine Biology* 21, pp. 341–453.
- Collins, M.; Knutti, R.; Arblaster, J.; Dufresne, J.-L.; Fichetfet, T.; Friedlingstein, P.; Gao, X.; Gutowski, W. J.; Johns, T.; Krinner, G.; Shongwe, M.; Tebaldi, C.; Weaver, A. J.; Wehner, M. (2013): Long-term Climate Change: Projections, Commitments and Irreversibility. In *Climate Change 2013: The Physical Science Basis. Contribution of Working Group I to the Fifth Assessment Report of the Intergovernmental Panel on Climate Change* (eds. T. F. Stocker, D. Qin, G.-K. Plattner, M. Tignor, S. K. Allen, J. Boschung, A. Nauels, Y. Xia, V. Bex, P. M. Midgley), pp. 1029-1136. Cambridge, UK and New York, NY, USA: Cambridge University Press.
- Corkum, C. P.; Gamperl, A. K. (2009): Does the ability to metabolically downregulate alter the hypoxia tolerance of fishes? A comparative study using cunner (*T. adspersus*) and Greenland cod (*G. ogac*). In *Journal of experimental zoology. Part A, Ecological genetics and physiology* 311 (4), pp. 231–239.
- Cottier, F.; Tverberg, V.; Inall, M.; Svendsen, H.; Nilsen, F.; Griffiths, C. (2005): Water mass modification in an Arctic fjord through cross-shelf exchange: The seasonal hydrography of Kongsfjorden, Svalbard. In *Journal of Geophysical Research* 110 (12).
- Craig, P. C.; Griffiths, W. B.; Haldorson, L.; McElderry, H. (1982): Ecological Studies of Arctic Cod (*Boreogadus saida*) in Beaufort Sea Coastal Waters, Alaska. In *Canadian Journal of Fisheries and Aquatic Sciences* 39 (3), pp. 395–406.
- Crawford, R. E.; Jorgenson, J. K. (1996): Quantitative Studies of Arctic Cod (*Boreogadus saida*) Schools: Important Energy Stores in the Arctic Food Web. In *Arctic* 40 (2), pp. 181–193.
- Crawford, R. E.; Vagle, S.; Carmack, E. C. (2012): Water mass and bathymetric characteristics of polar cod habitat along the continental shelf and slope of the Beaufort and Chukchi seas. In *Polar Biology* 35 (2), pp. 179–190.
- Curtin, N. A.; Kushmerick, M. J.; Wiseman, R. W.; Woledge, R. C. (1997): Recovery after contraction of white muscle fibres from the dogfish *Scyliorhinus canicula*. In *Journal of Experimental Biology* 200, pp. 1061–1071.
- Deutsch, C.; Penn, J. L.; Seibel, B. (2020): Metabolic trait diversity shapes marine biogeography. In *Nature* 585 (7826), pp. 557–562.

- Diaz, R. J.; Rosenberg, R. (2008): Spreading dead zones and consequences for marine ecosystems. In *Science* 321 (5891), pp. 926–929.
- Domenici, P.; Herbert, N. A.; Lefrançois, C.; Steffensen, J. F.; McKenzie, D. J. (2013): The Effect of Hypoxia on Fish Swimming Performance and Behaviour. In A. P. Palstra, J. V. Planas (Eds.): *Swimming Physiology of Fish*. Berlin, Heidelberg: Springer Berlin Heidelberg, pp. 129–159.
- Drost, H. E.; Carmack, E. C.; Farrell, A. P. (2014): Upper thermal limits of cardiac function for Arctic cod *Boreogadus saida*, a key food web fish species in the Arctic Ocean. In *Journal of fish biology* 84 (6), pp. 1781–1792.
- Drost, H. E.; Lo, M.; Carmack, E. C.; Farrell, A. P. (2016): Acclimation potential of Arctic cod (*Boreogadus saida*) from the rapidly warming Arctic Ocean. In *The Journal of experimental biology* 219 (19), pp. 3114–3125.
- Evseenko, S. A.; Bolshakova, Ya. Yu. (2020): Morphological Adaptations of Polar Cod *Boreogadus saida* (Gadidae) to a Life in the Ice Conditions. In *Journal of Ichthyology* 60 (2), pp. 230–235.
- Falk-Petersen, I.-B.; Frivoll, V.; Gulliksen, B.; Haug, T. (1986): Occurrence and size/age relations of polar cod, *Boreogadus Saida* (Lepechin), in Spitsbergen coastal waters. In *Sarsia* 71 (3-4), pp. 235–245.
- Farrell, A. P.; Richards, J. G. (2009): Defining Hypoxia. In J. G. Richards, A. P. Farrell (Eds.): *Hypoxia*, vol. 27. 1. ed. Amsterdam: Elsevier Acad. Press (*Fish Physiology*, 27), pp. 487–503.
- Farrell, A. Peter; Steffensen, J. F. (2005): *The Physiology of Polar Fishes*. Amsterdam, Boston: Elsevier.
- Fazel-Rastgar, F. (2020): Synoptic climatological approach associated with three recent summer heatwaves in the Canadian Arctic. In *Journal of Water and Climate Change* 11 (1), pp. 233–250.
- Fry, F. E. J. (1947): Effects of the environment on animal activity. In *Publications of the Ontario Fisheries Research Laboratory* 68, pp. 1–62.
- Fry, F. E. J. (1971): The effect of environmental factors on the physiology of fish. In *Fish Physiology*, pp. 1–98.
- Gilles, R.; Brouwer, M.; Carr, W. E. S.; Ellington, W. Ross; Engel, D. W.; Gleeson, R. A. et al. (Eds.) (1989): *Advances in Comparative and Environmental Physiology*. Berlin, Heidelberg: Springer Berlin Heidelberg.
- Gradinger, R. R.; Bluhm, B. A. (2004): In-situ observations on the distribution and behavior of amphipods and Arctic cod (*Boreogadus saida*) under the sea ice of the High Arctic Canada Basin. In *Polar Biology* 27 (10), pp. 595–603.

- Gray, I. E. (1954): Comparative study of the Gill Area of Marine Fishes. In *Biological Bulletin* 107 (2), pp. 219–225.
- Hemmingsen, E. A.; Douglas, E. L. (1970): Respiratory characteristics of the hemoglobin-free fish *Chaenocephalus aceratus*. In *Comparative Biochemistry and Physiology* 33 (4), pp. 733–744.
- Herbert, N. A.; Steffensen, J. F. (2005): The response of Atlantic cod, *Gadus morhua*, to progressive hypoxia: fish swimming speed and physiological stress. In *Marine Biology* 147 (6), pp. 1403–1412.
- Hochachka, P. W.; Mossey, M. K. (1998): Does muscle creatine phosphokinase have access to the total pool of phosphocreatine plus creatine? In *The American journal of physiology* 274 (3), 868-72.
- Holeton, G. F. (1974): Metabolic cold adaptation of polar fish: fact or artefact? In *Physiological Zoology* 47, pp. 137–152.
- Holeton, G. F. (1975): Respiration and morphometrics of hemoglobinless Antarctic icefish. In J. J. Cech, JR., D. W. Bridges, D. B. Horton (Eds.): *Respiration of Marine Organisms: Proceedings of the Marine Section, First Maine Biomedical Science Symposium*, pp. 198–211.
- Hop, H.; Graham, M. (1995): Respiration of juvenile Arctic cod (*Boreogadus saida*): effects of acclimation, temperature, and food intake. In *Polar Biology* 15, pp. 359–367.
- Hop, H.; Tonn, W. M.; Welch, H. E. (1997): Bioenergetics of Arctic cod (*Boreogadus saida*) at low temperatures. In *Canadian Journal of Fisheries and Aquatic Science* 54, pp. 1772–1784.
- Hop, Haakon; Gjøsæter, Harald (2013): Polar cod (*Boreogadus saida*) and capelin (*Mallotus villosus*) as key species in marine food webs of the Arctic and the Barents Sea. In *Marine Biology Research* 9 (9), pp. 878–894.
- Hu, S.; Zhang, L.; Qian, S. (2020): Marine Heatwaves in the Arctic Region: Variation in Different Ice Covers. In *Geophysical Research Letters* 47 (16).
- IPCC (2013): Annex I: Atlas of Global and Regional Climate Projections (eds. G. J. van Oldenborgh, M. Collins, J. Arblaster, J. H. Christensen, J. Marotzke, S. B. Power, M. Rummukainen, T. Zhou). In *Climate Change 2013: The Physical Science Basis. Contribution of Working Group I to the Fifth Assessment Report of the Intergovernmental Panel on Climate Change* (eds. T. F. Stocker, D. Qin, G-K Plattner, M. Tignor, S. K. Allen, J. Boschung, A. Nauels, Y. Xia, V. Bex, P. M. Midgley), pp. 1311-1393. Cambridge, UK and New York, NY, USA: Cambridge University Press.

- IPPC 2014: Climate Change 2014: Synthesis Report. Contribution of Working Groups I, II and III to the Fifth Assessment Report of the Intergovernmental Panel of Climate Change. With assistance of Core Writing Team, R. K. Pachauri and L. A. Meyer. Geneva, Switzerland.
- Jayne, B. C.; Lauder, G. V. (1994): How swimming fish use slow and fast muscle fibers: implications for models of vertebrate muscle recruitment. In *Journal of Comparative Physiology A* 175 (1), pp. 123–131.
- Johnston, I. A. (1977): A comparative study of glycolysis in red and white muscles of the trout (*Salmo gairdneri*) and mirror carp (*Cyprinus carpio*). In *J Fish Biology* 11 (6), pp. 575–588.
- Jourdan-Pineau, H.; Dupont-Prinet, A.; Claireaux, G.; McKenzie, D. J. (2010): An investigation of metabolic prioritization in the European sea bass, *Dicentrarchus labrax*. In *Physiological and Biochemical Zoology* 83 (1), pp. 68–77.
- Keeling, R. E.; Körtzinger, A.; Gruber, N. (2010): Ocean deoxygenation in a warming world. In *Annual review of marine science* 2, pp. 199–229.
- Kunz, K. L.; Claireaux, G.; Pörtner, H-O; Knust, R.; Mark, F. C. (2018): Aerobic capacities and swimming performance of polar cod (*Boreogadus saida*) under ocean acidification and warming conditions. In *The Journal of experimental biology* 221 (21).
- Kunz, K. L.; Frickenhaus, S.; Hardenberg, S.; Johansen, T.; Leo, E.; Pörtner, H-O et al. (2016): New encounters in Arctic waters: a comparison of metabolism and performance of polar cod (*Boreogadus saida*) and Atlantic cod (*Gadus morhua*) under ocean acidification and warming. In *Polar Biology* 39 (6), pp. 1137–1153.
- Larsen, J. N.; Anisimov, O. A., Constable, A.; Hollowed, A. B.; Maynard, N.; Prestrud, P.; Prowse, T. D.; Stone, J. M. R. (2014): Polar regions. In *Climate Change 2014: Impacts, Adaptation, and Vulnerability. Part B: Regional Aspects. Contribution of Working Group II to the Fifth Assessment Report of the Intergovernmental Panel on Climate Change* (eds. V. R. Barros, C. B. Field, D. J. Dokken, M. D. Mastrandrea, K. J. Mach, T. E. Bilir, M. Chatterjee, K. L. Ebi, Y. O. Estrada, R. C. Genova, B. Girma, E. S. Kissel, A. N. Levy, S. MacCracken, P. R. Mastrandrea, L. L. White), pp. 1567-1612. Cambridge, UK and New York, NY, USA: Cambridge University Press.
- Laurel, B. J.; Copeman, L. A.; Spencer, M.; Iseri, P. (2017): Temperature-dependent growth as a function of size and age in juvenile Arctic cod (*Boreogadus saida*). In *ICES Journal of Marine Science* 74 (6), pp. 1614–1621.
- Laurel, B. J.; Spencer, M.; Iseri, P.; Copeman, L. A. (2016): Temperature-dependent growth and behavior of juvenile Arctic cod (*Boreogadus saida*) and co-occurring North Pacific gadids. In *Polar Biology* 39 (6), pp. 1127–1135.

- Lefrançois, C.; Claireaux, G. (2003): Influence of ambient oxygenation and temperature on metabolic scope and scope for heart rate in the common sole *Solea solea*. In *Marine Ecology Progress Series* 259, pp. 273–284.
- Leo, E.; Kunz, K. L.; Schmidt, M.; Storch, D.; Pörtner, H-O; Mark, F. C. (2017): Mitochondrial acclimation potential to ocean acidification and warming of Polar cod (*Boreogadus saida*) and Atlantic cod (*Gadus morhua*). In *Frontiers in zoology* 14, p. 21.
- Lin, Y.; Dobbs, G. H.; Devries, A. L. (1974): Oxygen consumption and lipid content in red and white muscles of Antarctic fishes. In *The Journal of experimental zoology* 189 (3), pp. 379–386.
- Lønne, O. J.; Gulliksen, B. (1989): Site, age and diet of polar cod, *Boreogadus saida* (Lepechin 1773), in ice covered waters. In *Polar Biology* 9 (3), pp. 187–191.
- Love, J. W.; Rees, B. B. (2002): Seasonal differences in hypoxia tolerance in gulf killifish, *Fundulus grandis* (Fundulidae). In *Environmental Biology of Fishes* 63, pp. 103–115.
- Lowry, F. L.; Frost, K. J. (1981): Distribution, growth, and foods of Arctic cod (*Boreogadus saida*) in the Bering, Chukchi, and Beaufort seas. In *Canadian Field-Nature* 95, pp. 186–191.
- Lurman, G. J.; Bock, C. H.; Pörtner, H-O (2007): An examination of the metabolic processes underpinning critical swimming in Atlantic cod (*Gadus morhua* L.) using in vivo ³¹P-NMR spectroscopy. In *The Journal of experimental biology* 210 (21), pp. 3749–3756.
- Majewski, A. R.; Walkusz, W.; Lynn, Brittany R.; Atchison, S.; Eert, J.; Reist, J. D. (2016): Distribution and diet of demersal Arctic Cod, *Boreogadus saida*, in relation to habitat characteristics in the Canadian Beaufort Sea. In *Polar Biol* 39 (6), pp. 1087–1098.
- Mandic, M.; Todgham, A. E.; Richards, J. G. (2009): Mechanisms and evolution of hypoxia tolerance in fish. In *Proceedings. Biological sciences* 276 (1657), pp. 735–744.
- Marras, S.; Claireaux, G.; McKenzie, D. J.; Nelson, J. A. (2010): Individual variation and repeatability in aerobic and anaerobic swimming performance of European sea bass, *Dicentrarchus labrax*. In *The Journal of experimental biology* 213 (1), pp. 26–32.
- Masson-Delmotte, V.; Schulz, M.; Abe-Ouchi, A.; Beer, J.; Ganopolski, A.; Gonzalez Rouco, J. F.; Jansen, E.; Lambeck, K.; Luterbacher, J.; Naish, T.; Osborn, T.; Otto-Bliesner, B.; Quinn, T.; Ramesh, R.; Rojas, M.; Shao, X.; Timmermann, A. (2013): Information from Paleoclimate Archives. In *Climate Change 2013: The Physical Science Basis. Contribution of Working Group I to the Fifth Assessment Report of the Intergovernmental Panel on Climate Change* (eds. T. F. Stocker, D. Qin, G-K Plattner, M. Tignor, S. K. Allen, J. Boschung, A. Nauels, Y. Xia, V. Bex, P. M. Midgley), pp. 383-464. Cambridge, UK and New York, NY, USA: Cambridge University Press.

- Matey, V.; Richards, J. G.; Wang, Y.; Wood, C. M.; Rogers, J.; Davies, R. et al. (2008): The effect of hypoxia on gill morphology and ionoregulatory status in the Lake Qinghai scaleless carp, *Gymnocypris przewalskii*. In *Journal of Experimental Biology* 211 (7), pp. 1063–1074.
- McBryan, T. L.; Anttila, K.; Healy, T. M.; Schulte, P. M. (2013): Responses to temperature and hypoxia as interacting stressors in fish: implications for adaptation to environmental change. In *Integrative and comparative biology* 53 (4), pp. 648–659.
- McBryan, T. L.; Healy, T. M.; Haakons, K. L.; Schulte, P. M. (2016): Warm acclimation improves hypoxia tolerance in *Fundulus heteroclitus*. In *The Journal of experimental biology* 219 (4), pp. 474–484.
- McFarland, W. N.; Moss, S. A. (1967): Internal behavior in fish schools. In *Science* 156 (3772), pp. 260–262.
- Morozov, S.; McCairns, R. J. S.; Merilä, J. (2019): FishResp: R package and GUI application for analysis of aquatic respirometry data. In *Conservation physiology* 7 (1).
- Moulton, L. L.; Tarbox, K. E. (1987): Analysis of Arctic Cod Movements in the Beaufort Sea Nearshore Region, 1978-79. In *Arctic* 40, pp. 43–49.
- Nilsson, G. E. (2007): Gill remodeling in fish - a new fashion or an ancient secret? In *Journal of Experimental Biology* 210 (14), pp. 2403–2409.
- Nyack, A. C. (2006): Scaling of Post-contractile Phosphocreatine Recovery in White Muscle of Black Sea Bass, *Centropristis Striata*. Master's thesis. University of North Carolina, North Carolina Wilmington.
- Olsen, S. (1962): Observations on polar cod in the Barents Sea.
- Oppedal, F.; Dempster, T.; Stien, L. H. (2011): Environmental drivers of Atlantic salmon behaviour in sea-cages: A review. In *Aquaculture* 311 (1-4), pp. 1–18.
- Osuga, D. T.; Feeney, R. E. (1978): Antifreeze glycoproteins from Arctic fish. In *Journal of Biological Chemistry* 253 (15), pp. 5338–5343.
- Pavlov, A. K.; Tverberg, V.; Ivanov, B. V.; Nilsen, F.; Falk-Petersen, S.; Granskog, M. A. (2013): Warming of Atlantic Water in two west Spitsbergen fjords over the last century (1912–2009). In *Polar Research* 32 (1), p. 11206.
- Pörtner, H-O (2001b): Climate change and temperature-dependent biogeography: oxygen limitation of thermal tolerance in animals. In *Die Naturwissenschaften* 88 (4), pp. 137–146.

- Pörtner, H-O (2010): Oxygen- and capacity-limitation of thermal tolerance: a matrix for integrating climate-related stressor effects in marine ecosystems. In *The Journal of experimental biology* 213 (6), pp. 881–893.
- Pörtner, H-O; Bock, C.; Knust, R.; Lannig, G.; Lucassen, M.; Mark, F. C.; Sartoris, F. J. (2008): Cod and climate in a latitudinal cline: physiological analyses of climate effects in marine fishes. In *Climate Research* 37 (2-3), pp. 253–270.
- Pörtner, H-O; Bock, C.; Mark, F. C. (2017): Oxygen-and capacity-limited thermal tolerance: bridging ecology and physiology. In *The Journal of experimental biology* 220 (15), pp. 2685–2696.
- Pörtner, H-O; Farrell, A. P. (2008): Physiology and Climate Change. In *Science* 322 (5902), pp. 690–692.
- Pörtner, H-O; Walther, K.; Wittmann, A. (2013): Excess Oxygen in Polar Evolution: A Whole Organism Perspective. In Cinzia Verde, Guido Di Prisco (Eds.): *Adaptation and Evolution in Marine Environments, Volume 2*. Berlin, Heidelberg: Springer Berlin Heidelberg (From Pole to Pole), pp. 67–87.
- Precht, H. (1958): Concepts of the temperature adaptation of unchanging reaction systems of cold-blooded animals. In C. L. Prosser (Ed.): *Physiological Adaptation*. Washington, DC: American Physiological Society, pp. 50–78.
- Promińska, A.; Falck, E.; Walczowski, W. (2018): Interannual variability in hydrography and water mass distribution in Hornsund, an Arctic fjord in Svalbard. In *Polar Research* 37 (1), p. 1495546.
- Remen, M.; Oppedal, F.; Imsland, A. K.; Olsen, R. E.; Torgersen, T. (2013): Hypoxia tolerance thresholds for post-smolt Atlantic salmon: Dependency of temperature and hypoxia acclimation. In *Aquaculture* 416-417, pp. 41–47.
- Renaud, P. E.; Berge, J.; Varpe, Ø.; Lønne, O. J.; Nahrgang, J.; Ottesen, C.; Hallanger, I. (2012): Is the poleward expansion by Atlantic cod and haddock threatening native polar cod, *Boreogadus saida*? In *Polar Biology* 35 (3), pp. 401–412.
- Rhein, M.; Rintoul, S. R.; Aoki, S.; Campos, E.; Chambers, D.; Feely, R. A.; Gulev, S.; Johnson, G. C.; Josey, S. A.; Kostianoy, A.; Mauritzen, C.; Roemmich, D.; Talley, L. D.; Wang, F. (2013): Observations: Ocean. In *Climate Change 2013: The Physical Science Basis. Contribution of Working Group I to the Fifth Assessment Report of the Intergovernmental Panel on Climate Change* (eds. T. F. Stocker, D. Qin, G-K Plattner, M. Tignor, S. K. Allen, J. Boschung, A. Nauels, Y. Xia, V. Bex, P. M. Midgley), pp. 255-315. Cambridge, UK and New York, NY, USA: Cambridge University Press.
- Richards, J. G.; Farrell, A. P. (Eds.) (2009): *Hypoxia*. 1. ed. Amsterdam: Elsevier Acad. Press (Fish Physiology, 27).

- Righton, D. A.; Andersen, K. H.; Neat, F.; Thorsteinsson, V.; Steingrund, P.; Svedäng, H. et al. (2010): Thermal niche of Atlantic cod *Gadus morhua*: limits, tolerance and optima. In *Marine Ecology Progress Series* 420, pp. 1–13.
- Rodgers, E. M.; Franklin, C. E. (2021): Aerobic scope and climate warming: Testing the "plastic floors and concrete ceilings" hypothesis in the estuarine crocodile (*Crocodylus porosus*). In *Journal of experimental zoology. Part A, Ecological and integrative physiology* 335 (1), pp. 108–117.
- Rogers, N. J.; Urbina, M. A.; Reardon, E. E.; McKenzie, D. J.; Wilson, R. W. (2016): A new analysis of hypoxia tolerance in fishes using a database of critical oxygen level (P_{crit}). In *Conservation physiology* 4 (1).
- Rome, L. C.; Loughna, P. T.; Goldspink, G. (1984): Muscle fiber activity in carp as a function of swimming speed and muscle temperature. In *The American journal of physiology* 247 (2), 272–9.
- Roze, T.; Christen, F.; Amerand, A.; Claireaux, G. (2013): Trade-off between thermal sensitivity, hypoxia tolerance and growth in fish. In *Journal of Thermal Biology* 38 (2), pp. 98–106.
- Sampaio, E.; Santos, C.; Rosa, I. C.; Ferreira, V.; Pörtner, H-O; Duarte, C. M. et al. (2021): Impacts of hypoxic events surpass those of future ocean warming and acidification. In *Nature ecology & evolution* 5 (3), pp. 311–321.
- Sandblom, E.; Clark, T. D.; Gräns, A.; Ekström, A.; Brijs, J.; Sundström, L. F. et al. (2016): Physiological constraints to climate warming in fish follow principles of plastic floors and concrete ceilings. In *Nature communications* 7, p. 11447.
- Schurmann, H.; Christiansen, J. S. (1994): Behavioral thermoregulation and swimming activity of two Arctic teleosts (subfamily Gadinae)—the polar cod (*Boreogadus saida*) and the navaga (*Eleginus navaga*). In *Journal of Thermal Biology* 19 (3), pp. 207–212.
- Schurmann, H.; Steffensen, J. F. (1997): Effects of temperature, hypoxia and activity on the metabolism of juvenile Atlantic cod. In *Journal of fish biology* 50, pp. 1166–1180.
- Sidell, B. D. (1991): Physiological Roles of High Lipid Content in Tissues of Antarctic Fish Species. In : *Biology of Antarctic Fish*: Springer, Berlin, Heidelberg, pp. 220–231.
- Sidell, B. D. (1998): Intracellular oxygen diffusion: the roles of myoglobin and lipid at cold body temperature. In *Journal of Experimental Biology* 201 (8), pp. 1119–1128.
- Steffensen, J. F.; Bushnell, P. G.; Schurmann, H. (1994): Oxygen consumption in four species of teleosts from Greenland: no evidence of metabolic cold adaptation. In *Polar Biology* 14, pp. 49–54.

- Storch, D.; Menzel, L.; Frickenhaus, S.; Pörtner, H-O (2014): Climate sensitivity across marine domains of life: limits to evolutionary adaptation shape species interactions. In *Global change biology* 20 (10), pp. 3059–3067.
- van Waarde, A.; van den Thillart, G.; Kesbeke, F. (1983): Anaerobic energy metabolism of the European eel, *Anguilla anguilla* L. In *Journal of Comparative Physiology* 149, pp. 469–475.
- Welch, H. E. (1992): Energy Flow through the Marine Ecosystem of the Lancaster Sound Region, Arctic Canada. In *Arctic* 45 (4), pp. 343–357.
- Welch, H. E.; Crawford, R. E.; Hop, H. (1993): Occurrence of Arctic Cod (*Boreogadus saida*) Schools and Their Vulnerability to Predation in the Canadian High Arctic. In *Arctic* 48 (4), pp. 331–339.
- Wells, R. M. G. (1986): Cutaneous oxygen uptake in the antarctic icequab, *Rhigophila dearborni* (Pisces: Zoarcidae). In *Polar Biology* 5, pp. 175–180.
- Wells, R. M. G. (1987): Respiration of Antarctic Fish from McMurdo Sound. In *Comparative Biochemistry and Physiology* 88A (3), pp. 417–424.
- Whiteley, N. M.; Christiansen, J. S.; Egginton, S. (2006): Polar cod, *Boreogadus saida* (Gadidae), show an intermediate stress response between Antarctic and temperate fishes. In *Comparative biochemistry and physiology. Part A, Molecular & integrative physiology* 145 (4), pp. 493–501.
- Wood, C. M. (1991): Acid-Base and Ion Balance, Metabolism, and their Interactions, after Exhaustive Exercise in Fish. In *Journal of Experimental Biology* 160 (1), pp. 285–308.

Appendix

Table 8 **Solubility of oxygen at different temperatures.** Displayed is the oxygen content in sea water at 100% oxygen saturation and normal pressure (101.325 kPa). <https://www.internetchemie.info/chemielexikon/daten/s/sauerstoffgehalt-salzwasser.php>.

temperature [°C]	salinity [psu]	oxygen content [mg/l]
10	30	9.32
2	30	11.29

Acknowledgements

The implementation of a project like the present one is never possible without the help from many sides.

First, I would like to thank Prof. Dr. Hans-Otto Pörtner for giving me the chance to implement my master's thesis in his working group.

Then I would like to thank my first supervisor Dr. Felix Christopher Mark for accepting me as a master student, facilitating me to do my study research project abroad and for tackling this master's thesis with me in times of the corona virus. Thank you very much for your flexibility and your support!

I furthermore would like to thank my second supervisor Prof. Dr. Guy Claireaux. I appreciate the discussions we had and the input you gave me during my time in France and I would like to thank you for the examination of this thesis.

Further thanks go to the whole working group *Integrative Ecophysiology* at the AWI in Bremerhaven with special thanks to Sarah for your incredibly helpful support during the experiments and the calculations of the metabolic rates. Furthermore, Sandra, Anette, Isa and Nils thank you for being there for all my little questions. A big thank you goes to Amir Karamya and Fredy Véliz Moraleda who always had an eye on me and helped me so much by constructing the experimental setup and with all kinds of problems and questions around my fishes. Thank you!

Dann möchte ich als nächstes meinen Eltern Danken. Danke, dass ihr mich so gut vorbereitet habt, auf dieses Leben, mit mir durch alle Höhen und Tiefen geht und mir immer ein zu Hause seid! Danke!

Danke auch an meinen Bruder ohne dessen computertechnische Hilfe ich weder das Bachelor noch das Masterstudium gerockt hätte! Unbezahlbar!

Ein weiteres riesiges Dankeschön geht an Sara alias mermaid wife. Thank you so much for being there for me and giving me the support, I need! Thank you, dude!

Danke auch an Federica für deine wahnsinnige Unterstützung während der Endphase. Ich bin so dankbar, dass ich dich habe!

Merci beaucoup Olivier ! Pour m'équiper avec des vêtements de travail chauds et beaucoup de petits sourires ! Je suis incroyablement reconnaissant pour ton soutien polyvalent ! Danke !

Unfassbar dankbar bin ich auch für meine WG! Charlie, Anna, Melina, danke, dass das Zusammenleben mit euch so toll ist! Ihr habt mir das Durchführen dieser Masterarbeit um so vieles leichter gemacht!

Danke für eure Unterstützung und dass ihr so seid, wie ihr seid!

Ein riesiges Dankeschön geht auch an meine Familie auf Pellworm! Hanni und Andrea, danke, dass es euch gibt und ihr mich seit so vielen Jahren unterstützt und mir immer ein Zufluchtsort seid!

Des Weiteren möchte ich auch die 16 Polardorsche nicht unerwähnt lassen, die für diese Arbeit ihr Leben gegeben haben.

Und zu guter Letzt möchte ich gerne meiner Omma danken, die immer wusste, dass ich es schaffe.

The following declarations are to be included in every exemplar of the Bachelor's and Master's Thesis

Name: Carolin Julie Neven

Enrolment number: 316 40 95

Declaration of copyright

Hereby I declare that my Master's Thesis was written without external support and that I did not use any other sources and auxiliary means than those quoted. All statements which are literally or analogously taken from other publications have been identified as quotations.

Date: 30.06.2021

Signature



Declaration with regard to publishing theses

Two years after the final degree, the thesis will be submitted to the University of Bremen archive and stored there permanently.

Storage includes:

- 1) Master's Theses with a local or regional reference, as well as 10 % of all theses from every subject and year
- 2) Bachelor's Theses: The first and last Bachelor degrees from every subject and year

I agree that for research purposes third parties can look into my thesis stored in the University archive.

I agree that for research purposes third parties can look into my thesis stored in the University archive after a period of 30 years (in line with §7 para. 2 BremArchivG).

I do not agree that for research purposes third parties can look into my thesis stored in the University archive.

Date: 30.06.2021

Signature

